YEAST AIM21/TDA2 REDUCES BARBED END ASSEMBLY TO MAINTAIN FREE ACTIN POOL AND BALANCE ACTIN BETWEEN PATCHES AND CABLES

A Dissertation
Presented to the Faculty of the Graduate School
of Cornell University
In Partial Fulfillment of the Requirements for the Degree of
Doctor of Philosophy

by
Myungjoo Shin
December 2017

YEAST AIM21/TDA2 REDUCES BARBED END ASSEMBLY TO MAINTAIN FREE ACTIN POOL AND BALANCE ACTIN BETWEEN PATCHES AND CABLES

Myungjoo Shin, Ph. D.
Cornell University 2017

How cells balance the incorporation of actin into diverse structures is poorly understood. In budding yeast, a single actin monomer pool is used to build both actin cables involved in polarized growth and actin cortical patches involved in endocytosis. Here I report how Aim21/Tda2 is recruited to the membrane-proximal region of actin patches, how it negatively regulates actin assembly at patches to elevate the available actin monomer pool, and how an array of actin regulators is orchestrated to ensure proper assembly of both structures.

Aim21 has four polyproline regions and is recruited to actin patches by two SH3-containing patch proteins Bbc1 and Abp1. The C-terminal region, which is required for its function, binds to Tda2. Cell biological and biochemical data reveal that Aim21/Tda2 is a negative regulator of barbed end F-actin assembly and plays a pivotal role in balancing the distribution of actin between cables and patches, demonstrated by the rescue of the growth defect of *tpm1*Δ cells by *aim21*Δ. Additionally, this activity is necessary for efficient endocytosis. Aim21/Tda2 forms a complex with the F-actin barbed end capping protein Cap1/Cap2, revealing an interplay between regulators, and illustrating the complexity of regulation of barbed end assembly.

BIOGRAPHICAL SKETCH

Myungjoo Shin was born in Ansan, Korea, a small rural city close to Seoul, as a second son to Hongbae Shin, a mold carpenter, and Yoonsook Lee, a housewife. After two years, his family moved to Seoul. He was a curious child growing up and always showed interest in understanding how things work. He became fascinated by math first, and soon after, by science. He attended Hangaram high school, from where he graduated one year early to attend POSTECH in Pohang, Gyeongbuk, Korea.

In POSTECH, he majored in life science and participated in two research projects as an undergrad researcher. He studied how circadian rhythm is controlled in *Arabidopsis thaliana*, and how protein phosphatase 4 is involved in the development of *Xenopus laevis*. He also studied a wide range of subjects in POSTECH, including psychology, politics, intellectual property law, programming, economics, philosophy, architecture, and acting. He graduated *summa cum laude* in 2010.

In 2011, after a gap year, he came to Cornell to study more biology, in the graduate field of Biochemistry, Molecular and Cell Biology. Under the supervision of Dr. Anthony Bretscher, he studied how actin is regulated in yeast and how different actin structures are interconnected.

To my family

with all the love they deserve

ACKNOWLEDGMENTS

This journey would not have been possible without all the help I received along the way. Here, I would like to present my sincere appreciation for their support.

First, I would like to thank my adviser, Dr. Anthony Bretscher, for his contagious enthusiasm in science, excellent research mentorship, and overall guidance. This whole project and dissertation would not exist without him.

I also owe thanks my committee members, Dr. Tim Huffaker and Dr. Chris Fromme, for all their support and help.

I am very grateful to have all my family, friends, and lab mates, who supported, helped, taught, and accompanied me. They gave me emotional and moral support, especially when I felt discouraged. I would not have been able to finish this long journey without them.

And special thanks to Jinjoo, who has been with me through the highs and lows of this time.

This research has been generously supported and funded by National Institutes of Health grant GM39066.

TABLE OF CONTENTS

LIST OF FIGURES

LIST OF TABLES

LIST OF ABBREVIATIONS

5FOA	5-Fluoroorotic acid
ADFH	Actin depolymerizing factor homology domain
ADP	Adenosine diphosphate
ATP	Adenosine triphosphate
BAR	Bin-amphiphysin-Rvs
BSA	Bovine serum albumin
cAMP	Cyclic adenosine monophosphate
CIE	Clathrin-independent endocytosis
CME	Clathrin-mediated endocytosis
CMOS	Complementary metal-oxide-semiconductor
CPI	Capping protein interaction motif
CSI	CARMIL-specific interaction motif
CT	C-terminal region
DAD	Diaphanous autoregulatory domain
DIC	Differential interference contrast
DID	Diaphanous inhibitory domain
DNA	Deoxyribonucleic acid
ER	Endoplasmic reticulum
F-actin	Filamentous actin
FH	Formin homology domain
G-actin	Monomeric actin
GBD	GTPase-binding domain
GFP	Green fluorescent protein
GMF	Glia maturation factor
GTP	Guanosine triphosphate
IPTG	Isopropyl β-D-1-thiogalactopyranoside
Lat-A	Latrunculin-A

Lat-B	Latrunculin-B
mRNA	Messenger RNA
NPF	Nucleation promoting factors
PAGE	Polyacrylamide gel electrophoresis
PBS	Phosphate buffered saline
PCR	Polymerase chain reaction
PKA	Protein kinase A
$PI(4,5)P_2$	Phosphatidylinositol 4,5-bisphosphate
PM	Plasma membrane
PP	Polyproline
RNA	Ribonucleic acid
SC	Synthetic complete
SD	Synthetic deficient
SDS	Sodium dodecyl sulfate
SEM	Standard error of measurement
SH3	Src homology 3
SUMO	Small ubiquitin-like modifier
TB	Terrific broth
tRNA	Transfer RNA
VCA	Verprolin, central, and acidic domain
v/v	Volume / volume
WASP	Wiskott–Aldrich syndrome protein
WT	Wild type
YPD or YEPD	Yeast extract peptone dextrose

CHAPTER 1. INTRODUCTION

Introduction to the actin cytoskeleton

Cytoskeleton means 'cellular skeleton', from *cyto*-, which means cell, and skeleton. Like the skeleton in a human body, the cytoskeleton performs essential functions, some of which resemble the functions of the skeleton; it shapes the cell, provides mechanical support, makes movements possible, defines subcellular compartments, transmits signals, serves as track for transport, and many more. In eukaryotic cells, there are three components of the cytoskeleton, based on their thickness: from the thinnest to thickest, microfilaments, intermediate filaments, and microtubules (Figure 1.1). All three components of the cytoskeleton share dynamic properties; monomeric subunits assemble into linear filaments or higher order structures, and these structures disassemble back to monomeric subunits when the structures are no longer needed. Each component of the cytoskeleton makes up multiple different structures, and these structures are often built from the same pool of monomeric subunits. Also, the level of monomer pool often affects the initiation or rate of the assembly of these structures. Thus, cells need to maintain the pools of monomers at appropriate levels to build dynamic structures properly and keep them functional (Figure 1.2, microfilaments as an example).

Microfilaments (actin filaments)

Microfilaments are made of actin filaments (Korn, 1982). Like intermediate filaments and microtubules, microfilaments go through a cycle of assembly and disassembly; the monomers, monomeric actin (also known as G-actin, for globular actin), get incorporated into filaments (also

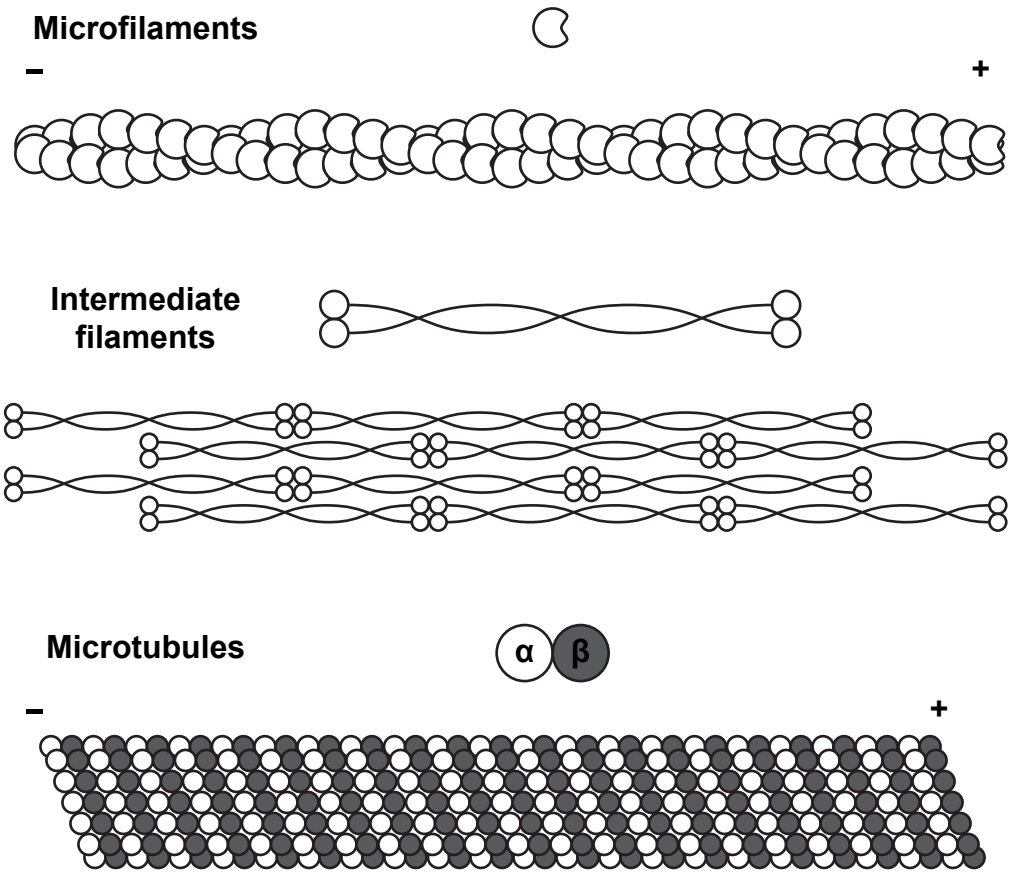

Figure 1.1. The three components of the cytoskeleton: microfilaments, intermediate filaments, and microtubules. Monomer form and filament form of each are shown. From the thinnest to the thickest, microfilaments (7nm diameter), intermediate filaments (usually 9-11nm), and microtubules (24nm diameter). Microfilaments and microtubules have polarity (+ end and – end). Intermediate filaments do not have polarity.

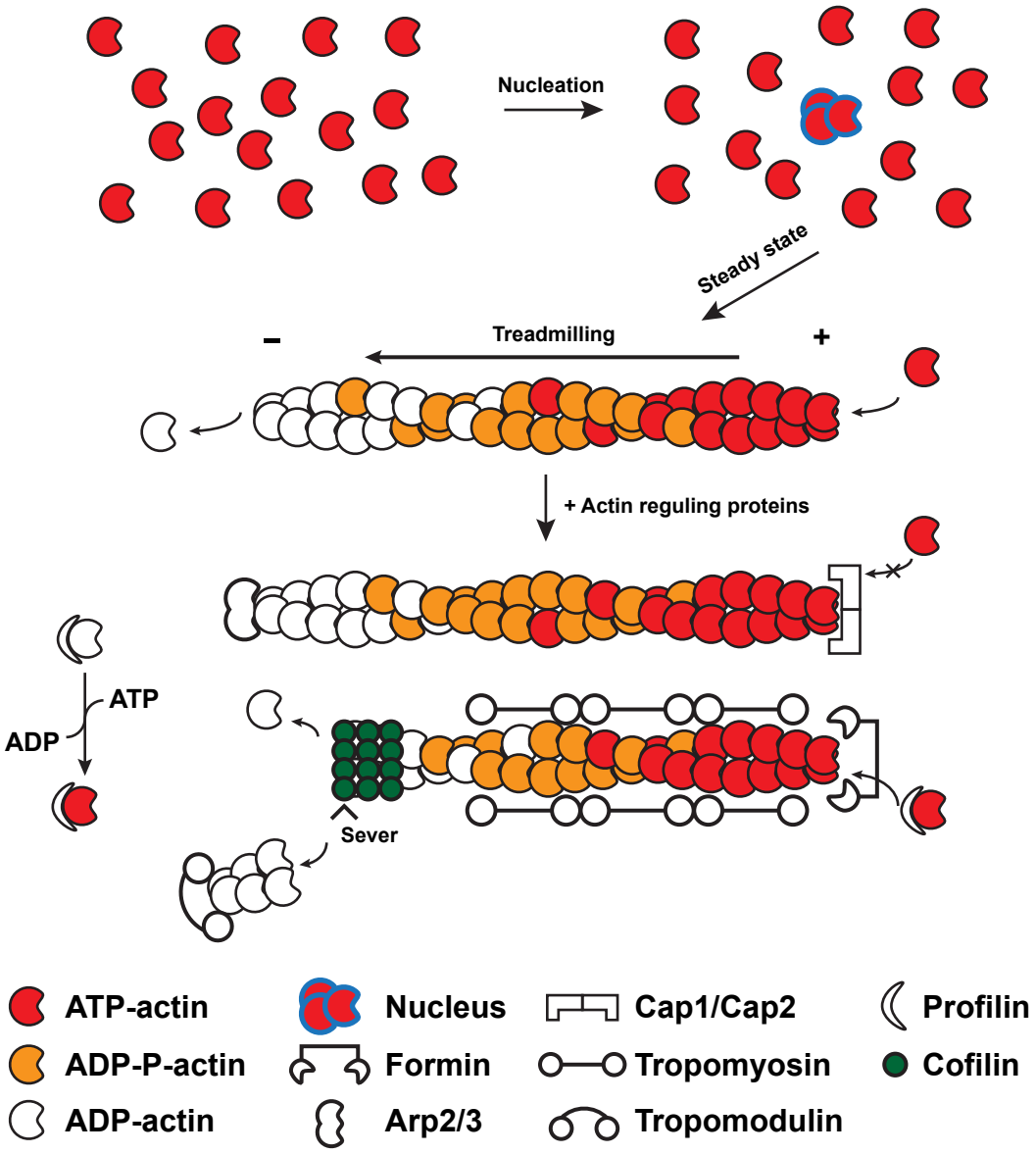

Figure 1.2. The actin cycle and actin regulating proteins. When the concentration is above the critical concentration, actin monomers assemble into filaments, with nucleation being the rate-limiting step. When addition rate at the barbed end equals the release rate at the pointed end, the filament undergoes treadmilling, without changing its length. Treadmilling is accompanied by the hydrolysis of ATP bound to actin. Actin regulating proteins include nucleators (the Arp2/3 complex and formin), actin monomer binding proteins (profilin), elongation regulating proteins (Cap1/Cap2 and tropomodulin), and stability regulating proteins (tropomyosin and cofilin).

known as filamentous actin, F-actin), and these filaments disassemble back to monomers (Figure 1.2) (Korn, 1982). While monomers naturally start to assemble into filaments when the concentration of actin is above the critical concentration, the nucleation step, where two or three actin monomers bind each other to form a nucleus, is the rate limiting step for filament assembly (Frieden, 1985; Korn, 1982; Pollard and Cooper, 1986). Thus, *in vivo*, this nucleation step is usually aided by nucleators, such as the Arp2/3 complex or formin, which gives the cell better control over where, and how much, assembly happens (Campellone and Welch, 2010). Actin is also an ATPase and its nucleotide state changes its likelihood of polymerization. Actin is more likely to assemble into filaments when bound to ATP, compared to when bound to ADP, meaning ATP-actin has lower critical concentrations for assembly than ADP-actin. Actin filaments have directionality as well. Actin monomers are assembled into filaments with a certain orientation, and one end is preferred for addition of new monomers, with a lower critical concentration, than the other end (Carlier et al., 1985; Pollard, 1986; Pollard, 1990). The end with lower critical concentration is called the growing end, which is also known as the plus end or barbed end, and the end with higher critical concentration is called the minus end or pointed end; barbed and pointed ends are named from their appearances when decorated with the F-actin binding fragment of myosin (Huxley, 1963). This directionality and different critical concentrations at ends create treadmilling. At steady state, actin monomers are added to barbed ends and released from pointed ends. Thus, when the assembly rate at barbed ends equals the disassembly rate at pointed ends, there is no net growth and filaments are constantly undergoing treadmilling (Korn, 1982). This treadmilling is also accompanied by hydrolysis of ATP-actin into ADP-actin; the ATPase activity of actin is stimulated when actin is incorporated into filaments. ATP-actin is added to the barbed end, ATP is hydrolyzed into ADP-P, phosphate is released, and ADP-actin is released from the

pointed end (Korn et al., 1987; Pollard, 1990). As a result, recently assembled areas of filaments mostly contain ATP bound actin (ATP-F-actin), followed by ADP-P-F-actin, and then followed by ADP-F-actin, the oldest part of the filaments (Figure 1.2). The cell utilizes multiple sets of proteins to regulate this cycle of actin (Figure 1.2) (Campellone and Welch, 2010; Pollard, 2016):

(1) Nucleators and their regulators control where, and how many, filaments are assembled (Campellone and Welch, 2010). *e.g.* Arp2/3 complex, formin, and cordon-bleu.

(2) Actin monomer binding proteins regulate the level of free actin and direct assembly to one structure over another. It should be noted that the concentration of actin monomers is usually higher than the critical concentration of barbed end, yet these G-actin binding proteins keep the effective concentration of actin monomers in the pool low by sequestering them. This prevents uncontrolled nucleation and elongation, but allows efficient nucleation and elongation when needed. *e.g.* profilin and β-thymosin. Profilin is the first protein discovered to bind to G-actin, and it has many functions, including (i) it facilitates the exchange of ADP to ATP in G-actin, (ii) it decreases the effective concentration by sequestering G-actin, and (iii) profilin bound actin (profilin-actin) can only add to barbed end and profilin-actin feeds assembly by formins (Carlsson et al., 1977; Evangelista et al., 2002; Mockrin and Korn, 1980; Pollard and Cooper, 1984; Pruyne et al., 2002; Schutt et al., 1993; Tilney et al., 1983; Vinson et al., 1998). β-thymosin is another G-actin sequestering protein. *In vivo,* most of free actin is bound to either profilin or β-thymosin (Pollard, 2016; Safer et al., 1991; Safer et al., 1990).

(3) Proteins that regulate the elongation of filaments. After being nucleated, the elongation of filaments is modulated to ensure an appropriate degree of growth, neither too little nor too excessive. The addition of monomers to—and release from—filaments happen at ends and a set

of proteins adjust the rate of elongation either by directly interacting with the ends or by binding to the sides of the filaments and inducing conformational change of filaments (an allosteric regulation). *e.g.* barbed end and pointed end capping proteins, such as Cap1/Cap2 and tropomodulin (respectively), bind ends with high affinity to inhibit further addition or release of actin monomers (Casella et al., 1986; Fowler, 1987; Fowler, 1990; Fowler et al., 1993; Maruyama, 1965a; Maruyama, 1965b; Maruyama et al., 1977; Maruyama et al., 1990; Weber et al., 1994).

(4) Proteins that control the stability of filaments or the actin structures; some proteins stabilize the assembled structures and other proteins destabilize them to stimulate their disassembly back to actin monomers. *e.g.* tropomyosin binds and stabilizes F-actin, and cofilin binds, destabilizes, and severs F-actin.

Although these are main categories of actin regulators, there are other types of proteins that provide further and more fine-tuned regulation of the assembly and disassembly of F-actin, managing the G-actin pool (Brieher, 2013; Campellone and Welch, 2010; Pollard, 2016).

Actin in yeast: two main actin structures and actin pool

Actin is highly conserved throughout eukaryotes, and it has been extensively studied in budding yeast, *Saccharomyces cerevisiae*. Budding yeast has a single actin gene and the actin cytoskeleton is responsible for all its cellular transport (Drees et al., 1995; Gallwitz and Seidel, 1980; Kubler and Riezman, 1993; Ng and Abelson, 1980; Pruyne et al., 1998; Shortle et al., 1982). In contrast, in larger eukaryotic cells, transport is also mediated by microtubules, especially long-range transport (Atkinson et al., 1992). This gives the yeast an unusual dependence on actin,

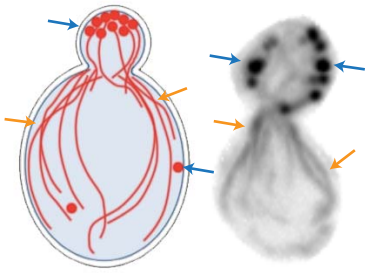

Figure 1.3. Actin structures in actively growing yeast. Right panel shows actual actin structures in yeast, visualized by phalloidin staining (maximum projection of center 4 planes), and left panel shows a schematic representation. Blue arrows indicate actin cortical patches, and yellow arrows indicate actin cables.

making it a great model system to study the regulation of the actin cytoskeleton, along with its many available experimental tools.

There are two main actin structures in actively growing yeast: actin cables and actin cortical patches (Figure 1.3) (Adams and Pringle, 1984; Kilmartin and Adams, 1984). Both structures perform distinct functions and are essential for proper growth (Kubler and Riezman, 1993; Pruyne et al., 1998).

Actin cables: tracks for myosin V-mediated transport

Actin cables are bundled filaments that are built by the formins, Bni1 and Bnr1, cross-linked by fimbrin Sac6, and stabilized by tropomyosin, Tpm1 and Tpm2, and they serve as tracks for myosin V motor (Myo2 and Myo4 in yeast)-mediated polarized transport of secretory vesicles, organelles, and mRNAs (Adams et al., 1989; Catlett and Weisman, 1998; Chernyakov et al., 2013; Drubin et al., 1988; Evangelista et al., 2002; Fagarasanu et al., 2006; Hill et al., 1996; Hoepfner et al., 2001; Itoh et al., 2004; Itoh et al., 2002; Johnston et al., 1991; Lipatova et al., 2008; Pruyne et al., 2002; Pruyne et al., 1998; Sagot et al., 2002a; Sagot et al., 2002b; Schott et al., 1999; Yin et al., 2000). While a formin is essential for building actin cables, two isoforms, Bni1 and Bnr1, are functionally redundant: *bnr1*Δ cells grow as well as wild type cells, and *bni1*Δ cells have only minor growth defects (Evangelista et al., 2002; Vallen et al., 2000). However, Bni1 and Bnr1 have some key differences between them. Bni1 localizes to the bud tip in small- or medium-budded cells and then to the bud neck in large-budded cells, but Bnr1 localizes to the bud neck throughout the cell cycle (Fujiwara et al., 1998; Gao et al., 2010; Kamei et al., 1998; Ozaki-Kuroda et al., 2001). Bni1 treadmills back on actin cables, whereas Bnr1 does not (Buttery et al., 2007). Both

Bni1 and Bnr1 can cap the barbed ends of the filaments, but Bnr1 caps more tightly. Bnr1 is about 10 times more potent at nucleation than Bni1. Bnr1 can bundle F-actin, but Bni1 cannot (Graziano et al., 2011; Graziano et al., 2013; Moseley and Goode, 2005). Bni1 and Bnr1 are also regulated differently, which will be discussed in detail in *Regulation of actin cables*.

Tropomyosin binds to the sides of actin filaments, with one coiled-coil dimer spanning several subunits of actin. They perform multiple functions, such as stabilization of the filaments and regulating interactions between the filaments and other proteins (Gunning et al., 2015). In yeast, the tropomyosins, Tpm1 and Tpm2, stabilize cables built by formins and, like formins, cells can tolerate loss of either Tpm1 or Tpm2, but loss of both Tpm1 and Tpm2 is lethal (Drees et al., 1995; Liu and Bretscher, 1989a; Liu and Bretscher, 1989b; Pruyne et al., 1998). However, unlike Bni1 and Bnr1, Tpm1 is five times more abundant than Tpm2, making Tpm1 the major isoform and Tpm2 the minor isoform (Drees et al., 1995). Consistent with this, *tpm1*Δ cells have few short cables and, as a result, grow very poorly, but *tpm2*Δ cells do not show any phenotype regarding actin morphology or growth (Drees et al., 1995; Liu and Bretscher, 1992; Liu and Bretscher, 1989a). The poor growth of *tpm1*Δ cells signifies the importance of actin cables and myosin V-mediated transport (Pruyne et al., 2004).

Once actin cables are built and stabilized, now they can serve as tracks for myosin V motors, Myo2 and Myo4 in yeast. Myo2 and Myo4 bind both actin cables through their ATPase domain, and their cargos by interacting with cargo-specific adapters. Then, they use ATP to walk towards the barbed ends of actin cables, which usually localize at the bud tip or the bud neck, delivering the cargos (Pruyne et al., 2004). Although Myo2 and Myo4 are both myosin V motors, Myo2 and Myo4 carry different cargos. Myo2 transports secretory vesicles, trans-Golgi, mitochondria,

vacuoles, and peroxisomes, and it also orients the spindle through an adaptor Kar9, while Myo4 transports mRNAs and endoplasmic reticulum (ER) (Chernyakov et al., 2013; Fagarasanu et al., 2006; Itoh et al., 2004; Itoh et al., 2002; Lipatova et al., 2008; Pruyne et al., 2004). Another difference between Myo2 and Myo4 is that Myo2 is essential, while Myo4 is not. This is likely to be due to the fact that Myo2 is directly responsible for the transport of essential cargos, such as secretory vesicles and mitochondria, while Myo4 cargos, such as mRNAs and ER, are nonessential or can be inherited indirectly (Chernyakov et al., 2013; Diehl and Pringle, 1991; Haarer et al., 1994; Itoh et al., 2004; Johnston et al., 1991; Prendergast et al., 1990; Schott et al., 1999).

Actin cortical patches: sites of endocytosis

Actin cortical patches are branched F-actin structures nucleated by the Arp2/3 complex, whose seven subunits are encoded by seven separate genes in yeast, that provide mechanical force for endocytosis (Goode et al., 2015; Kubler and Riezman, 1993; Winter et al., 1997; Winter et al., 1999b). The force generated by actin assembly is transmitted to the plasma membrane (PM) through adapter proteins (Figure 1.4). This transmitted force bends the membrane to create an endocytic membrane invagination and later drives the newly formed endocytic vesicles into the cytoplasm (Figure 1.4) (Goode et al., 2015; Lu et al., 2016). While actin assembly and the force generated by it also play a role in endocytosis in other eukaryotes, they carry a bigger importance in yeast, because endocytic invagination needs to overcome turgor pressure (Aghamohammadzadeh and Ayscough, 2009; Mooren et al., 2012).

Endocytosis removes lipids and proteins from the plasma membrane, and takes up molecules from outside of the cell, such as ligands and nutrients. There are several types of

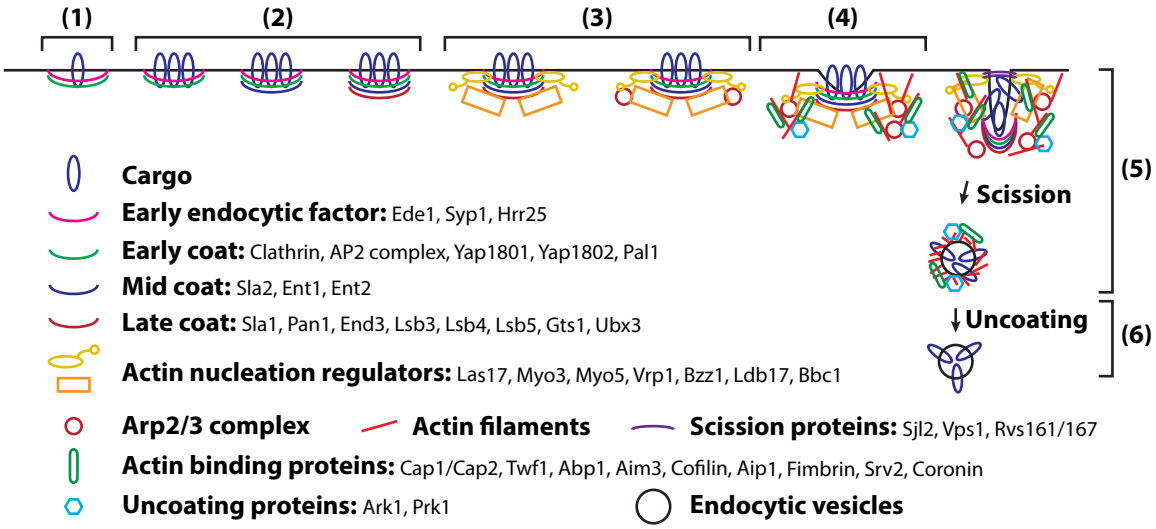

Figure 1.4. Timeline for clathrin-mediated endocytosis in yeast. CME goes through (1) site selection and recruitment of early endocytic factors and early coat proteins, (2) cargo concentration and recruitment of mid and late coat, (3) recruitment of the Arp2/3 complex, NPFs, and their regulators, (4) F-actin assembly and endocytic invagination, (5) scission at the neck of the endocytic invagination, and (6) uncoating of endocytic vesicles.

endocytosis, but they can be divided into clathrin-mediated endocytosis (CME) and clathrin-independent endocytosis (CIE) (Doherty and McMahon, 2009; Kirchhausen et al., 2014; Mayor et al., 2014; Merrifield and Kaksonen, 2014). Although the existence of CIE has been proposed in yeast and some evidence has recently been presented, currently, little is known about CIE and CME seems to be the major endocytic pathway (Aghamohammadzadeh et al., 2014; Prosser et al., 2011; Prosser and Wendland, 2012).

CME in yeast starts with cells choosing where to initiate endocytosis on their PM (Figure 1.4). While the mechanism of how cells choose a site for endocytosis is not clearly understood, there is a strong correlation with the region involved in exocytosis, implying cargoes delivered by exocytosis play a role in site selection (Brach et al., 2014; Gao et al., 2003; Pruyne et al., 1998). Nonetheless, several early endocytic factors and early coat proteins, such as Ede1, Syp1, Hrr25, and clathrin, mark sites that later progress into endocytosis (Brach et al., 2014; Carroll et al., 2012; Peng et al., 2015). After early endocytic factors and early coat proteins arrive, endocytic cargos are concentrated and sorted into these selected sites (Carroll et al., 2012; Ehrlich et al., 2004; Layton et al., 2011). Then, mid and late coat proteins, such as Sla1, Sla2, and Ent1, are recruited to the sites (Kaksonen et al., 2003; Kaksonen et al., 2005). Next, the Arp2/3 complex is recruited together with its regulators to assemble actin filaments (Goode et al., 2015; Kaksonen et al., 2003; Kaksonen et al., 2005; Lu et al., 2016). Although the yeast Arp2/3 complex, unlike the Arp2/3 complexes from other organisms, has some nucleation activity on its own, it becomes further activated by nucleation promoting factors (NPF) and their activators, including Las17, Myo3, Myo5, Vrp1, Abp1, Bzz1, and Pan1 (Goode et al., 2015; Wen and Rubenstein, 2005). Nucleation activity of the Arp2/3 complex is also negatively regulated by Arp2/3 complex inhibitors or NPF

inhibitors, which includes yeast coronin Crn1, Syp1, Lsb1, Lsb2, Sla1, Sla2, and Bbc1 (Goode et al., 2015). With this complex interplay among these players, the Arp2/3 complex builds branched F-actin structures, and the force generated by them is transmitted to the PM by adapter proteins Sla2 and Ent1. Sla2 and Ent1, which are also coat proteins, bind to both F-actin and the PM, to transmit the force from actin assembly to the PM, causing membrane invagination (Avinoam et al., 2015; Skruzny et al., 2012; Skruzny et al., 2015). Endocytic invagination is followed by scission at the neck of the invagination to generate an endocytic vesicle. The mechanism by which scission happens in yeast is not yet known, but it involves the Bin-amphiphysin-Rvs (BAR) proteins Rvs161/Rvs167, which forms an obligate heterodimer, and Bzz1, and a synaptojanin Sjl2 (Friesen et al., 2006; Idrissi et al., 2008; Kishimoto et al., 2011; Picco et al., 2015). The endocytic vesicles generated by scission are then driven into the cell by actin assembly, where they fuse with endosomes. Before fusing with endosomes, the endocytic coats and F-actin structures on the endocytic vesicles need to be removed, and kinases Ark1 and Prk1 are implicated in this process (Cope et al., 1999; Sun et al., 2007; Toret et al., 2008).

Balance between cables and patches

Because both actin cables and cortical patches carry out crucial functions and are assembled from the same actin monomer pool, yeast needs mechanisms to ensure appropriate assembly for each structure (Carlier and Shekhar, 2017; Pollard, 2016). For example, barbed end capping protein Cap1/Cap2, which forms an obligate heterodimer, effectively inhibits F-actin elongation at actin patches and prevents excessive growth of F-actin (Amatruda et al., 1990; Amatruda and Cooper, 1992; Amatruda et al., 1992; Kim et al., 2004). In cells lacking Cap1 or

Cap2, excessive assembly of F-actin at patches depletes free actin pool and, as a result, actin cables are severely down-regulated (Amatruda et al., 1990; Amatruda et al., 1992). The opposite case has also been reported. Overexpressing a fragment of Bnr1 that is capable of nucleation but lacks autoinhibition generates excessive cables and kills the cell, but this lethality is rescued by co-overexpressing Las17, a major NPF for actin patch assembly (Gao and Bretscher, 2008).

Regulation of actin cables

As discussed in *Actin cables: tracks for myosin V-mediated transport*, actin cables are nucleated and built by two formin isoforms, Bni1 and Bnr1. Bni1 and Bnr1 share a similar domain structure: from N-terminus to C-terminus, GTPase-binding domain (GBD), diaphanous inhibitory domain (DID), formin homology domain 1 (FH1), formin homology domain 2 (FH2), and, inside the C-terminal part of FH2, diaphanous autoregulatory domain (DAD) (Higgs and Peterson, 2005; Pruyne et al., 2004). FH1 and FH2 are the parts of proteins that initiate actin assembly. FH1 domain interacts with actin monomer bound to profilin and feeds it into the barbed end, while FH1-FH2 stays on the barbed ends and protects them from barbed end capping proteins during the elongation process, which is known as processive capping (Chang et al., 1997; Goode and Eck, 2007; Kovar et al., 2006; Pruyne et al., 2002; Romero et al., 2004; Sagot et al., 2002b). DID and DAD interact with each other to keep the molecule in the inhibited form and this autoinhibitory interaction is released upon interaction with GTPases through the GBD (Alberts, 2001; Goode and Eck, 2007; Li and Higgs, 2003; Li and Higgs, 2005; Watanabe et al., 1999). However, it is unclear which GTPases Bni1 and Bnr1 interact with to become active. Cdc42, Rho1, and Rho3 for Bni1, and Rho4 for Bnr1 have been implicated as interacting GTPases, but the results are not yet conclusive

(Dong et al., 2003; Fujiwara et al., 1998; Imamura et al., 1997; Kamei et al., 1998; Kohno et al., 1996; Pruyne et al., 2004). The activity of formins is regulated by proteins other than GTPases as well. For instance, the activities of Bni1 and Bnr1 are both regulated by Bud6. There are also specific regulators for each isoform (Buttery et al., 2007; Graziano et al., 2011; Graziano et al., 2013; Moseley and Goode, 2005; Park et al., 2015). Bni1 is a component of the polarisome and is regulated by phosphorylation by Prk1 (Fujiwara et al., 1998; Sheu et al., 1998; Wang et al., 2009). Bni1, not Bnr1, gets degraded upon cell wall or membrane damage, and this degradation is mediated by activation of Pkc1 (Kono et al., 2012). Bnr1 is regulated by Bud14/Kel1/Kel2, septin Shs1, septin-associated kinase Gin4, and the BAR protein Hof1 (Buttery et al., 2012; Chesarone et al., 2009; Gould et al., 2014; Graziano et al., 2014; Kamei et al., 1998; Kikyo et al., 1999).

These cables then get cross-linked by fimbrin Sac6, and stabilized by tropomyosin, Tpm1 and Tpm2. Although this cross-linking is crucial and the stabilization is essential for the proper morphology of actin cables, regulation of them has not been extensively studied (Adams et al., 1989; Drees et al., 1995; Liu and Bretscher, 1992; Liu and Bretscher, 1989a; Pruyne et al., 1998). What is known about their regulation is summarized below. Tpm1 and Tpm2 are acetylated at their N-terminus by Nat3/Mdm20 complex (NatB), one of the three N-terminal acetyltransferase complexes in yeast, and this acetylation is critical for their cooperative binding to actin cables and the stabilization of them (Maytum et al., 2000; Polevoda et al., 2003; Singer and Shaw, 2003). Fimbrin has been shown to be regulated by calcium binding and phosphorylation by cAMP-dependent protein kinase A (PKA) in human cells, and Sac6 in budding yeast has been shown to be regulated by Cdk1 to modulate the stability of cables (Janji et al., 2006; Miao et al., 2016; Namba et al., 1992). Abp140 is another actin binding protein that bundles F-actin *in vitro* and

preferentially localizes to actin cables *in vivo*. Although its *in vitro* bundling activity and *in vivo* cable localization have suggested that it regulates actin cable dynamics, *abp140*Δ cells do not display defects in cable dynamics. Interestingly, Abp140 was later found to be a methyltransferase for tRNAs and to be involved in the localization of its own mRNA to the mother cell. This implies that its actin binding property can be to localizes its mRNAs, not to regulate cable dynamics, but more studies need to be done to determine its physiological relevance regarding actin cables (Asakura et al., 1998; D'Silva et al., 2011; Gao and Bretscher, 2008; Kilchert and Spang, 2011; Yang and Pon, 2002).

Regulation of actin patches: nucleation, elongation, and disassembly

Actin cortical patches provide mechanical force for endocytic invagination and, for efficient endocytosis, actin assembly needs to be properly regulated to ensure an adequate level of force and invagination. F-actin at patches goes through three stages, nucleation, elongation, and disassembly, and multiple sets of proteins are employed to regulate actin at all three stages (Goode et al., 2015; Lu et al., 2016).

Regulation of F-actin nucleation at patches

As briefly discussed in *Actin cortical patches: sites of endocytosis*, actin filaments at cortical patches are nucleated by the Arp2/3 complex (Goode et al., 2015; Kelleher et al., 1995; Schwob and Martin, 1992; Welch et al., 1997). The Arp2/3 complex binds to the sides of an existing filament and nucleates F-actin at a 70° angle from it to generate a branched F-actin structure (Goley and Welch, 2006; Mullins et al., 1998). This nucleation activity is regulated by

multiple nucleation promoting factors (NPFs) and inhibitors, some of which are also regulated by other proteins (Goley and Welch, 2006; Goode et al., 2015). For example, Las17, a yeast homologue of Wiskott–Aldrich syndrome protein (WASP), was the first discovered NPF for the Arp2/3 complex, and it is essential for proper assembly of actin cortical patches and functional endocytosis (Li, 1997; Madania et al., 1999; Winter et al., 1999a). Las17 binds the Arp2/3 complex through its VCA domain (a domain containing Verprolin, Central, and Acidic motives) and induces conformational changes to activate the nucleation activity of the Arp2/3 complex (Goley et al., 2004; Higgs et al., 1999; Rodal et al., 2005). The NPF activity of Las17 is inhibited by Syp1, Sla1, and Bbc1, through interaction between Src homology 3 (SH3) domains of these proteins and polyproline region of Las17 (Boettner et al., 2009; Feliciano and Di Pietro, 2012; Rodal et al., 2003).

In addition to this complex interplay of proteins regulating the Arp2/3 complex activity, the nucleation of F-actin is further controlled by the existence of mother filaments, and proteins that modulate branching. The Arp2/3 complexes need to bind to existing actin filaments to be fully active, and glia maturation factor (GMF), Aim7 in yeast, binds to the Arp2/3 complex to dissociate it from the mother filaments (Gandhi et al., 2010; Higgs et al., 1999; Luan and Nolen, 2013; Machesky et al., 1999; Ydenberg et al., 2013). Beside these regulatory mechanisms, the nucleation or branching activity of the Arp2/3 complex is also managed by other mechanisms, such as the nucleotide status of Arp2 or Arp3 (Dayel et al., 2001; Dayel and Mullins, 2004; Goley et al., 2004; Ingerman et al., 2013; Le Clainche et al., 2001; Le Clainche et al., 2003; Martin et al., 2006; Martin et al., 2005).

Regulation of F-actin elongation at patches

The Arp2/3 complex, the nucleator for actin cortical patches, binds to the pointed end, leaving the barbed end free, in contrast to formin, which binds to the barbed end and protects it from barbed end capping proteins (Kelleher et al., 1995; Pruyne et al., 2002; Welch et al., 1997). These free barbed ends allow actin monomers to be added quickly, but also make it imperative for cells to make sure that excessive assembly does not occur (Amatruda et al., 1990; Amatruda et al., 1992). There are two different inhibitors of barbed end actin assembly in yeast: F-actin barbed end capping protein Cap1/Cap2, and Abp1/Aim3 (Michelot et al., 2013; Nadkarni and Brieher, 2014).

Cap1 and Cap2 are well-known F-actin barbed end assembly inhibitors, and their homologues are found throughout eukaryotes. Cap1 and Cap2 form a heterodimer that binds the barbed end of F-actin with high affinity and inhibits further addition of monomers (Edwards et al., 2014; Maruyama, 1965a; Maruyama, 1965b; Maruyama et al., 1977; Maruyama et al., 1990). The importance of Cap1/Cap2 can be seen when *CAP1* or *CAP2* is deleted; much more actin is assembled into patches, endocytosis becomes very inefficient, and actin cables are largely gone (Amatruda et al., 1990; Amatruda et al., 1992). Capping activity by barbed end capping proteins can be modulated by other proteins, especially by those containing the capping protein interaction (CPI) motif or CARMIL-specific interaction (CSI) motif (Edwards et al., 2015; Edwards et al., 2014; Stark et al., 2017; Uruno et al., 2006; Yang et al., 2005). For instance, CARMIL, which has both motifs, has been shown to bind capping protein and decrease its affinity for the barbed end (Edwards et al., 2014; Jung et al., 2001; Stark et al., 2017; Yang et al., 2005). Although such proteins have not been found in yeast yet, a recent study showed that similar interactions might exist (Farrell et al., 2017). Also, phosphatidylinositol 4,5-bisphosphate ($PI(4,5)P_2$), which is

enriched in the plasma membrane, has also been shown to decrease capping activity of barbed end capping proteins in yeast and in other organisms (Amatruda and Cooper, 1992; Edwards et al., 2014; Heiss and Cooper, 1991).

Abp1, Actin Binding Protein 1, is a well-known actin binding protein in yeast (Drubin et al., 1988). Abp1 has an actin depolymerizing factor homology domain (ADFH), which binds to the sides of actin filaments, and a Src homology 3 (SH3) domain (Drubin et al., 1990; Moon et al., 1993). Although Abp1 has an ADFH domain, it does not disassemble actin filaments on its own. Rather it activates the Arp2/3 complex, and recruits other endocytic proteins, including Ark1 and Prk1, to actin patches (Cope et al., 1999; Fazi et al., 2002; Goode et al., 2015; Goode et al., 2001). Michelot et al. (2013) found that Abp1 interacts with Aim3, supposedly through the interaction between its SH3 domain and polyproline region of Aim3, to inhibit actin assembly at barbed ends *in vitro*. This result implies that Aim3 can work as a capping protein when recruited by Abp1, but as Michelot et al. (2013) indicated, it is also possible that Abp1/Aim3 induces a conformational change in the filament to reduce the addition of actin monomers to the barbed end.

Regulation of F-actin disassembly at patches

Disassembly of F-actin structures at patches has been an interesting topic in actin regulation, because the disassembly of actin patches *in vivo* seems to be far faster than the disassembly of actin filaments *in vitro* (Brieher, 2013; Chen et al., 2000; Moseley and Goode, 2006; Zigmond, 1993). This suggested that there are more players involved in this process than originally thought, and that led to the discoveries of multiple disassembly factors. According to the current view, it is believed that disassembly at actin patches is mediated by cofilin Cof1 with its cofactor Aip1,

coronin Crn1, twinfilin Twf1, and Srv2 (or cyclase-associated protein (CAP)) (Pollard, 2016). These factors have different mechanisms of action and are orchestrated to accomplish fast and robust disassembly of F-actin structures at patches.

Cofilin has been believed to be the main player in this process. It directly binds, destabilizes and severs actin filaments (Bamburg et al., 1980; Carlier et al., 1997; Carlier and Shekhar, 2017; Harris et al., 1980; Moon et al., 1993; Nishida et al., 1984; Okada et al., 2006; Ono et al., 2004). Cofilin has an ADFH domain and preferentially binds ADP-actin over ATP-actin (Carlier et al., 1997). It binds cooperatively to F-actin, making a cofilin-decorated domain on it. This decoration induces a conformational change to the filament, which in turn causes a twist and breakage at the junction between the cofilin-decorated domain and the bare domain, severing the filament (Hayakawa et al., 2014; McGough et al., 1997; Nadkarni and Brieher, 2014; Suarez et al., 2011; Wioland et al., 2017). This conformational change also alters what proteins bind to it, as some proteins have different affinities to F-actin, depending on the conformation (McGough et al., 1997; Nishida et al., 1984; Wioland et al., 2017). Interestingly, except at the junctions, the cofilin-decorated domain is rather stable and long-living *in vitro*, which is at odds with *in vivo* data where cofilin destabilizes, severs, and disassembles ADP-F-actin into monomers rapidly (Suarez et al., 2011; Wioland et al., 2017; Zigmond, 1993).

Aip1, a cofactor of cofilin, greatly increase severing activity by cofilin, especially inside of this domain, partially solving the disagreement between *in vivo* and in *vitro* data (Brieher et al., 2006; Kueh et al., 2008; Okada et al., 2006; Ono et al., 2004). Aip1 is recruited to F-actin by cofilin, and destabilizes the interaction between cofilin and decorated F-actin, increasing the rate severing (Aggeli et al., 2014; Rodal et al., 1999). In addition to its function to stimulate the activity of cofilin,

Aip1 has also been found to be associated with barbed ends, and the role of this interaction had been unclear (Okada et al., 2002). Yet, several recent studies gave some insights in this matter. Michelot et al. (2013) presented convincing evidence that Aip1 and Cap1/Cap2 compete for barbed ends generated by cofilin severing and proposed that Aip1 blocks addition of new actin monomers to the resulting barbed ends, like Cap1/Cap2. However, Nadkarni and Brieher (2014) argued that Aip1 does not inhibit addition of monomers to barbed ends, but rather accelerates disassociation of monomers from F-actin at both ends, indicating that Aip1 capping serves a different function from Cap1/Cap2 capping. A more recently study by Wioland et al. (2017) shows that once cofilin decorates filaments, it can decrease the binding affinity of barbed end capping protein, even without Aip1. In summary, these recent findings suggest that Aip1 stimulates the severing activity of cofilin, caps the barbed ends of severed F-actin to block Cap1/Cap2 from stabilizing barbed ends, and promotes disassociation of monomers from the ends, contributing to the fast disassembly of F-actin. Coronin, Crn1 in yeast, is also found to interact with cofilin to accelerate disassembly of F-actin (Gandhi et al., 2009; Kueh et al., 2008; Mikati et al., 2015). While coronin has also been known to regulate the activity of the Arp2/3 complex, as discussed in *Regulation of F-actin nucleation at patches*, it also binds to the sides of the filaments and changes their dynamics (Cai et al., 2007a; Cai et al., 2007b; de Hostos et al., 1991; Humphries et al., 2002; Rodal et al., 2005). It decorates F-actin and regulates the severing activity by cofilin, depending on the nucleotide status of actin; it recognizes the conformational difference between ADP-F-actin and ATP-F-actin (or ADP-P-F-actin), and increases the severing of ADP-F-actin by cofilin, but protects ATP-F-actin (or ADP-P-F-actin) (Gandhi et al., 2009; Ge et al., 2014; Mikati et al., 2015).

Twinfilin and CAP, Twf1 and Srv2 in yeast, also greatly increase the disassembly of F-actin (Goode et al., 2015). Twinfilin was found as a protein with two ADFH domains and a linker between them (Goode et al., 1998). With its ADFH domains, twinfilin binds to both G-actin and F-actin. With these dual binding ability, twinfilin has been shown to sequester actin monomers to suppress actin assembly; cap barbed ends and compete with capping proteins; and stimulates disassembly of F-actin with Srv2/CAP (Goode et al., 1998; Helfer et al., 2006; Johnston et al., 2015; Ojala et al., 2002; Paavilainen et al., 2007; Paavilainen et al., 2008). The *in vivo* significance of capping activity of Twf1 is unclear, but it is worth noting that localization of Twf1 is dependent on Cap1/Cap2, and both the capping activity by Cap1/Cap2 and monomer sequestering activity of Twf1 are negatively regulated by $PI(4,5)_2P$ (Falck et al., 2004; Palmgren et al., 2001). Srv2/CAP was found as a protein associated with adenyl cyclase, which converts ATP to cAMP, in budding yeast (Field et al., 1990). Since its discovery, CAP has been found in other organisms, including mammals, but the eponymic interaction with adenyl cyclase has only been found in yeasts (Hubberstey and Mottillo, 2002). Srv2/CAP has been reported to have several functions in actin dynamics, such as binding to actin monomers, especially ADP-G-actin; increasing severing by cofilin on its own or in conjunction with Aip1 and profilin; and accelerating dissociation of monomers from both ends with twinfilin (Balcer et al., 2003; Chaudhry et al., 2013; Johnston et al., 2015; Mattila et al., 2004; Normoyle and Brieher, 2012).

This complex actin regulation is crucial for efficient endocytosis: losing some components of this regulation causes endocytic defects–slowed down uptake of cargo with abnormal actin morphology. Interestingly, this even includes the loss of proteins that inhibit actin assembly, such

as *cap1*Δ. This suggests that not only is actin assembly itself important, but also the coordination of actin assembly and actin turnover (Goode et al., 2015; Lu et al., 2016).

Overview of presented work

As described in *Actin cables: tracks for myosin V-mediated transport*, *tpm1*Δ cells grow poorly because of their lack of functional cables (Liu and Bretscher, 1992; Liu and Bretscher, 1989a). This phenotype has led to several fruitful discoveries about how actin cables are built, stabilized, and utilized for polarization and growth (Pruyne et al., 1998). In 2011, Dr. Jolanda van Leeuwen and Dr. Charlie Boone in University of Toronto found that a spontaneous loss of function mutation in Altered Inheritance rate of Mitochondria 21 gene (*AIM21*) rescues the growth defect of *tpm1*Δ cells, from their high-throughput suppressor screen, while *aim21*Δ cells do not have any growth phenotype; the results from this screen, including *aim21*Δ rescuing *tpm1*Δ, was later published in 2016 (van Leeuwen et al., 2016). Dr. Charlie Boone informed us about this finding and I started this journey of figuring out how *aim21*Δ rescues the growth defect of *tpm1*Δ cells.

In 2011, when I started working on Aim21, little was known about this protein, especially regarding its function. It was recovered from two different screens; first, as one of the genes whose deletion causes defects in mitochondrial inheritance, and, second, as one of the genes whose deletion causes defects in Snc1 endocytosis. However, how it caused those defects was not discussed (Burston et al., 2009; Hess et al., 2009). It is conserved in yeasts, but no homologues were known at that time, and Aim21 itself does not seem to have any known domains, at least from its sequence. Aim21 has four polyproline regions that are all predicted to bind to SH3 domains, and Abp1 has been predicted to be one of its binding partners (Fazi et al., 2002; Tonikian

et al., 2009). Its localization to actin patches was known, but neither the mechanism of this localization nor what functions it performs at patches was known–it was suggested to be a part of a regulatory module of the Arp2/3 complex activity (Tonikian et al., 2009).

My initial studies on how *aim21*Δ rescues the growth defect of *tpm1*Δ cells showed that *aim21*Δ not only rescues the growth defect of *tpm1*Δ cells, but also restores actin cables to *tpm1*Δ cells, while *aim21*Δ cells have less cables than wild type cells. This apparent paradox asked for further investigation of the cellular function of Aim21, and this led me to the finding that Aim21 is a new inhibitor of F-actin barbed end assembly at patches and this activity is necessary to balance actin assembly between cortical patches and cables. More specially, (1) Aim21 is recruited to the membrane-proximal region of actin patches by Bbc1 and Abp1, both of which are SH3 domain containing proteins and regulate actin at patches on their own. (2) It recruits and forms a complex with Tda2, a recently discovered dynein light chain structural homologue (Farrell et al., 2017), and together they inhibit actin assembly at barbed ends. (3) By inhibiting actin assembly at patches, Aim21 plays a significant role in maintaining the free actin pool, and *aim21*Δ rescues the growth defect of *tpm1*Δ cells by reducing the level of free actin and inhibiting actin cable assembly by Bni1. (4) I also found that Aim21/Tda2 physically interacts with, and possibly modulates, the capping activity of Cap1/Cap2, revealing a complex interplay between actin regulators. This project has given meaningful insights and advances in our understanding of how actin is regulated to achieve best functional efficiency and ensure balance among different actin structures. These results have been written into a manuscript titled "Yeast Aim21/Tda2 both regulates free actin by reducing barbed end assembly and forms a complex with Cap1/2 to balance actin assembly between patches and cables", which is co-authored by Dr. Jolanda van Leeuwen, Dr. Charlie

Boone, and Dr. Anthony Bretscher. This manuscript has been submitted to MBoC at the time of submitting this dissertation and some parts of this dissertation are adapted from it.

CHAPTER 2. AIM21/TDA2 IS A NEW ACTIN ASSEMBLY INHIBITOR AT BARBED ENDS

***aim21*Δ rescues the growth defect of *tpm1*Δ cells**

Initial observation: spontaneous suppressor mutation for the growth defect of tpm1Δ cells lies in AIM21

As described in Chapter 1. Introduction, I was informed by Dr. Jolanda van Leeuwen and Dr. Charlie Boone that *aim21*Δ rescues the growth defect of *tpm1*Δ cells. More specifically, they noticed that their *tpm1*Δ cells grew well, which was inconsistent with the previous literature descriptions. They found that, in those cells, *AIM21* was mutated at position 427 of the coding sequence from A to T, causing K143 (AAA) to become a premature stop codon (TAA). Additionally, they found the deletion of the whole gene, *aim21*Δ, also rescues the growth defect of *tpm1*Δ cells (personal communication in 2011, and published in 2016) (van Leeuwen et al., 2016).

Characterizing the growth of tpm1Δ cells and their rich-medium sensitivity

To verify this result, I remade *aim21*Δ, *tpm1*Δ, *aim21*Δ *tpm1*Δ cells, from wild type, BY4742. However, I got inconsistent results with the growth of *tpm1*Δ cells. Some of the colonies grew better than others, and some colonies displayed differently sized colonies when streaked, while others displayed more similarly sized colonies (data not shown). This varying growth phenotype can also be seen in the published literature. Liu and Bretscher (1992) showed that their *tpm1*Δ cells grew at almost half the rate of WT and were temperature-sensitive at 37°C, though not a tight temperature sensitivity. However, Adams et al. (1993) showed that their *tpm1*Δ cells

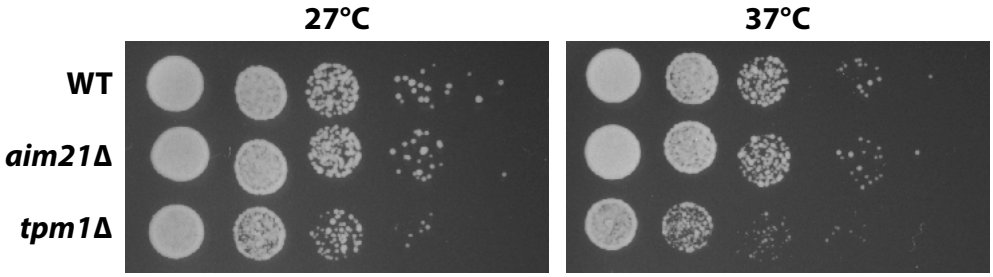

Figure 2.1. Good growth of the existing *tpm1*Δ strain. Cells with the indicated genotypes were grown to OD600=0.2, subjected to 1:10 dilutions on YPD plates, and incubated at 27°C or 37°C for 1-1.5 day.

had only modest growth defects, compared to WT. Okada et al. (2006) showed that the growth defect of their *tpm1*Δ cells was marginal at 25°C, but close to lethal at 37°C. *tpm1*Δ strain I had at that time was from the deletion consortium that was purchased from Invitrogen, and they grew almost as well as WT at low temperature, and displayed growth defects at high temperatures, such as 37°C, which is at odds with the previous literature (Figure 2.1). I also had *tpm1*Δ cells from Dr. Charlie Boone and these cells exhibited strong growth defects. However, these cells quickly picked up suppressor mutations, resulting in inconsistent results. I decided to make *tpm1*Δ cells freshly, from WT, with different methods, in the hope that one method might result in more consistent results than others. However, the heterogeneity and spontaneous suppressor mutation problem persisted regardless of what genetic modification method was used (data not known). Because of this inconsistency among the results from literature and the results I got, it was hard to determine what the correct phenotypes of *tpm1*Δ cells are.

When I was making *tpm1*Δ cells in several different ways, I noticed that *tpm1*Δ cells grow differently between on YPD plates and synthetic media plates; *tpm1*Δ cells grew very poorly and yielded colonies with vastly different sizes on YPD plates, but grew better and yielded more similarly sized colonies on synthetic media plates (Figure 2.2 A, as an example). This YPD specific growth defect has been found and characterized in the mutants that are defective in nutrient signaling and its subsequent transcription regulation (Hinnebusch, 1988). It is believed to be caused by defects in releasing the overall transcription repression of amino acid synthesis involved genes that is induced by excessive amount of certain amino acids in YPD. This prompted the name "rich-medium sensitivity" (Hinnebusch, 1988). However, when the same phenotypes were also reported for mutants that are defective in actin regulation or actin-related processes, the

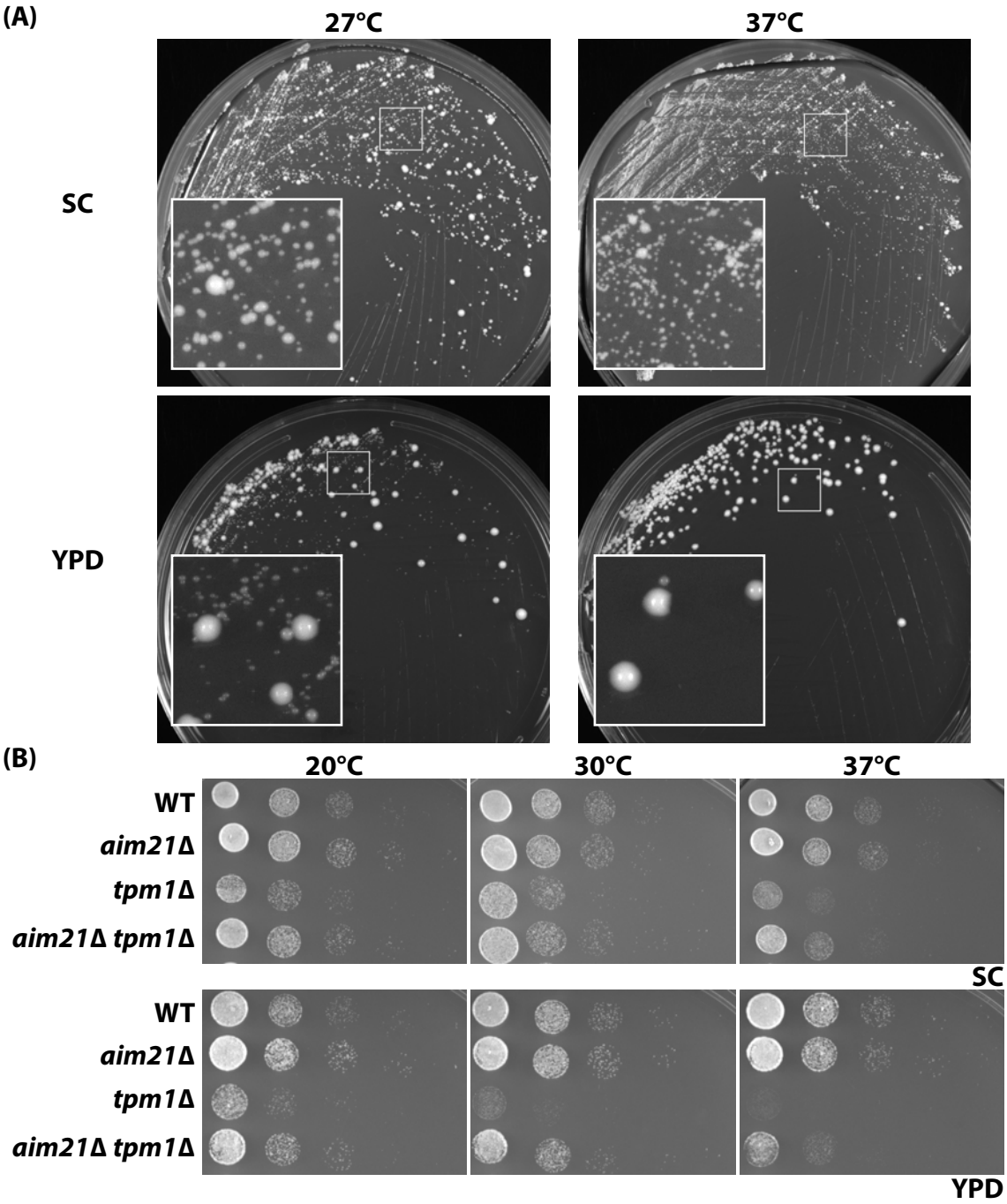

Figure 2.2. *tpm1*Δ cells have rich-medium sensitivity and *aim21*Δ rescues the growth defect of *tpm1*Δ cells. (A) An equal volume of *tpm1*Δ liquid culture was streaked on YPD or SC plates and incubated at 27°C or 30°C for 2-3 days. The boxed images indicate zoomed-in portion of plates. There was some variability in colony sizes even on SC plates, but this was exaggerated on YPD plates. (B) Cells with the indicated genotypes were grown to OD600=0.2, subjected to 1:10 dilutions on YPD or SC plates, and incubated at 20°, 30°C, or 37°C for 1-2 days.

mechanistic explanation was not provided. Field et al. (1990) showed that *srv2*Δ cells cannot grow well on YPD, while they can on synthetic media plate. Gerst et al. (1991), by adding the components of YPD to synthetic media and measuring the growth rate, found that the high concentration of valine and alanine in YPD was the cause of the rich-medium sensitivity of *srv2*Δ cells. However, the authors also showed that this lethality could not be rescued by activating the transcription of amino acid synthesis involved genes, suggesting that their sensitivities are rooted in other causes, which they could not specify. Protopopov et al. (1993) and Haarer et al. (1996) also found this rich-medium sensitivity in their *snc1*Δ *snc2*Δ cells and *sec3* mutants cells (respectively), both of which display secretion defects (Schott et al., 1999). Like Gerst et al. (1991), Haarer et al. (1996) found that peptone in YPED was the cause of the growth difference from synthetic media, but this time they found that the high levels of amino acids, including valine, in peptone were not the cause of the rich-medium sensitivity; it was still unclear why adding peptone would cause the growth retardation in *sec3* mutants. Interestingly, several mutants of *MYO2*, whose phenotype resembles that of *tpm1*Δ—decreased polarized transport to the bud, also displayed the rich-medium sensitivity, though the reason was unresolved in this case as well (Schott et al., 1999).

Regardless, I could show that *tpm1*Δ cells have the rich-medium sensitivity as well (Figure 2.2, as an example). Thus, I decided to remake *tpm1*Δ strains only using synthetic media throughout the process to avoid potential suppressor mutations, repeat several times to obtain multiple *tpm1*Δ strains, and compare their growth phenotypes. When I compared their growth, they showed consistent growth phenotypes, suggesting that the growth phenotype I got was correct and the new *tpm1*Δ strains did not pick up suppressor mutations on synthetic media (representative

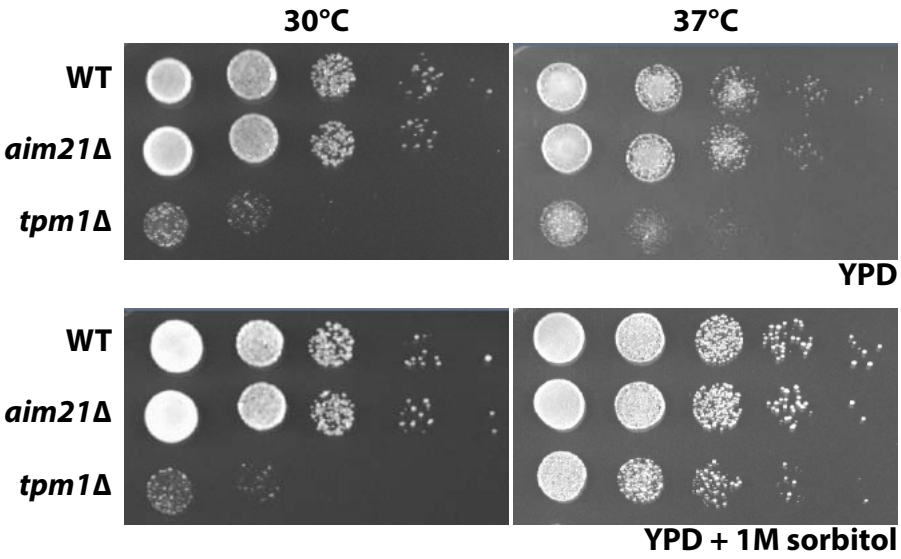

Figure 2.3. *tpm1*Δ cells grow better at 37°C on YPD plates when supplemented with 1M sorbitol. Cells with the indicated genotypes were grown to OD600=0.2, subjected to 1:10 dilutions on YPD or YPD + 1M sorbitol plates, and incubated at 30°C, or 37°C for 1-2 days.

growth phenotype of *tpm1*Δ cells is shown in Figure 2.2 B). Also, I could show that newly made *tpm1*Δ cells grew very poorly on YPD, but relatively well on synthetic media plates (Figure 2.2 B). *tpm1*Δ cells showed some degree of temperature sensitivity as well; they grew even more poorly at 37°C, while growing the best at 20°C (Figure 2.2 B). There are two things should be noted: (1) When I streaked *tpm1*Δ on YPD plates, they showed differently sized colonies, but the frequency of bigger colonies was too high to be caused by spontaneous suppressor mutations. (2) *tpm1*Δ cells grew almost as well as WT cells when grown on YPD plates supplemented with 1M sorbitol at 37°C (Figure 2.3). While it is possible that 1M sorbitol mitigates the growth defect of *tpm1*Δ cells by shrinking the cells and allowing the short actin cables to transport more cargos, why it only happens at 37°C is still unclear. Both phenotypes will be discussed more in Chapter 3. Discussion and Future Directions**.**

Although the reason was indeterminate, *tpm1*Δ cells displayed rich-medium sensitivity, so when I made, grew, and maintained *tpm1*Δ cells, I used synthetic media and grew them at 20°C to minimize spontaneous suppressor mutations and obtain better growth. For experiments, unless noted otherwise, I grew *tpm1*Δ cells in synthetic media, changed the media to YPD, and grew them for at least two cell cycles, in order to show the stronger phenotypes of *tpm1*Δ cells in YPD. Also, when multiple genetic modifications needed to be done, *tpm1*Δ was introduced last, to avoid any possible suppressor mutations for *tpm1*Δ in the course of subsequent genetic modifications.

Verifying that aim21Δ rescues the growth defect of tpm1Δ cells

With the correctly made *tpm1*Δ strains, I tested if *aim21*Δ could rescue the growth defect of *tpm1*Δ cells. I found *aim21*Δ *tpm1*Δ cells grew much better than *tpm1*Δ cells, while *aim21*Δ

cells grew as well as WT cells (Figure 2.2). *aim21*Δ also seemed to rescue the rich-medium sensitivity of *tpm1*Δ cells, which made the rescue more prominent on YPD plates than on synthetic media plates, though the rescue could still be seen on synthetic media plates (Figure 2.2).

aim21Δ rescues the growth defect of tpm1Δ cells by bringing back cables

Because *tpm1*Δ cells are known to have defects in actin morphology and Aim21 is an actin patch protein, I decided to look at the actin structures of *aim21*Δ, *tpm1*Δ, and *aim21*Δ *tpm1*Δ cells, and compare them to those of WT. In initial studies using fluorophore-conjugated phalloidin, both *tpm1*Δ cells and *aim21*Δ *tpm1*Δ cells showed no actin cables. Because actin cables are essential for growth and *tpm1*Δ cells can still grow, albeit slowly, I supposed that *tpm1*Δ cells should retain some cables and suspected that this lack of visible cables in *tpm1*Δ cells was due to loss of unstable cables during the staining process and their low signal (Pruyne et al., 1998). Based on the phalloidin actin staining protocol provided by Pringle et al. (1989), I made several modifications to preserve cables better and improve the signal from cables, which is discussed in detail in Appendix 1. Materials and Methods.

With the improved actin staining, I could see that *tpm1*Δ cells indeed had few short cables, *aim21*Δ cells had less cables than WT cells, and, surprisingly, *aim21*Δ brought back some cables to *tpm1*Δ cells (Figure 2.4). While this explained the rescue of the growth defect of *tpm1*Δ cells, how *aim21*Δ restores cables to *tpm1*Δ cells was not clear. To understand this, I set out to investigate the function of Aim21. The mechanism of this rescue will be discussed in ***aim21*Δ reduces actin assembly by Bni1 to suppress the growth defect imposed by *tpm1*Δ.**

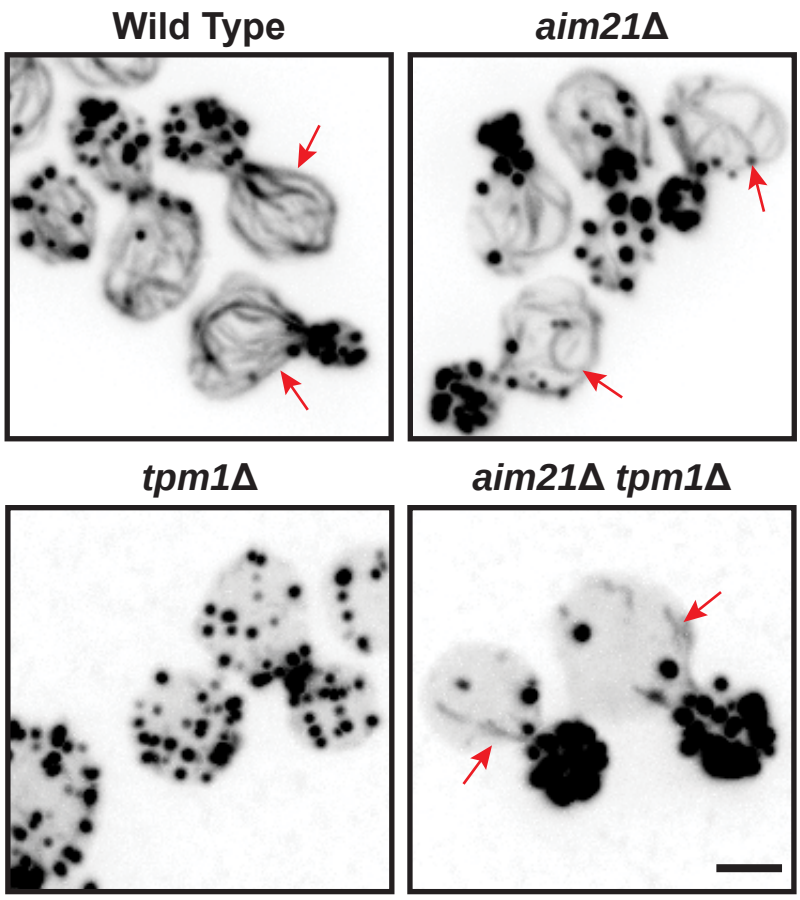

Figure 2.4. *aim21*Δ restores actin cables to *tpm1*Δ cells. Actin structures as visualized by Alexa Fluor 568-phalloidin. Inverted images of maximum projection of whole cells. Red arrows indicate actin cables. Bar 2μm.

Localization of Aim21

Aim21 is an actin patch protein

After verifying the rescue phenotype, I wanted to confirm the localization of Aim21 to patches. To do so, I decided to tag the endogenous copy of *AIM21* with fluorescent proteins using homologous recombination, as described by Longtine et al. (1998), which I will call the Longtine method throughout this dissertation. Because I had limited combinations of selectable markers and fluorescent proteins, I generated an array of plasmid constructs to use throughout this project, which is discussed in Appendix 1. Materials and Methods in more detail.

When I successfully tagged endogenous *AIM21* with mNeonGreen and *ABP1*, an actin patch marker, with mCherry, I could verify their co-localization to patches, consistent with previous finding (Figure 2.5 A) (Tonikian et al., 2009). Interestingly, this localization was not perfect; while all Aim21-mNeonGreen patches co-localized with Abp1-mCherry patches, there were some Abp1-mCherry patches without Aim21-mNeonGreen signal. Because actin patches are transient structures and their composition varies throughout their lifespan, I took movies of the localizations of both proteins and found that Aim21-mNeonGreeen and Abp1-mCherry appear at the same time, but Aim21-mNeonGreen disappears when the Abp1-mCherry patch starts moving inward, leaving Abp1-mCherry patches alone about 2 seconds before its disappearance (Figure 2.5 B). Because the inward movement of Abp1-mCherry in WT usually signifies the formation of an endocytic vesicle, this timing relationship between Aim21-mNeonGreen and Abp1-mCherry suggests that Aim21 leaves before, or soon after, endocytic scission, and does not associate with the endocytic vesicle (Kaksonen et al., 2003).

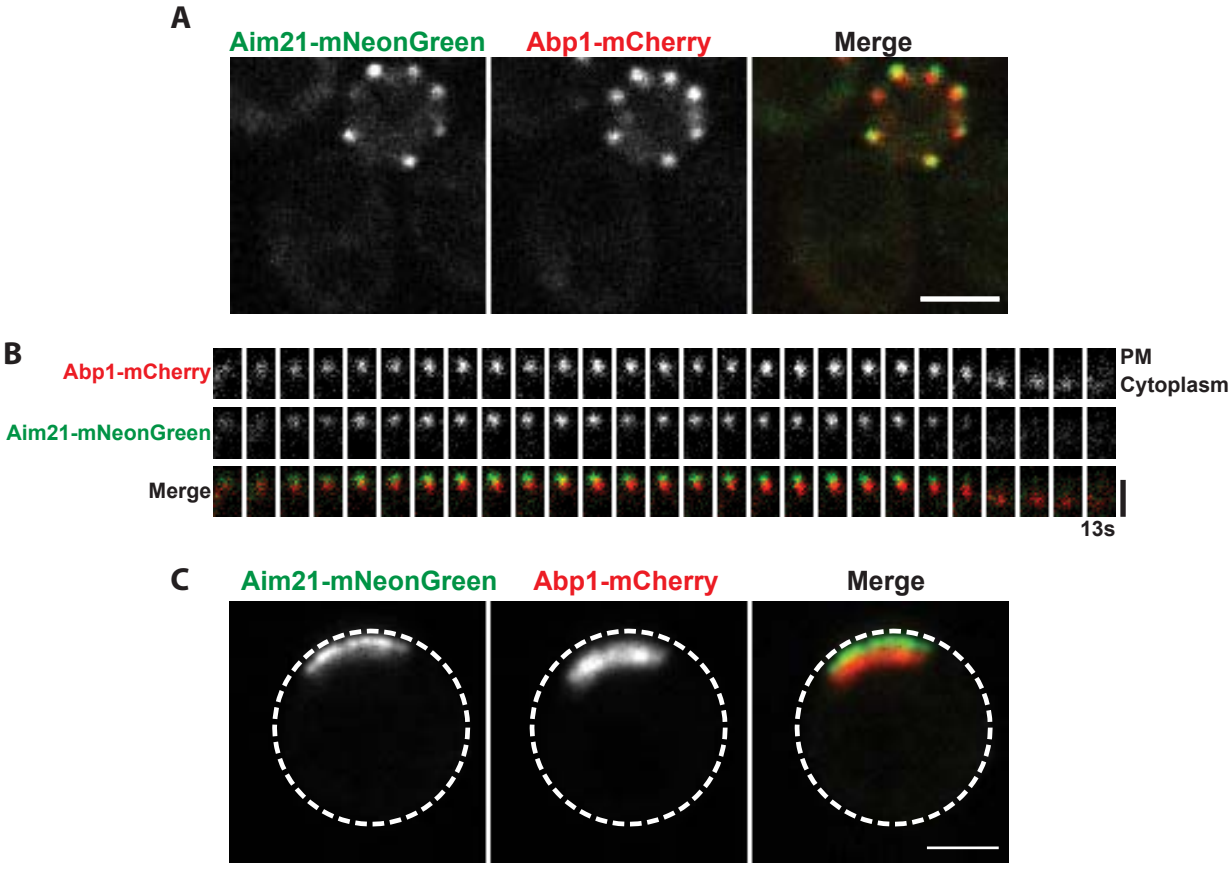

Figure 2.5. Aim21 localizes to actin cortical patches. (A) Aim21-mNeonGreen co-localizes with Abp1-mCherry, an actin patch marker. Bar 2µm. (B) Single frame images of a cortical patch showing the duration of Abp1-mCherry and Aim21-mNeonGreen. Bar 1µm. (C) Localization of Aim21-mNeonGreen and Abp1-mCherry in *sla2*Δ cells. Bar 2µm.

Aim21 localizes to the membrane-proximal region of actin patches

A careful examination of the localization of Aim21-mNeonGreen with respect to Abp1-mCherry showed that Aim21 localizes more closely to the plasma membrane than Abp1-mCherry. This prompted me to look at the localization of Aim21 in *sla2*Δ cells to find its sub-localization at actin patches. Sla2 is an adapter protein that binds to both F-actin and membrane, linking two and transferring the force generated by actin assembly to the plasma membrane (Avinoam et al., 2015; Skruzny et al., 2012; Skruzny et al., 2015). Without Sla2, actin assembly becomes uncoupled from the PM and, as a result, F-actin is continuously assembled adjacent to the plasma membrane and then moves inwards, thus showing actin tails reflecting a linear readout of this dynamic process and making possible differentiating sub-localizations during the process (Kaksonen et al., 2003; Kaksonen et al., 2005; Michelot et al., 2013; Okreglak and Drubin, 2007; Okreglak and Drubin, 2010). I imaged Aim21-mNeonGreen and Abp1-mCherry in *sla2*Δ cells and it revealed a tight localization of Aim21 close to the membrane-proximal region of the tails, similar to the localization seen for Sla1, Las17, and Pan1, and not with the older actin filaments in the Abp1-mCherry tail (Figure 2.5 C) (Kaksonen et al., 2003).

The localization of Aim21 to cortical patches is dependent on Bbc1, Abp1, and Tda2

Once I determined that Aim21 localizes to the membrane-proximal region of actin patches, then I wanted to know how Aim21 is localized there. From its lack of known actin binding motif or domains, I speculated that Aim21 needs to be recruited to patches by other actin patch proteins. To test that, I deleted 20 known cortical patch proteins each individually in cells with

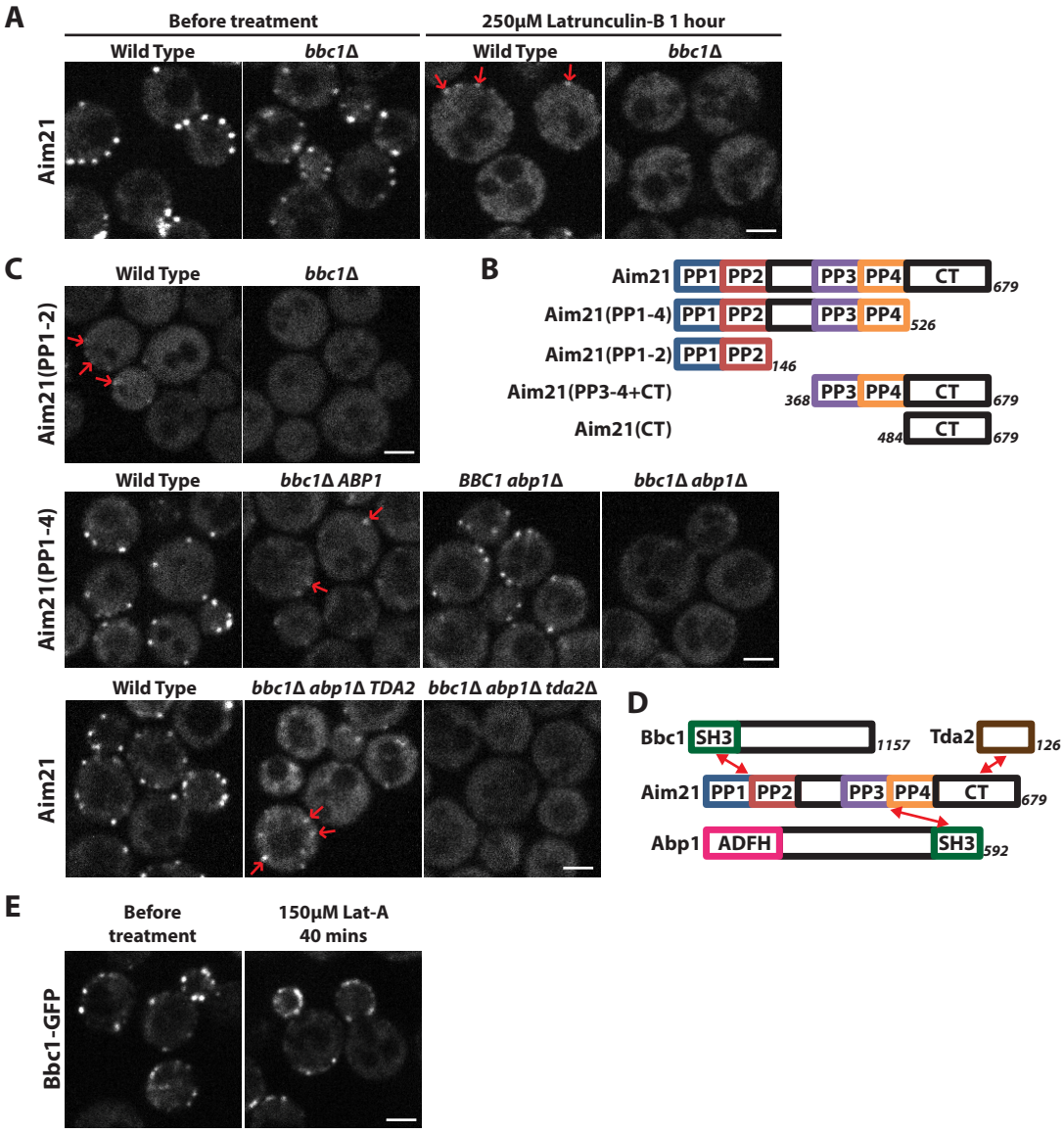

Figure 2.6. Localization of Aim21 to actin patches is dependent on Bbc1, Abp1, and Tda2. (A) Localization of Aim21-mNeonGreen before and after 1-hour treatment with 250µM latrunculin-B (lat-B). Red arrows indicate localization to actin patches. (B) Schematic showing Aim21 protein structure and truncations used. Not to scale. (C) Aim21(PP1-2)-GFP, Aim21(PP1-4)-GFP, and Aim21-GFP in wild type, *bbc1*Δ, *bbc1*Δ *abp1*Δ, and *bbc1*Δ *abp1*Δ *tda2*Δ cells. Red arrows indicate localization to actin patches. (D) Schematic showing the interactions that contribute to the localization of Aim21 to patches. ADFH, Actin Depolymerizing Factor Homology domain. (E) Bbc1-GFP in WT cells before and after 40-minutes treatment of 150µM lat-A. (A, C, E) All bars 2µm.

chromosomally tagged Aim21-GFP, but none completely eliminated cortical patch localization of Aim21-GFP. I reasoned that several proteins might contribute to Aim21 localization.

Then, in order to narrow down the number of candidate proteins that may recruit Aim21, I tested if the localization of Aim21 depended on F-actin. Cells treated with latrunculin, a toxin that sequesters monomeric actin to disassemble all F-actin, resulted in loss of much, but not all, cortical patch localization of Aim21-mNeonGreen (Figure 2.6 A). Thus, there appeared to be both actin-associated and actin-independent mechanisms of localization. Aim21 is a 679-residue protein with four polyproline regions (PP1-PP4), and a ~150 residue C-terminal (CT) domain (Figure 2.6 B). All four of these polyproline sequences are predicted to associate with SH3 domains, and it has been suggested that Aim21 binds the SH3 domains of Bbc1 and Abp1 (Fazi et al., 2002; Tonikian et al., 2009). I therefore generated GFP-tagged chromosomal constructs of Aim21 lacking various domains and assessed their localizations. Out of many constructs, Aim21(PP1-2)-GFP was the minimal region that could localize to cortical patches, and this localization was abolished in *bbc1*Δ cells (Figure 2.6 C, upper panel). Loss of Bbc1 also caused complete delocalization of Aim21 in latruculin treated cells (Figure 2.6 A). Thus, Bbc1, which localizes to patches independently of actin, is necessary to localize this region of Aim21, most likely by direct interaction, and is responsible for the actin-independent localization of Aim21 (Figure 2.6 E).

Aim21(PP1-4), lacking the CT domain, localized well to cortical patches in wild type and weakly in *bbc1*Δ cells; all localization was abolished in *bbc1*Δ *abp1*Δ cells (Figure 2.6 C, middle panel). Thus, Aim21 requires Abp1 to enhance its localization through PP3-4. Despite the involvement of Bbc1 and Abp1 in localizing Aim21, full-length Aim21-GFP still showed some

localization in *bbc1*Δ *abp1*Δ cells, indicating some localization through the C-terminal domain (Figure 2.6 C, lower panel).

Tda2 is a small protein that high-throughput interaction data suggests interacts with Aim21 (Gavin et al., 2006; Yu et al., 2008). Because Tda2 does not have an SH3 domain, Tda2 was a likely candidate to interact with Aim21(CT). I therefore examined the localization of Aim21-GFP in *bbc1*Δ *abp1*Δ *tda2*Δ cells and found that it was no longer localized (Figure 2.6 C, lower panel). Overall, the data reveals that Aim21 has a complex interaction pattern, being localized by the two SH3-containing proteins Bbc1 and Abp1, with a contribution through the C-terminal domain involving Tda2 (summarized in Figure 2.6 D).

While analyzing the images of Aim21(PP1-4)-GFP, I noticed that Aim21(PP1-4)-GFP patches were bigger and more diffuse in *bbc1*Δ cells, compared to the ones in WT cells, and a similar phenotype could be observed with Aim21-GFP in *bbc1*Δ *abp1*Δ cells (Figure 2.6 C). This prompted me to check if actin patch sub-localization of Aim21 in *sla2*Δ cells is changed by *bbc1*Δ. I found that Aim21-mNeonGreen localized throughout the entire length of elongated actin tails in *bbc1*Δ *sla2*Δ, in contrast to its tight cortical localization in *sla2*Δ (Figure 2.5 and Figure 2.7, upper left panel). Thus, interaction of Aim21(PP1-2) with Bbc1, which itself is tightly associated with the cortex (Figure 2.7, upper right panel) restricts Aim21 to the cortex. Because Bbc1 has an inhibitory function on actin assembly in patches through Las17, this phenotype could be due to the changed actin dynamics in *bbc1*Δ cells (Kaksonen et al., 2005; Rodal et al., 2003). To exclude this possibility, I examined the localization of Aim21(PP3-4+CT) in *BBC1 sla2*Δ cells. Loss of PP1-2 released Aim21 from the cortex, and it was now found in the recently assembled two-thirds of the tail (Figure 2.7, lower left panel), very similar to the localization of capping protein Cap1 (Figure

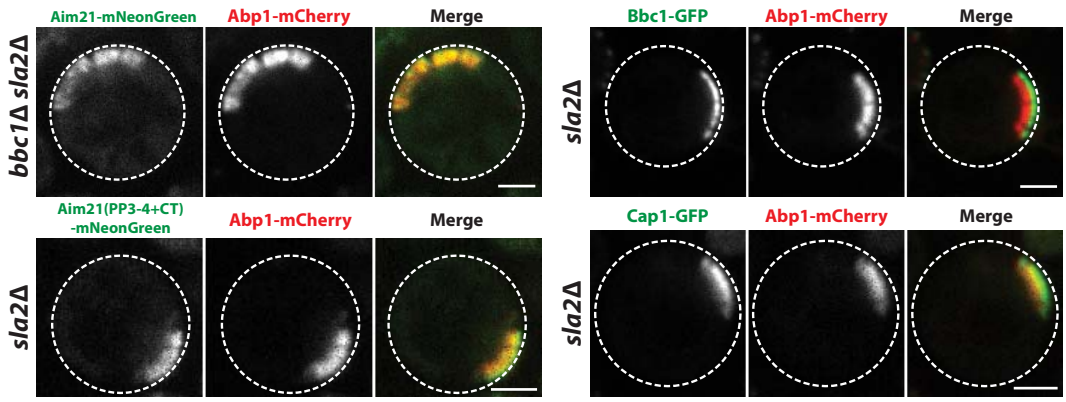

Figure 2.7. Aim21 is localized to the membrane-proximal region through the interaction between Aim21(PP1-2) and Bbc1. Aim21-mNeonGreen in *bbc1*Δ *sla2*Δ cells, Bbc1-GFP in *sla2*Δ cells, Aim21(PP3-4+CT)-mNeonGreen in *sla2*Δ cells, and Cap1-GFP in *sla2*Δ cells. Abp1-mCherry as actin marker. Dotted lines outline the cells. Bar 2μm.

2.7, lower right panel). Thus, I concluded that Bbc1 is critical for localizing and restricting Aim21 to the cell cortex, but interactions requiring Abp1 and Tda2 also play a role.

Then, I decided to measure the number of Aim21 molecules per patch, using Cse4 as a standard; Cse4 is a component of kinetochore and there are 79±14 molecules per kinetochore cluster (Lawrimore et al., 2011). I tagged both Aim21 and Cse4 with GFP in separate cells, and compared their fluorescence intensity to calculate the number of Aim21 per patch. I determined that there are, on average, around 41±4.4 (SEM) Aim21 molecules per patch throughout their lifespan; the actual number of Aim21 molecules at the patch would vary depending on how mature the patch is.

Cellular function of Aim21

Aim21 regulates both the abundance of actin in cortical patches and the level of free actin

After exploring how Aim21 is localized to patches, the next question I asked was what cellular function it performs. I went back to the actin staining images and, in addition to fewer actin cables, I also noticed that *aim21*Δ cells have bigger actin patches. I quantified the amount of F-actin in cortical patches by measuring the phalloidin fluorescence intensity of the patches, and I found it is modestly enhanced in *aim21*Δ cells (Figure 2.8 A). Using Abp1-mNeonGreen as a surrogate for quantifying cortical patch actin in living cells, patches in *aim21*Δ cells had significantly more Abp1 signal than in wild type cells, consistent with results from actin staining, (Figure 2.8 B, C), and the lifespan of patches increased from about 11.9s in wild type cells to 17.3s in *aim21*Δ cells (Figure 2.8 D, E). These phenotypes are reminiscent of cells lacking capping protein Cap1 or Cap2, in which filaments in cortical patches overgrow, resulting in a reduced level

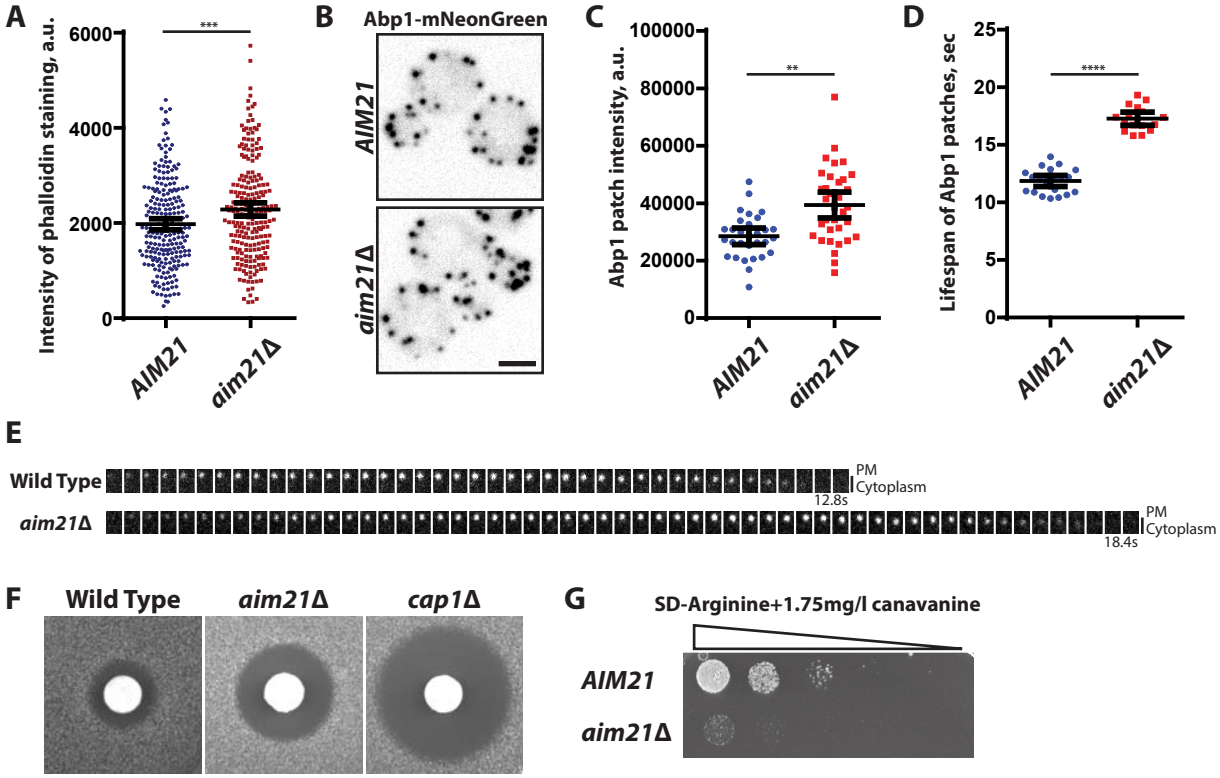

Figure 2.8. Aim21 inhibits actin assembly at actin patches. (A) Quantification of actin patch intensity in wild type and *aim21*Δ cells. Actin structures were visualized by Alexa Fluor 568-phalloidin. Multiple planes, spanning entire cell, were taken and sum projection of the planes was used to calculate the amount of actin per patch. n=231 for wild type and n=216 for *aim21*Δ. p<0.001. (B) Inverted images of Abp1-mNeonGreen in WT and *aim21*Δ cells. Bar 2µm. (C) Relative intensity of Abp1-mNeonGreen patches in WT and *aim21*Δ cells. n=30 for WT and n=34 for *aim21*Δ. p<0.01. (D) Lifespan of Abp1-mNeonGreen in patches. Middle five planes were taken and only patches that stayed in these five planes for their lifetime were included in the calculation. The average lifespan was 11.9±0.23 (SEM) seconds (n=21) for WT and 17.3±0.27 (SEM) seconds (n=16) for *aim21*Δ. p<0.0001. (E) Single frame images of Abp1-mNeonGreen patches in WT and *aim21*Δ cells. Bar 1µm. (F) Latrunculin sensitivity assay of WT, *aim21*Δ, and *cap1*Δ cells. 6mm filter paper disks with 5µl of 0.2mM latrunculin-A (lat-A) were used. (G) Growth assay of the indicated cells spotted on synthetic arginine-deficient media plate with 1.75mg/l of canavanine (SD-Arg+1.75mg/l canavanine). (A, C, D) Bars indicate 95% confidence interval (CI).

of free actin available for assembly (Kaksonen et al., 2005; Michelot et al., 2013). I therefore wished to examine the level of free actin in *aim21*Δ cells compared with *cap1*Δ cells. The level of free actin can be indirectly assessed by testing the sensitivity of cells to growth inhibition by latrunculin: a low level of free actin renders the cells very sensitive to the drug. When a filter paper disk containing 5µl of 0.2mM latrunculin-A was placed on a thin lawn of either wild type, *aim21*Δ, or *cap1*Δ cells, the halo-shaped zone of growth inhibition of *aim21*Δ cells was larger than wild type cells, but smaller than *cap1*Δ cells, suggesting that loss of Aim21 reduces the pool of actin available for assembly (Figure 2.8 F). These results were consistent with the results of Hoepfner et al. (2014) where gene deletion strains were tested for their sensitivities to different chemicals in a high throughput screen. Combined with the reduction in cables seen in *aim21*Δ cells, these results imply that Aim21 negatively regulates actin assembly at patches, and influences the balance of actin between patches and cables at least in part by regulating the level of free actin for assembly.

To further test this hypothesis that Aim21 negatively regulates actin assembly at patches, I decided to check the genetic interactions of *AIM21*. If the hypothesis is correct, *aim21*Δ should rescue mutants that are defective in actin assembly activation at patches, but have synthetic growth defects with the mutants that are defective in actin assembly inhibition at patches. Indeed, *aim21*Δ rescued the growth defect of cells lacking verproline Vrp1, a major NPF at actin patches, but showed synthetic growth defect and more abnormal actin morphology with the deletion of *SLA1*, an actin assembly inhibitor (Donnelly et al., 1993; Geli et al., 2000; Lechler et al., 2001; Rodal et al., 2003; Sun et al., 2006) (Figure 2.9).

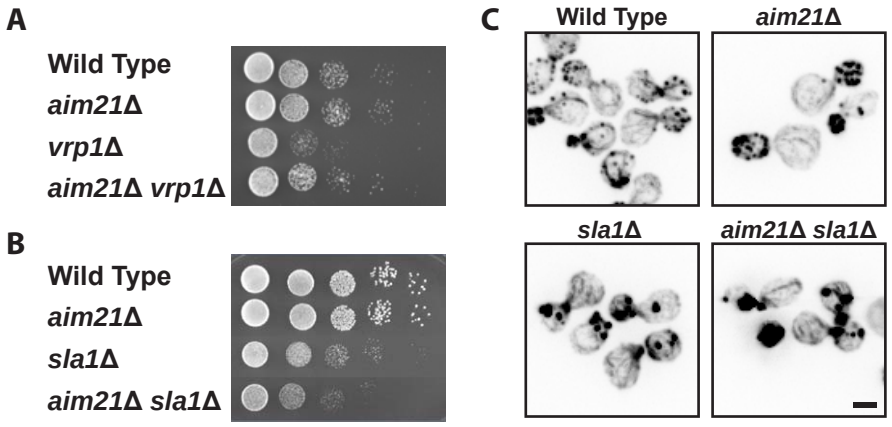

Figure 2.9. *aim21*Δ rescues the growth defect of *vrp1*Δ cells, but makes *sla1*Δ cells grow slower. (A, B) Cells with the indicated genotypes were grown to OD600=0.2, subjected to 1:10 dilutions on YPD plates, and incubated at 20°C (for *vrp1*Δ *aim21*Δ), or 35°C (for *sla1*Δ *aim21*Δ) for 1-2 days. (C) Actin structures as visualized by Alexa Fluor 568-phalloidin. *aim21*Δ *sla1*Δ cells showing more abnormal actin structures than *aim21*Δ and *sla1*Δ cells. Bar 2μm.

Aim21 is necessary for efficient endocytosis

Aim21 has been recovered in two high-throughput functional screens. In the first screen, from which it derives its name (Altered Inheritance of Mitochondria 21), *aim21*Δ cells showed a defect in mitochondrial inheritance, presumably because mitochondrial inheritance requires active transport along actin cables (Hess et al., 2009). In the second screen, *aim21*Δ cells showed a defect in endocytosis of Snc1 (Burston et al., 2009). To verify this endocytic defect, I carried out a simple test of endocytosis is to test cells for their sensitivity to a toxic arginine analogue, canavanine. In the presence of arginine, wild type cells down-regulate the arginine transporter, Can1, from the plasma membrane by endocytosis. Cells compromised for endocytosis cannot do this efficiently and consequently retain more transporter in the plasma membrane, which render the cells more sensitive to growth inhibition by canavanine. Consistent with earlier results, I found that *aim21*Δ cells were indeed more sensitive to canavanine, reflecting a partial defect in endocytosis (Figure 2.8 G). Thus, the altered distribution of actin towards cortical patches influences their function, namely endocytosis.

Two possible mechanisms for the inhibition of actin assembly by Aim21

Although it became clear that Aim21 negatively inhibits actin assembly at patches, how Aim21 does so was not clear. I came up with two possible molecular mechanisms that are not mutually exclusive: (1) Aim21 inhibits the Arp2/3 complex or its NPFs. *e.g.* like Sla1 or Bbc1, or (2) Aim21 inhibits elongation of actin filaments. *e.g.* like Cap1/Cap2 or Abp1/Aim3 (Michelot et al., 2013; Rodal et al., 2003). Interestingly, the results from synthetic genetic array analysis showed that *aim21*Δ cells have the most similar genetic interaction patterns to those of *bbc1*Δ, *cap1*Δ, and

*cap2*Δ, consistent with both hypotheses (Costanzo et al., 2010; Costanzo et al., 2016; Usaj et al., 2017; van Leeuwen et al., 2016).

Physical interactions of Aim21

The C-terminal region of Aim21 is required for its function and this region interacts with Tda2

In order to determine which hypothesis is correct, I decided to investigate which part of Aim21 is needed for its function and what proteins that part interacts with. Since loss of Aim21 restores the growth of *tpm1*Δ cells, this rescue of growth inhibition provided an assay for Aim21 function. While *AIM21* or *AIM21-GFP* cells in combination with *tpm1*Δ grew poorly, *tpm1*Δ *AIM21(PP1-4)-GFP* cells grew well, indicating that the C-terminal domain of Aim21, which I speculated to interact with Tda2 from the *in vivo* localization study of Aim21, is necessary for function (Figure 2.6 C, D and Figure 2.10 A). Now with this information about Aim21(CT), I wanted to verify if Aim21(CT) directly interacts with Tda2 and indeed, *in vitro* data with recombinant proteins showed that 6His-SUMO-Tda2 co-precipitates with full-length Aim21 and Aim21(CT), but not Aim21(PP1-4) (Figure 2.10 B). Thus, Tda2 binds directly to the C-terminal domain of Aim21. Consistent with this data, Tda2 localized to cortical patches in wild type cells, but was delocalized in cells expressing chromosomal Aim21(PP1-4), and re-localized in *aim21*Δ cells in which the CT domain of Aim21 is fused to the cortical patch protein Bbc1 (Figure 2.10 C and Figure 2.11). Thus, the interaction between Aim21(CT) and Tda2 not only contributes to the localization of Aim21 to patches (Figure 2.6 C, D), but also recruits Tda2 to patches. Because Aim21 and Tda2 are present in similar number of molecules per cell, this interaction suggested that Aim21 and Tda2 exist as a complex *in vivo* (Farrell et al., 2017; Kulak et al., 2014).

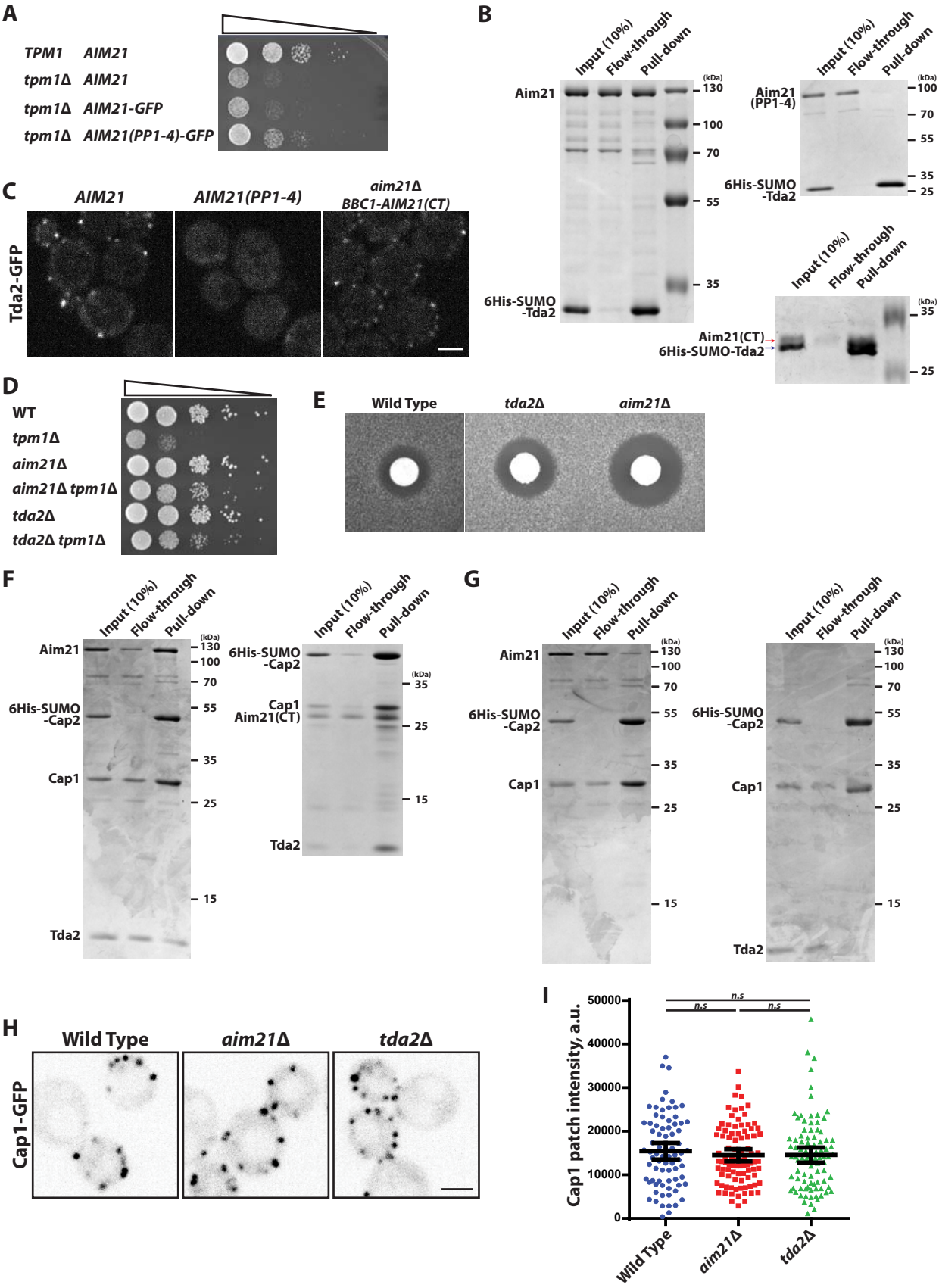
A
TPM1 AIM21
tpm1Δ AIM21
tpm1Δ AIM21-GFP
tpm1Δ AIM21(PP1-4)-GFP
B
Input (10%)
Flow-through
Pull-down
Aim21
6His-SUMO -Tda2
Aim21 (PP1-4)
Aim21(CT)
6His-SUMO-Tda2
(kDa)
130
100
70
55
35
25
C
AIM21
AIM21(PP1-4)
aim21Δ BBC1-AIM21(CT)
Tda2-GFP
D
WT
tpm1Δ
aim21Δ
aim21Δ tpm1Δ
tda2Δ
tda2Δ tpm1Δ
E
Wild Type
tda2Δ
aim21Δ
F
Aim21
6His-SUMO -Cap2
Cap1
Tda2
Cap1 Aim21(CT)
15
G
H
Wild Type
aim21Δ
tda2Δ
Cap1-GFP
I
Cap1 patch intensity, a.u.
50000
40000
30000
20000
10000
0
n.s

Figure 2.10. The C-terminal region (CT) of Aim21 is important for its cellular function and Aim21 interacts with Tda2, Cap1, and Cap2 through this region. (A) Serial dilution assay showing that *AIM21(PP1-4)-GFP* does not inhibit the growth of *tpm1*Δ cells as much as *AIM21*. YPD plate incubated at 30°C for 1 day. (B) Pull-down assay of Aim21, Aim21(PP1-4), or Aim21(CT), by 6His-SUMO-Tda2 using Ni-NTA resin. Red arrow indicates Aim21(CT) and blue arrow indicates 6His-SUMO-Tda2. Aim21 forms a complex with Tda2 through Aim21(CT). (C) Localization of Tda2-GFP in WT, *aim21*Δ, and *aim21*Δ *BBC1-AIM21(CT)*. Bar 2μm. (D) Serial dilution assay that shows *tda2*Δ partially rescues the growth defect of *tpm1*Δ cells. YPD plate incubated at 35.5°C for 1 day. (E) Latrunculin sensitivity assay of *tda2*Δ cells. 6mm filter paper disks with 5μl of 0.2mM lat-A were used. Images of wild type and *aim21*Δ from Fig. 3F are shown for comparison. (F) Pull-down assay of Aim21 or Aim21(CT), Tda2, Cap1, and 6His-SUMO-Cap2, using Ni-NTA resin. Cap1/Cap2 forms a complex with Aim21/Tda2 or Aim21(CT)/Tda2. (G) Pull-down assay of Aim21, Cap1, and 6His-SUMO-Cap2; Tda2, Cap1, and 6His-SUMO-Cap2, using Ni-NTA resin. Cap1/Cap2 can only interact with Aim21 or Tda2 when both are present. (H) Inverted images of Cap1-GFP in WT, *aim21*Δ, and *tda2*Δ cells. Bar 2μm. (I) Brightness of Cap1-GFP patches in WT, *aim21*Δ, and *tda2*Δ cells. n=77 for WT, n=91 for *aim21*Δ, and n=91 for *tda2*Δ. No statistically significant difference among them ($p>0.4$). Bars indicate 95% confidence interval (CI). *n.s.*, not significant. (B, F, G) Note: Aim21, Aim21(PP1-4), and Aim21(CT) all run higher than their calculated molecular weights (74.7kDa, 57.6kDa, and 21.7kDa, respectively).

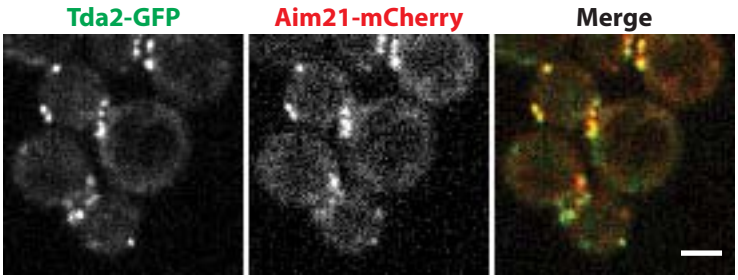

Figure 2.11. Tda2 colocalizes with Aim21. Tda2-GFP colocalizes with Aim21-mCherry in cortical patches. Bar 2µm.

As Aim21(CT) is important for the function of Aim21 and this region recruits Tda2, I explored if Tda2 contributes to Aim21 function. Indeed, *tda2*Δ could partially rescue the growth defect imposed by *tpm1*Δ (Figure 2.10 D) and also reduced the level of free actin in cells as assayed by the latrunculin sensitivity assay (Figure 2.10 E). Neither the rescue of *tpm1*Δ nor the increase in latrunculin sensitivity by *tda2*Δ is as significant as seen for *aim21*Δ, indicating that Aim21 has additional functions to recruiting Tda2.

Aim21, Tda2, Cap1, and Cap2 form a complex

In addition to binding to Tda2, high-throughput screens suggest that Aim21 might interact with the F-actin barbed end capping protein Cap1 and Cap2, which form an obligate heterodimer (Gavin et al., 2006). To explore these relationships, I used *in vitro* pull-down assays to explore possible interactions.

When resin-bound 6His-SUMO-Cap2 was incubated with Cap1, Aim21, and Tda2, all four proteins were recovered, indicating that Cap1/Cap2 binds to Aim21, Tda2, or the Aim21/Tda2 complex (Figure 2.10 F, left panel). In a similar experiment, but employing Aim21(CT) in place of full-length Aim21, a complex of Cap1/Cap2/Tda2/Aim21(CT) formed (Figure 2.10 F, right panel). The complex only formed when all components were present – without Aim21 or Tda2, the complex failed to form (Figure 2.10 G). This interaction was consistent with what I found with Aim21(PP3-4+CT)-GFP in *sla2*Δ cells, where Aim21(PP3-4+CT) localized to the newer two thirds of the extended actin tails.

I next explored if loss of Aim21 or Tda2 had an effect on the localization of Cap1/Cap2. Although actin cortical patches are larger and more persistent in *aim21*Δ cells (Figure 2.8 A, C,

D), Cap1-GFP remained localized to cortical patches and the amount of Cap1-GFP per patch in *aim21*Δ or *tda2*Δ cells did not differ significantly from that of wild type cells, which was at odds with what Farrell et al. (2017) found (Figure 2.10 I, H). Thus, Aim21 and Tda2 are not necessary to recruit Cap1/Cap2 to patches, and the effect Aim21/Tda2 has on patches seems to be largely independent of Cap1/Cap2 recruitment.

Molecular mechanism of actin assembly inhibition by Aim21

Aim21/Tda2 functions to reduce barbed end actin assembly

The fact that Aim21/Tda2 formed a complex with Cap1/Cap2 strongly suggested that Aim21/Tda2 inhibits actin assembly by inhibiting the elongation of filaments, possibly as a positive cofactor for Cap1/Cap2, rather than by inhibiting the Arp2/3 complex or its NFPs.

To explore the potential capping activities of these proteins, I decided to perform *in vitro* actin assembly assays using pyrene-actin; sheared filaments served as actin nuclei, with a level of free actin so that most of elongation should occur at the barbed end of the growing filament. In this assay, assembly was dependent on the addition of the sheared filaments, with inclusion of 200nM Cap1/Cap2 significantly inhibiting assembly (Figure 2.12 A). When I tested 200nM Aim21/Tda2, surprisingly, it too reduced actin assembly, but not as efficiently as Cap1/Cap2 (Figure 2.12 B). Tda2 alone had no effect on actin assembly, whereas Aim21 alone had some activity, but less than the Aim21/Tda2 complex (Figure 2.12 B). These results meant that Aim21 can inhibit actin assembly, independently of Cap1/Cap2, and Tda2 enhances this inhibition. This explained why actin patches are bigger and the level of free actin in *aim21*Δ cells, or *tda2*Δ cells, is lower than in wild type cells.

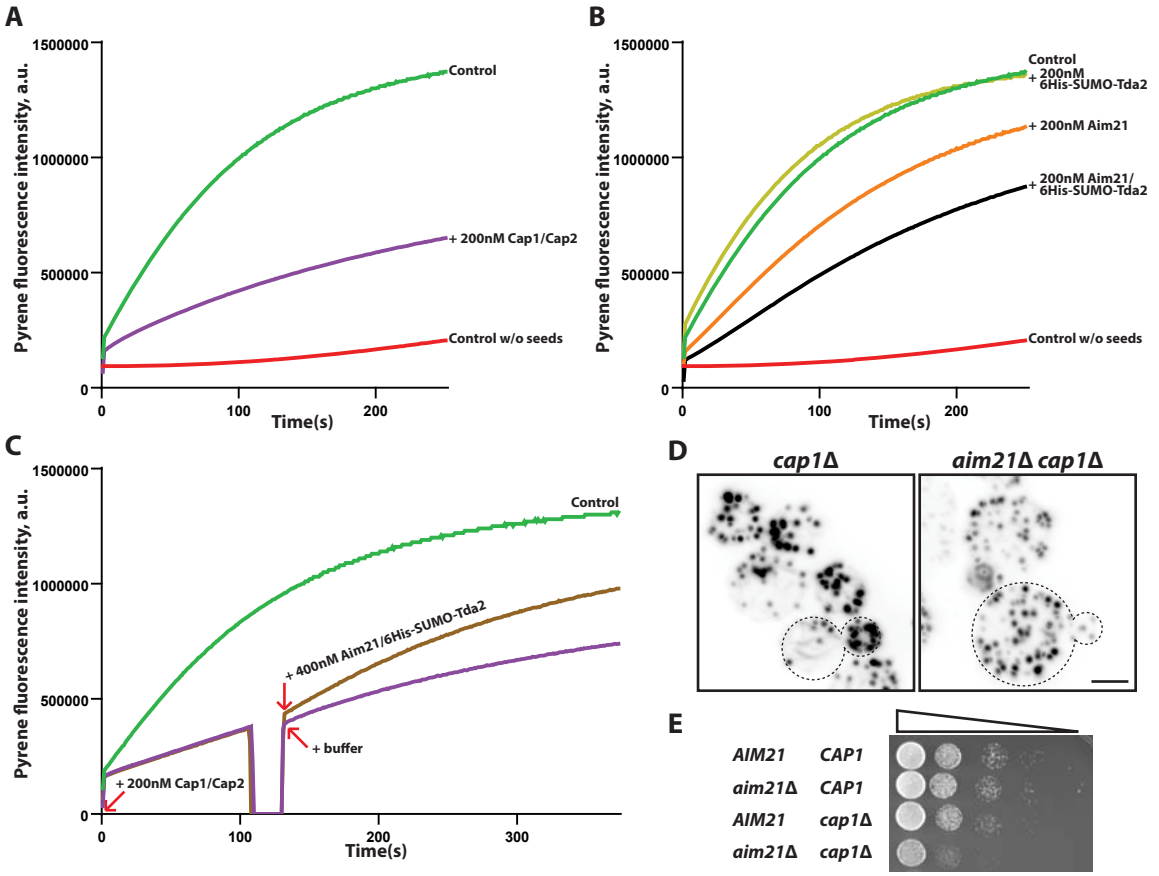

Figure 2.12. Aim21/Tda2 reduces assembly at the barbed end of actin filaments. (A) Pyrene actin assembly assays with 200nM Cap1/Cap2. Cap1/Cap2 caps barbed ends of F-actin seeds and significantly slows down the rate of actin assembly. (B) Pyrene actin assembly assays with 200nM Aim21, or 200nM 6His-SUMO-Tda2, or 200nM Aim21/6His-SUMO-Tda2. Aim21/6His-SUMO-Tda2 also slows down the rate of actin assembly. (C) Pyrene actin assembly assays with both Cap1/Cap2 and Aim21/Tda2. Assembly was initiated in the presence of 200nM Cap1/Cap2 and 120 seconds later either buffer or 400nM Aim21/6His-SUMO-Tda2 added. (D) Inverted images of actin structures in *cap1*Δ and *aim21*Δ *cap1*Δ cells, visualized by Alexa Fluor 568-phalloidin. Maximum projection of the entire cell. Dotted lines outline the cells. Bar 2μm. (E) Serial dilution assay that shows *aim21*Δ and *cap1*Δ have synthetic growth defect. YPD plate incubated at 37°C for 31 hours. (A, B) Representative curves are shown, typical of >3 independent experiments. (A, B, C) Control w/o seeds contains G-actin and 10x F-actin buffer. Control contains G-actin, 10x F-actin buffer, and F-actin seeds. All additions were made at t=0 and the assembly reaction was initiated by the addition of 10x F-actin buffer.

Because Aim21/Tda2 might still modulate the capping activity by Cap1/Cap2 in addition to being an actin assembly inhibitor on its own, I decided to perform more assembly assays to test this possibility. Assembly assays were set up with 200nM Cap1/Cap2, and then 400nM Aim21/Tda2 was subsequently added. After the addition of Aim21/Tda2, actin assembly increased, showing that Aim21/Tda2 reduced the ability of Cap1/Cap2 to inhibit assembly at the barbed ends of actin filaments (Figure 2.12 C). Thus, Aim21/Tda2 has the properties of a barbed end capping protein that can function independently of Cap1/Cap2, and may modulate the activity of, or compete with, Cap1/Cap2.

If Cap1/Cap2 and Aim21/Tda2 work at least partially independently to reduce barbed end assembly, the effect of *aim21*Δ and *cap1*Δ should have an additive effect on actin structures *in vivo*. Indeed, *aim21*Δ *cap1*Δ cells show more abnormal actin structures than either *aim21*Δ or *cap1*Δ alone (Figure 2.12 D), and at 37°C, *aim21*Δ *cap1*Δ cells grow more slowly than either *aim21*Δ or *cap1*Δ alone (Figure 2.12 E). Thus, Cap1/Cap2 and Aim21/Tda2 function, at least in part, independently.

***aim21*Δ favors actin cable assembly by Bnr1 over Bni1 to suppress the growth defect imposed by *tpm1*Δ**

aim21Δ rescues the growth defect of tpm1Δ cells by lowering the level of free actin

By using cell biological and biochemical methods, I could show that Aim21 functions to reduce assembly at the growing ends of actin filaments within patches to elevate the level of free actin available for assembly. However, it was still unclear how *aim21*Δ, which reduces the number

of cables on its own, probably by funneling more actin into patches, rescues the growth defect of *tpm1*Δ cells.

Because Aim21 is an actin patch protein and *tpm1*Δ cells have defects in cables, I speculated that the genetic interaction between *aim21*Δ and *tpm1*Δ is likely to mediated by the free actin pool, which is reduced in *aim21*Δ cells. I hypothesized that *aim21*Δ suppresses the growth defect of *tpm1*Δ cells by lowering the level of available actin, and tested if loss of other proteins that regulate free actin levels could also suppress *tpm1*Δ. Indeed, loss of capping protein Cap1, which reduces free actin levels (Figure 2.8 F), also partially suppressed the growth defect of *tpm1*Δ cells (Figure 2.13 A). This suggests that lowering the level of free actin is a general mechanism for suppressing the growth defect of *tpm1*Δ cells. If correct, *tpm1*Δ cells should grow better in a low level of latrunculin. Indeed, in a latrunculin sensitivity assay, *tpm1*Δ cells displayed a double halo; a region adjacent to the filter paper disk that inhibited growth by the high latrunculin level, surrounded by a region of better growth where the latrunculin level is reduced, with reduced growth on the periphery with too low latrunculin levels (Figure 2.13 B). Thus, *aim21*Δ restores growth to *tpm1*Δ cells by reducing the level of free actin for assembly.

*Lower free actin level reduces actin assembly by Bni1 to suppress the growth defect of tpm1*Δ *cells*

In yeast, tropomyosin is an essential protein as it is required to stabilize actin cables (Liu and Bretscher, 1989a; Liu and Bretscher, 1989b; Pruyne et al., 1998). Yeast has two tropomyosin isoforms: a major one, Tpm1 and, a minor one, Tpm2, that is present at about one sixth the level of Tpm1 (Drees et al., 1995). Thus, in *tpm1*Δ cells, survival is dependent on the low level of Tpm2.

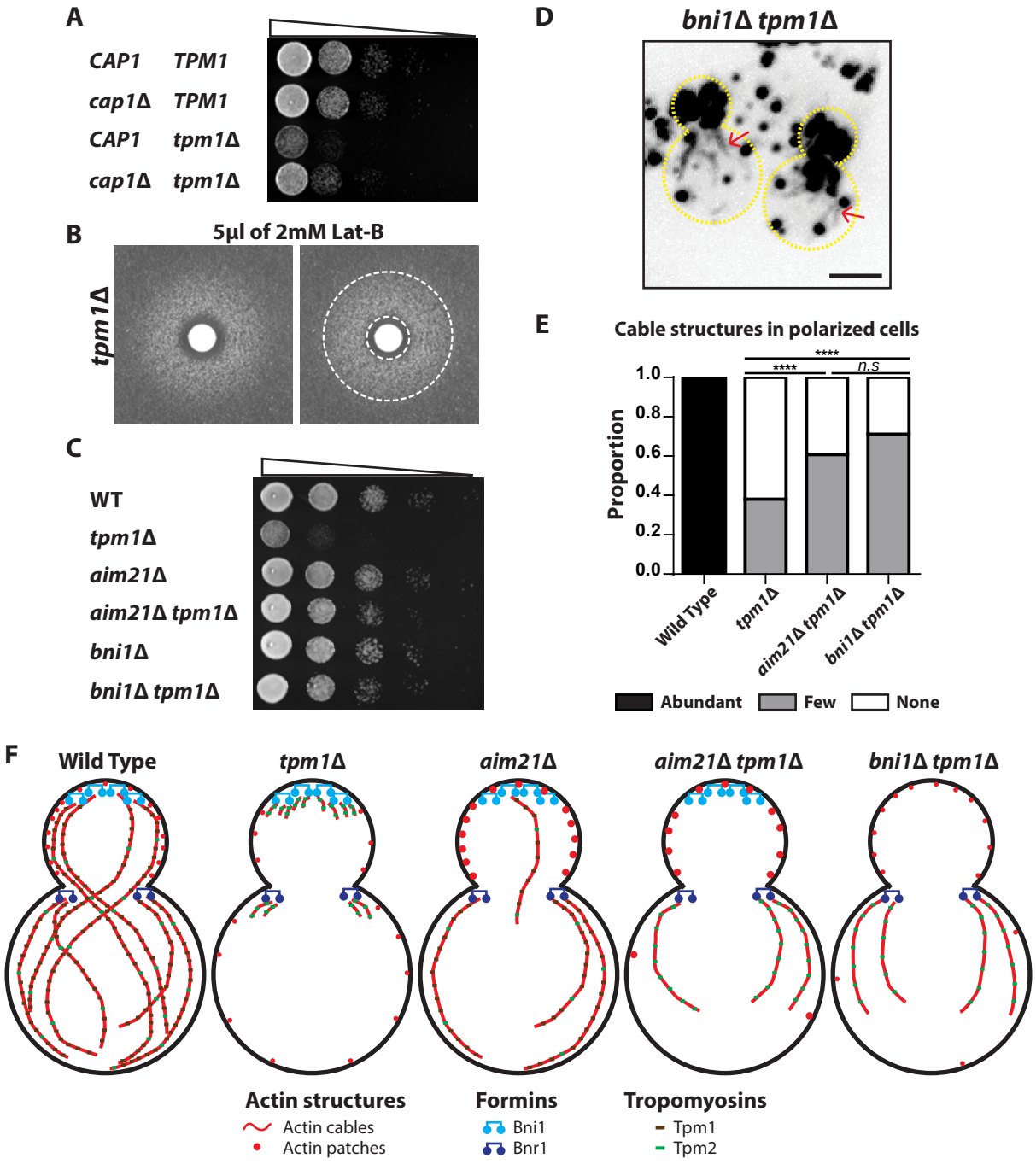

Figure 2.13. Decreasing the number of actin cables being initiated rescues the growth defect of *tpm1*Δ cells. (A) Serial dilution assay that shows *cap1*Δ partially rescues the growth defect of *tpm1*Δ cells. YPD plate incubated at 30°C for 1 day. (B) Latrunculin sensitivity assay on *tpm1*Δ cells. 6mm filter paper disks with 5µl of 2mM lat-B were used. The image on the right is the same as the one on the left, but with dotted lines added to outline two halos. (legend continued on next page)

(C) Serial dilution assay that shows *bni1*Δ rescues the growth defect of *tpm1*Δ cells. YPD plate incubated at 35.5°C for 1 day. (D) Inverted image of actin structures in *bni1*Δ *tpm1*Δ cells, visualized by Alexa Fluor 568-phalloidin. Maximum projection of the entire cell. Dotted lines outline the cells. Red arrows indicate actin cables. (E) Quantification of actin cables in wild type, *tpm1*Δ, *aim21*Δ *tpm1*Δ, and *bni1*Δ *tpm1*Δ cells. Only cells with small- or medium-sized buds were included in the analysis. Abundant is defined as more than 8 actin cables from the bud neck or bud tip. Few is defined as 1-8 actin cables from the bud neck or bud tip. None is defined as no detectable actin cables. n=85 for WT, n=189 for *tpm1*Δ n=125 for *aim21*Δ *tpm1*Δ, and n=194 for *bni1*Δ *tpm1*Δ. ****, $p<0.0001$. *n.s.*, not significant. (F) Model: *aim21*Δ rescues the growth defect of *tpm1*Δ cells by increasing the amount of actin in actin patches, thereby reducing G-actin availability in the cytoplasm, and favoring the generation of fewer, but longer and stabilized actin cables nucleated by Bnr1. Supporting this model, *bni1*Δ also restores growth and cables to *tpm1*Δ cells.

Actin cables are nucleated and elongated by the two formin isoforms, Bni1 in the bud and Bnr1 at the bud neck. In *tpm1*Δ cells, both formin isoforms are active and generate actin cables, but they are very unstable due to the limiting supply of Tpm2, and as a result, *tpm1*Δ cells grow poorly (Liu and Bretscher, 1992; Liu and Bretscher, 1989a). Since polarized actin cables are essential for growth and *aim21*Δ *tpm1*Δ cells grew better than *tpm1*Δ cells, I wanted to know if *aim21*Δ *tpm1*Δ cells have better cables than *tpm1*Δ cells (Pruyne et al., 1998). After quantifying the percentage of WT cells, *tpm1*Δ cells, and *aim21*Δ *tpm1*Δ cells that have cables from phalloidin staining images, I found that indeed more *aim21*Δ *tpm1*Δ cells have cables than *tpm1*Δ cells (Figure 2.13 E). While examining cable structures in those strains, I noticed that in *aim21*Δ *tpm1*Δ cells, the majority of cables emerged from the bud neck, the location of Bnr1. It has been found, at least in vitro, that the FH1-FH2-COOH region of Bnr1 is a much more potent nucleator than the equivalent region of Bni1 (Moseley and Goode, 2005). This immediately suggests a mechanism for suppression: whereas in *tpm1*Δ cells short ineffective cables are assembled by both Bni1 and Bnr1 (Figure 2.13 F, second panel), in *aim21*Δ *tpm1*Δ cells where the level of free actin is low, Bni1 becomes less active and cables are preferentially assembled from the bud neck by Bnr1. This partially restores the balance between the number of tropomyosin molecules and the number of cables generated: more tropomyosin molecules per each actin cable. This allows the limiting Tpm2 to generate longer cables, which in turn permits more effective transport of secretory vesicles for polarized growth (Figure 2.13 F, fourth panel). If this hypothesis is correct, it should also be possible to suppress the growth defect of *tpm1*Δ cells by directing all cable assembly to Bnr1 by deleting *BNI1* (Figure 2.13 F, fifth panel). Indeed, *bni1*Δ *tpm1*Δ cells grow better than *tpm1*Δ cells, and actin cables are restored, like in *aim21*Δ *tpm1*Δ (Figure 2.13 C, D, E). Two things worth noting with this this rescue are (1) that cables in *aim21*Δ *tpm1*Δ cells and *bni1*Δ *tpm1*Δ cells were longer than

the ones in *tpm1*Δ cells, and (2) that in *tpm1*Δ cells, but not in *aim21*Δ *tpm1*Δ or *bni1*Δ *tpm1*Δ cells, there were some cables that were not attached to bud tip or bud neck, suggesting that actin cables in *aim21*Δ *tpm1*Δ and *bni1*Δ *tpm1*Δ cells are oriented better than the ones in *tpm1*Δ cells. These explain the disproportionately dramatic growth rescue, compared to the more modest rescue of cables.

CHAPTER 3. DISCUSSION AND FUTURE DIRECTIONS

Rich-medium sensitivity of tpm1Δ cells

This study originated from the question of how *aim21*Δ rescues the growth defect of *tpm1*Δ. One of the hardships that I encountered during the process of answering this question was the inconsistent growth of *tpm1*Δ strains and the contradictory results about it from the previous literature. After analyzing their growth on different media, I found that *tpm1*Δ cells have rich-medium sensitivity and by growing on synthetic media, I could suppress the generation of spontaneous mutations in *tpm1*Δ cells to obtain consistent results and verify the original phenotype I started with–*aim21*Δ rescues the growth defect of *tpm1*Δ cells.

Although it was not the main topic of this study, this rich-medium sensitivity of *tpm1*Δ cells is an intriguing phenomenon, especially given that *tpm1*Δ cells not only grew slowly on YPD plates, but also displayed differently sized colonies when streaked on YPD plates. Because the rate of bigger colonies on YPD plates was too high and the bigger colonies resulted in different sized colonies when streaked back on YPD plates, it seems that the different sized colonies of *tpm1*Δ cells cannot be explained by mutations. This suggests that *tpm1*Δ cells have some form of heterogeneity in them related to the rich-medium sensitivity, which could be something similar to heterogeneity for bet hedging, as described by Levy et al. (2012). Also, it is still unclear why high temperature worsens the growth defect of *tpm1*Δ on YPD plates, but rescues it when supplemented with 1M sorbitol. This suggests the involvement of the Hog1 pathway and Pkc1 pathway with the growth defect of *tpm1*Δ cells. However, more studies need to be done to test both hypotheses. Identifying the cause of the rich-medium sensitivity of *tpm1*Δ cells would help advance our understanding how nutrients affects polarized growth, as both secretion mutants (*e.g. sec3* and

myo2 mutants) and Ras signaling mutant (*e.g. srv2*Δ) have been shown to display this phenotype (Field et al., 1990; Gerst et al., 1991; Haarer et al., 1996; Schott et al., 1999).

Aim21/Tda2 as a new inhibitor for barbed end actin assembly

Cells lacking Tpm1 are dependent on the minor tropomyosin isoform Tpm2 to stabilize actin cables, giving rise to few detectable cables and consequent slow growth (Liu and Bretscher, 1989a). Cells lacking Aim21 grow well, although they have a reduced number of cables. This study originated from the paradox that *aim21*Δ *tpm1*Δ cells grow better and have more cables than *tpm1*Δ cells. Three lines of investigation initially pointed to a role for Aim21 in restricting actin assembly in cortical patches. First, Aim21 localized to cortical patches and loss of Aim21 enhanced the amount of actin in patches. Second, *aim21*Δ cells, like *cap1*Δ cells, were more sensitive to the monomer-sequestering drug latrunculin, indicating a low level of free actin available for assembly. Third, *aim21*Δ rescues the growth defect caused by loss of actin assembly activator Vrp1, but worsens the actin morphological defect and the slow growth of *sla1*Δ cells, which lack proper inhibition of actin assembly (Donnelly et al., 1993; Geli et al., 2000; Lechler et al., 2001; Rodal et al., 2003; Sun et al., 2006).

I could corroborate this hypothesis, derived from *in vivo* data, by performing *in vitro* pull-down and actin assembly assays with purified recombinant proteins. A series of pull-down experiments revealed that (1) Aim21 physically interacts with Tda2 through its C-terminal region and (2) the Aim21/Tda2 complex can bind to Cap1/Cap2, through an interaction requiring Aim21(CT) and Tda2. The actin assembly assays showed that (1) Aim21 itself could reduce actin assembly at barbed ends of filaments, whereas Tda2 cannot, (2) the Aim21/Tda2 complex is a

better inhibitor than Aim21 alone, but still less potent than Cap1/Cap2, and (3) addition of Aim21/Tda2 decreased the actin assembly inhibition by Cap1/Cap2. Along with the synthetic growth defect and exacerbated actin morphological abnormality of *aim21*Δ *cap1*Δ cells, this suggests that Aim21/Tda2 is not only an inhibitor in its own right, but also a regulator of Cap1/Cap2. The formation of an Aim21/Tda2/Cap1/Cap2 complex is surprising given the different localizations of Aim21/Tda2 and Cap1/Cap2. I will return to this issue in *The potential role of interaction between Aim21/Tda2 and Cap1/Cap2*.

Localization of Aim21 and its implications

By analyzing the localization and functionality of Aim21 truncations *in vivo*, I was able to identify the mechanism for cortical patch localization of Aim21, as well as the region required for its function. This revealed that Bbc1 binding to the N-terminal polyproline regions (PP1-2) of Aim21 is a major determinant in the localization of Aim21. Consistent with this, I showed that both Aim21 and Bbc1 are tightly associated with the membrane-proximal region of the actin tails in *sla2*Δ cells, and Aim21 is redistributed throughout the tail when *BBC1* is deleted. Further, I also identified another region contributing to the localization Aim21 and its interaction partner; the third and fourth polyproline region (PP3-4) of Aim21 interacts with Abp1. By testing the ability of *AIM21* truncations to rescue the growth defect of *tpm1*Δ cells, I identified C-terminal region, Aim21(CT), as necessary for its function and localization of Tda2 to cortical patches. Although Tda2 contributed to the localization of Aim21, especially in *bbc1*Δ *abp1*Δ, it is unlikely Tda2 recruits Aim21 to patches, given Tda2 does not localize to patches without Aim21. How Tda2

contributes to the localization and the function of Aim21 will be discussed later in *The potential role of Tda2 in the Aim21/Tda2 complex*.

The membrane-proximal localization of Aim21 is very distinct from other actin assembly inhibitors. F-actin in cortical patches is nucleated by the Arp2/3 complex, leaving barbed ends available for assembly. In order to prevent excessive assembly and depletion of the free actin pool, cells need to regulate the elongation of filaments on barbed ends, and there were two sets of proteins known to be involved in this process (Michelot et al., 2013; Nadkarni and Brieher, 2014). The first and major factor identified was capping protein Cap1/Cap2, which form an obligate heterodimer. Cap/Cap2 has high affinity for barbed ends and prevents further addition of actin monomers to the barbed ends. Second, Aim3 functions with Abp1 to inhibit actin assembly at barbed ends (Michelot et al., 2013). Here, I add Aim21/Tda2 as a third inhibitor for actin assembly. Interestingly, in *sla2*Δ cells where membrane invagination is uncoupled from actin assembly, all three barbed end actin elongation inhibitors show very different and distinct localizations: membrane-proximal region for Aim21/Tda2 with Bbc1, two thirds of the recently assembled actin tail for Cap1/Cap2, and the entire length of the actin tail for Abp1/Aim3. At least for Aim21, this distinct localization is necessary for full functionality; *AIM21(PP3-4+CT)* is only partially functional as it partially restores the growth defect to *aim21*Δ *tpm1*Δ cells (Figure 2.7 and Figure 3.1). This suggests that the distinct localizations of three inhibitors have functional consequences, which will be discussed more in *The physiological significance of three inhibitors*. Aim21 is conserved in yeast, including *Schizosaccharomyces pombe*, though not clearly present in other eukaryotes. However, the fact that Aim21/Tda2, Cap1/Cap2, and Abp1/Aim3 all have different

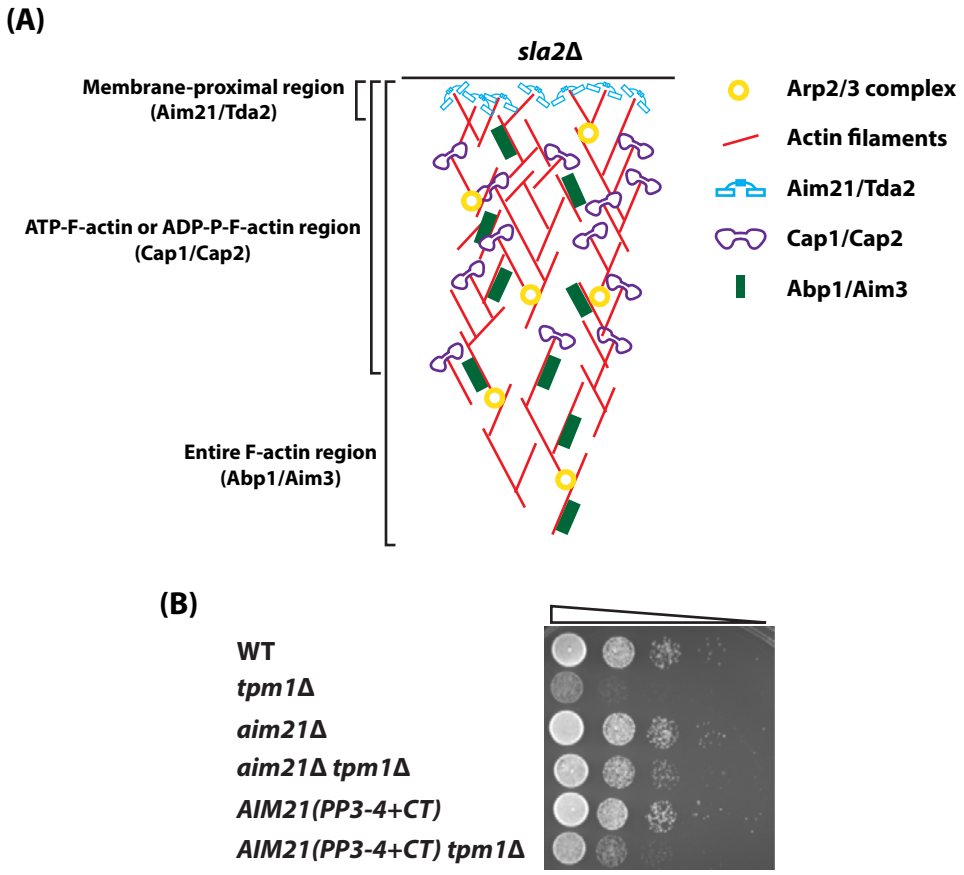

Figure 3.1. All three barbed end actin assembly inhibitors have distinct sub-localizations and the sub-localization of Aim21 is important for it function. (A) Simplified schematic diagram showing distinct sub-localizations of Aim21/Tda2, Cap1/Cap2, and Abp1/Aim3 in *sla2*Δ cells. (B) Serial dilution assay that shows *AIM21(PP3-4+CT)* partially rescues the growth defect of *tpm1*Δ cells. YPD plate incubated at 30°C for 1 day.

localizations raises a possibility that other organisms may also have additional barbed end assembly inhibitors with specific localizations and functions.

Understanding the molecular mechanism of barbed end assembly by Aim21/Tda2

Although I could draw a conclusion that Aim21/Tda2 is a barbed end assembly inhibitor, the molecular mechanism by which Aim21/Tda2 inhibits actin assembly is yet to be discovered. There are two hypotheses: (1) Aim21/Tda2 directly binds to and caps barbed ends and (2) Aim21/Tda2 binds to the sides of filaments and induces a conformational change to inhibit addition of monomers by allosteric effects. To determine which hypothesis is correct, I would propose two experiments: (1) electron microscopy of Aim21/Tda2 with actin filaments to determine whether Aim21/Tda2 localizes to barbed ends or to the sides of filaments, as was done for Aip1 by Okada et al. (2002), and (2) disrupting the interaction between Aim21/Tda2 and Cap1/Cap2, and checking if this causes *aim21*Δ like phenotypes *in vivo* and if Aim21/Tda2 can still decrease the capping activity by Cap1/Cap2. The rationale for this experiment will be discussed in detail in *The potential role of interaction between Aim21/Tda2 and Cap1/Cap2*.

The potential role of Tda2 in the Aim21/Tda2 complex

I showed that Tda2 performs three functions regarding Aim21: (1) improving the localization of Aim21 to patches, (2) increasing the inhibition of barbed end actin assembly by Aim21, and (3) bridging the interaction between Aim21 and Cap1/Cap2 complex. While mechanisms remain unclear, the recent results from Farrell et al. (2017) can give some insights. Farrell et al. (2017) presented convincing evidence that Tda2 dimerizes *in vivo* and *in vitro*, which

suggests that Tda2 can dimerize Aim21 as well. The finding that a small amount of Aim21 still localized to cortical patches in *bbc1*Δ *abp1*Δ cells and this is abolished by the additional deletion of *TDA2*, may reflect the possibility that Tda2 dimerizes Aim21 to enhance otherwise weak interactions of the Aim21 monomer. It is worth noting that it is unlikely that Tda2 directly recruits Aim21 to patches, given that Tda2 needs Aim21 for its patch localization, even though it was first found to contribute to the patch localization of Aim21. Dimerization can also explain the increased inhibition of actin assembly by Aim21 when Tda2 was present; Tda2 dimerizes Aim21 to increase its affinity for the sides or barbed ends of actin filaments. While the same speculation can be made for the function of Tda2 to mediate the interaction between Aim21 and Cap1/Cap2, the lack of physical interaction between Aim21 and Cap1/Cap2 makes it unlikely that Tda2 dimerizes Aim21 to increase its affinity for Cap1/Cap2, but rather suggested that Tda2 is directly involved in this interaction. However, I later found that Aim21, but not Tda2, can actually interact with Cap1/Cap2 without Tda2, when their concentrations are exceedingly high. Although the interaction between Aim21 alone and Cap1/Cap2 might not happen *in vivo*, as the concentrations used are too high to be physiological, it certainly favors the dimerization model over direct involvement model (Figure 3.2).

The potential role of interaction between Aim21/Tda2 and Cap1/Cap2

The fact that Aim21/Tda2 and Cap1/Cap2 form a complex was intriguing, because of their distinct sub-localizations in *sla2*Δ: Aim21/Tda2 is localized to the membrane-proximal region by Bbc1 and Abp1, but Cap1/Cap2 localizes to the newer two thirds of the extended actin tails. It is still uncertain what role this interaction plays. Farrell et al. (2017) suggested that Aim21/Tda2

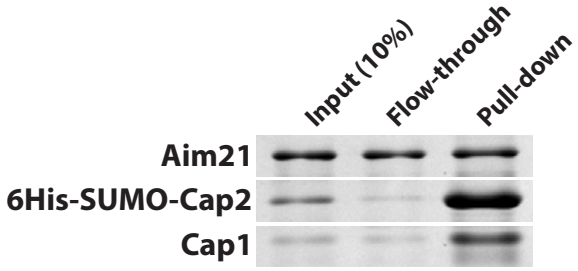

Figure 3.2. At high concentration, Aim21 interacts with Cap1/Cap2 without Tda2. Pull-down assay of Aim21, Cap1, and 6His-SUMO-Cap2, using Ni-NTA resin. Aim21, Cap1, and 6His-SUMO-Cap2 were more than five times more concentrated than in Figure 3.10.

recruits Cap1/Cap2 to actin patches through this interaction. However, I did not see any difference in the recruitment of Cap1/Cap2 to actin patches in the absence of Aim21. Also, given the nanomolar affinity of Cap1/Cap2 for barbed ends, it is unlikely that it needs help for its recruitment to patches (Kim et al., 2004).

It has been shown that Cap1/Cap2 homologues in humans can be negatively regulated by proteins with a capping protein interaction (CPI) motif or CARMIL-specific interaction (CSI) motif (Edwards et al., 2015; Edwards et al., 2014; Stark et al., 2017; Uruno et al., 2006; Yang et al., 2005). Although neither Aim21 nor Tda2 seems to have CPI or CSI motif, Farrell et al. (2017) showed that the mutations on Cap2 that have been shown to destroy CPI-motif-mediated interaction in Cap1/Cap2 human homologues also remove the interaction between Aim21/Tda2 and Cap1/Cap2 (Edwards et al., 2015). Thus, the interaction between Aim21/Tda2 and Cap1/Cap2 is likely to be analogous to CPI-motif-mediated interactions observed in other organisms. This likely explains its ability to negatively regulate the capping activity of Cap1/Cap2, which was shown as an increase in actin assembly when Aim21/Tda2 is added to actin assembly assay with Cap1/Cap2 (Figure 2.12).

As described in *Understanding the molecular mechanism of barbed end assembly by Aim21/Tda2*, I proposed two possible molecular mechanism for actin assembly inhibition by Aim21/Tda2: Aim21/Tda2 as a capping complex and Aim21/Tda2 as an allosteric inhibitor. While both models have their own merits, the fact that Cap1/Cap2 has high affinity for barbed ends suggests that, if it is a capping complex, Aim21/Tda2 would need an extra mechanism *in vivo* to bind to barbed ends in the presence of Cap1/Cap2, and the interaction between Aim21/Tda2 and Cap1/Cap2 is a likely candidate as discussed above. If Aim21/Tda2 is indeed a capping complex

and the interaction between Aim21/Tda2 and Cap1/Cap2 is to allow Aim21/Tda2 to compete with Cap1/Cap2 for barbed ends, cells with the *CAP2* mutations that disrupt the interaction should display *aim21*Δ-like phenotypes, as Aim21/Tda2 cannot compete as effectively. Also, using this cap2 mutant instead of wild type Cap2 in actin assembly assays should prevent Aim21/Tda2 from decreasing the capping activity of Cap1/Cap2. It is worth noting that the close localization of Aim21/Tda2 to the plasma membrane *in vivo* suggests that it can specifically reduce the activity of Cap1/Cap2 near the PM, perhaps in conjunction with the known inhibition of Cap1/Cap2 by the plasma membrane regulatory lipid $PI(4,5)P_2$ (Amatruda and Cooper, 1992).

Regulation of Aim21

Aim21 has been reported to be phosphorylated on many sites, possibly by casein kinase Hrr25 (Albuquerque et al., 2008; Peng et al., 2015). The role of this phosphorylation will be an interesting topic to follow up. Many endocytic proteins are known to be phosphorylated and dephosphorylated during the course of endocytosis, to regulate their function and coordinate their recruitment and departure (Lu et al., 2016). Interestingly, a coat and adapter protein Ent1 binds to actin through an unconventional actin binding domain, and the actin binding ability of this domain is regulated by phosphorylation, suggesting that the ability of Aim21 to bind to actin filaments and inhibit their growth can also be regulated by phosphorylation (Skruzny et al., 2012).

How aim21Δ rescues the growth defect of tpm1Δ cells

The finding that Aim21 negatively regulates actin assembly at patches and maintains the free actin pool did not initially explain how *aim21*Δ restores growth to *tpm1*Δ cells. A number of

subsequent observations indicated that reducing actin availability is indeed a part of the mechanism of the growth restoration. First, *tda2*Δ cells are also slightly more sensitive to latrunculin and *tda2*Δ also partially restores growth to *tpm1*Δ cells. Second, *cap1*Δ cells are very sensitive to latrunculin because of their low levels of free actin and *cap1*Δ also partially restores growth to *tpm1*Δ cells. Third, whereas a high level of latrunculin inhibits the growth of *tpm1*Δ cells, an intermediate level can enhance their ability to grow. I traced the mechanism to the potency difference between formins, Bni1 and Bnr1 (Moseley and Goode, 2005). The data indicated that lowering the level of free actin decrease the activity of Bni1 and biases cable nucleation to Bnr1, thereby allowing the limiting supply of Tpm2 to stabilize longer cables from the bud neck. This enhances essential cable-dependent processes, such as the delivery of secretory vesicles and organelle segregation.

The physiological significance of three inhibitors

While the distinct sub-localizations of three actin barbed end elongation inhibitors, Aim21/Tda2, Cap1/Cap2, and Abp1/Aim3, show the complexity of actin assembly regulation at barbed ends, it also raises a question of what the physiological significance of having three different assembly inhibitors is (Figure 3.1). Although more studies need to be done to conclude anything decisively, the membrane-proximal localization of Aim21/Tda2 and its negative effect on Cap1/Cap2 suggest that the physiological role of Aim21/Tda2 in this trio is to prevent Cap1/Cap2 from capping newly nucleated filaments prematurely near the cortex, while providing some level of inhibition. Shorter actin tails in *aim21*Δ *sla2*Δ cells, compared to those in *sla2*Δ cells, showed that the rate of actin assembly can be slowed down in the absence of Aim21 (Figure 3.3). This can contribute to larger patches in *aim21*Δ cells; the coordination of actin assembly and

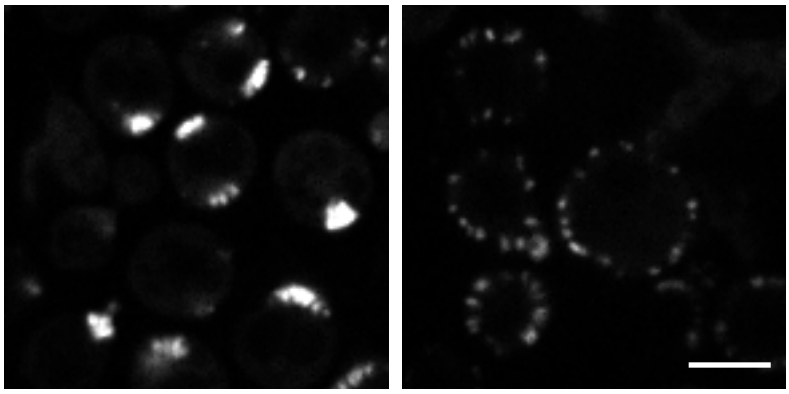

Figure 3.3. *aim21*Δ *sla2*Δ cells have shorter actin tails than *sla2*Δ cells. Actin structures as visualized by Alexa Fluor 568-phalloidin. Bar 2μm.

disassembly at patches might be compromised without Aim21, so it takes longer time and more actin assembly to reach the same level of invagination. Certainly, this is just one possibility and further studies need to be performed to understand and dissect the role of each inhibitor.

Summary

Actin and its functions have been studied for several decades, yet it is only recently that we are beginning to understand the exact molecular mechanism of its *in vivo* dynamics and regulation, with newly found actin regulators (Pollard, 2016). In this study, I started from a question of how *aim21*Δ rescues the growth defect of *tpm1*Δ cells, a seemingly paradoxical phenomenon, and in the process of answering the question, I established Aim21, with its cofactor Tda2, as a new complex that reduces barbed end actin assembly and whose activity in actin cortical patches is necessary both for efficient endocytosis and for regulating actin distribution between cables and cortical patches. Also, I could elucidate how *aim21*Δ restores cables and growth back to *tpm1*Δ cells–by decreasing nucleating activity of Bni1 by lowering the level of free actin. In conclusion, this study uncovered a novel barbed end assembly inhibitor, and demonstrated the complex interplay among actin regulators and the surprising degree of connectedness among different actin structures.

APPENDICES

Appendix 1. Materials and Methods

DNA constructs

Longtine et al. (1998) developed several pFA6a plasmids that can be used for gene deletion or GFP-tagging, with different markers. However, the selection was quite limited, so I decided to expand it by adding more selectable markers and fluorescent proteins.

Because all BY4741 (Mat a), BY4742 (Mat α), and BY4743 (Mat a/α) strains have *leu2*Δ0 and *ura3*Δ0 genotypes, I decided to make pFA6a constructs with *LEU2* and *URA3* markers. I first checked how *LEU2* and *URA3* were deleted in BY4741, BY4742, and BY4743 strains (Brachmann et al., 1998). After checking the region of deletion, I carefully designed primers so that *LEU2* and *URA3* that I was putting into pFA6a vector (1) do not have overlapping sequences with remnant sequences at *leu2*Δ0 or *ura3*Δ0 locus, to avoid nonspecific integration of the future PCR products into *leu2*Δ0 or *ura3*Δ0 locus, but (2) still have a functional promoter, coding region, and terminator. I tested the newly made pFA6a-LEU2 and pFA6a-URA3 vectors, with pFA6a-HIS3MX as a positive control, by deleting *AIM21* as described by Longtine et al. (1998). All three transformations gave comparable numbers of colonies with low false positive rates. DNA constructs made and used in this dissertation are listed in Table 1.

Yeast strains

Yeast transformations were performed using polyethylene glycol, lithium acetate, and single-stranded carrier DNA, according to Gietz and Schiestl (2007). Chromosomal manipulation

was done using homologous recombination-based integration using PCR products, as described as Longtine et al. (1998), and their genotypes were confirmed by PCR for correct integration. Strains used in this dissertation are listed in Table 2.

Obtaining PCR products from pFA6a constructs was often unsuccessful, probably because the primers are long and have high melting temperature, but the annealing temperature has to be set low because of the limited homology with primer binding sites on the plasmids (especially R1) (Longtine et al., 1998). Thus, I decided to optimize the protocol for better success and yield. The factors I considered in this optimization process included amount of template, annealing temperature, number of cycles, elongation time, and which polymerase and buffer to use. Here is the optimized protocol used throughout the study: (1) use 5ng of template (pFA6a plasmid) per 50µl reaction, (2) use Phusion Hot Start polymerase and HF (high fidelity) buffer from NEB or Thermo Fisher Scientific, (3) employ thermocycling program of 98°C (5 min), 25 cycles of 98°C (30 sec), 50°C (1 min), and 72°C (1 min per kb + 30 sec), and 72°C (10 min).

While all other genetic modifications were done according to Longtine et al. (1998), the same method could not be used to generate *AIM21(PP3-4+CT)* strains. Thus, to make them, chromosomal *AIM21* was deleted first and then replaced by *AIM21(PP3-4+CT)-GFP* or *AIM21(PP3-4+CT)-mNeonGreen*. Similarly, to generate *aim21*Δ *BBC1-AIM21(CT)* strain, I first made a *AIM21-mCherry* strain and then, from its genomic DNA, amplified the *AIM21(CT)-mCherry* region including the selectable marker with flanking sequences that target the C-terminus of *BBC1* by PCR. This PCR product was transformed into *aim21*Δ to make *aim21*Δ *BBC1-AIM21(CT)-mCherry*.

To prevent spontaneous suppressor mutation, *aim21*Δ *sla1*Δ strain was made by selecting the *aim21*Δ *sla1*Δ *pRS316-SLA1* cells that lost URA3 marker using 5'FOA.

Microscopy and analysis

Images were acquired using a spinning disk confocal microscope (Intelligent Imaging Innovations, Denver, CO). It consisted of an inverted microscope (Leica DMI6000B), a spinning disk confocal unit (Yokogawa CSU-X1), a fiber-optic laser light source, a 100x 1.47NA PL APO objective lens, and a sCMOS camera (Hamamatsu ORCA Flash 4.0v2+). SlideBook 6.0 software was used to operate the microscope system and analyze the images. Multiplane images were taken at 0.28μm steps and maximum or sum intensity projections were created with SlideBook software.

Cells were grown at room temperature to log phase for both live cell imaging and phalloidin staining. All imaging was done at 26°C. Cells were immobilized on concanavalin A-coated glass bottom culture dishes (MatTek) and supplemented with synthetic complete media, or on 1.5% agarose gel beds made with synthetic complete media. Differential interference contrast (DIC) images were taken together with fluorescence images and used to outline the cells, when they cannot be clearly defined from fluorescence images alone.

For analysis of actin patch intensity, Abp1 patch intensity, and Cap1 patch intensity, the background was set by selecting the same sized area inside the cell next to the patches that were selected for analysis. For analysis of Abp1 patch lifespan, the central 5 planes (0.28μm distance between planes) were taken and only the patches that disappeared in the center 3 planes were included for analysis, to exclude the patches that simply moved out of the capture area.

For statistically analysis, Student's *t*-test was used to determine *p*-values.

Actin staining using fluorophore-conjugated phalloidin

Visualization of F-actin in yeast cells using fluorophore-conjugated phalloidin was done as described by Pringle et al. (1989), with some modifications to better preserve actin cables and increase signals from them. The modifications I made and why they were implemented are following. (1) To obtain more consistent results and avoid damaging actin structures by methanol, I made a 20% paraformaldehyde solution in water, and used it at 4% to fix the cells. Paraformaldehyde solution was heated up to 60° for 5 minutes to break up polymers might have formed during frozen storage. (2) I found that longer fixation can lead to actin cable deterioration. I fixed the cells for 1-2 minutes. (3) To minimize damage to cables, I avoided strong shaking, including vortexing, and centrifugation of the cells. Because centrifugation is usually needed to change the liquid – spinning down the cells and discarding the supernatant, I had to come up with another way for liquid change. I developed a liquid change method that utilizes agarose gel beds and their absorption of liquid. I made a 1.5% agarose gel bed with 1xPBS, placed the fixed cells on it, let the gel absorb the fixing solution, then added the staining solution, and waited for it to be absorbed by the gel bed, and put a coverslip over the gel bed for imaging. (4) With shortened fixation and less perturbation of the cells, I noticed that the plasma membrane of the fixed cells stayed more intact and did not allow phalloidin molecules to permeate through. To solve this, I added 0.2% triton to the staining solution to increase permeability of the membrane during the staining process. Also, by permeating the membrane and staining the actin structures at the same time, phalloidin could stabilize the cables immediately, so I could prevent the potential degradation

of cables by the detergent. (5) I found that higher concentration of Alexa Fluor™ 568 phalloidin (Thermo Fisher Scientific A12380), up to 50% (v/v), helps increase the signal of actin cables. Because Alexa Fluor™ 568 phalloidin is dissolved and stored in 100% methanol, as recommended by Thermo Fisher Scientific, it was possible for 50% methanol in 50% (v/v) phalloidin staining solution to damage the actin structures. To avoid this, I dried the Alexa Fluor™ 568 phalloidin solution, and dissolved it in two volumes of 1xPBS+0.2%triton, and used that as a staining solution.

Latrunculin sensitivity assay

Latrunculin sensitivity assay was done as described by Winder et al. (2003). Yeast cells were grown to log phase in synthetic complete media and 40µl of the cultures were diluted into the 2ml of 2xYPD. 2ml of 1% molten agarose cooled down to 55-60°C was added. The mixture was briefly vortexed and poured on a YPD plate evenly. The plates were then incubated for 3 hours at room temperature for the agarose to solidify and for yeast cells to recover from the heat shock. Sterile 6mm filter paper disks that absorbed 5µl of 0.2mM latrunculin-A (lat-A) or 2mM latrunculin-B (lat-B) were then placed on top of the cells embedded in the agarose gel. The plates were incubated at 27°C for 24-48 hours.

Protein purification

pE-SUMOpro from LifeSensors Inc. was used to create plasmids that express 6His-SUMO-Aim21, 6His-SUMO-Aim21(PP1-4), 6His-SUMO-Aim21(CT), 6His-SUMO-Cap1, 6His-SUMO-Cap2, and 6His-SUMO-Tda2. These plasmids were transformed into Rosetta 2 (DE3) pLysS cells from Novagen. Bacterial cells transformed with the plasmids were grown in terrific

broth (TB) to log phase, and treated with 1mM IPTG at 37°C for 3.5 hours to induce the expression of recombinant proteins. Expressed recombinant proteins then were purified using Ni-NTA agarose resin from Qiagen. 20mM sodium phosphate, 300mM NaCl, 20mM imidazole, pH7.4 was used for lysis buffer and wash buffer, and 20mM sodium phosphate, 300mM NaCl, 500mM imidazole, pH7.4 was used for elution buffer. For cleaving 6His-SUMO tags off the purified proteins, recombinant 6His-Ulp1 was used. Cleaved 6His-SUMO tags and 6His-Ulp1 were removed using Ni-NTA resin. Purity of proteins was determined by SDS-PAGE. Proteins were dialyzed into 20mM sodium phosphate, 150mM NaCl, 20mM imidazole, pH7.4 for pull-down assays or into 50mM KCl, 2mM $MgCl_2$, 1mM ATP, pH7.5 (F-actin buffer) for actin assembly assays. Concentration of proteins was determined by using Coomassie stained SDS-PAGE gels with BSA standards.

Pull-down assay

Pull-down assays were performed in 20mM sodium phosphate, 150mM NaCl, 20mM imidazole, pH7.4. Ni-NTA resins was washed with the pull-down buffer first, then incubated with proteins at 4°C overnight. Resins were washed three times with the buffer to remove unbound proteins. The volume of washing buffer was equivalent to the volume of pull-down reaction, to better preserve interactions that might not be very strong, such as the interaction between Aim21/Tda2 and Cap1/Cap2. Equivalent molar concentrations of proteins were added, except for Tda2, which was added in excess as it was hard to detect due to its low molecular weight.

Actin assembly assay

Rabbit skeletal actin was purified by Dr, Anthony Bretscher, as described by MacLean-Fletcher and Pollard (1980) (Nefsky and Bretscher, 1992). Purified actin was stored in 5mM Tris-HCl, 0.2mM $CaCl_2$, pH8.0 (monomeric actin (G-actin) buffer) to prevent assembly into filamentous actin (F-actin). F-actin seeds were prepared by incubating purified rabbit skeletal actin in 50mM KCl, 2mM $MgCl_2$, 1mM ATP, pH7.5 (F-actin buffer) overnight and sonicating the solution to shear assembled F-actin into smaller pieces; I used 6 cycles of 10 seconds sonification with 10% power and 30 second reset on ice (Branson Digital Sonifier 250). Purified actin in G-actin buffer was mixed with pyrene-labelled actin (Cytoskeleton bk003) at 5%, and then diluted to 0.53mg/ml for assembly assays (final concentration 0.4mg/ml after the addition of 10xF-actin buffer, F-actin seeds, and protein solutions). Right before the assay, the G-actin was centrifuged at 100,000g for 30 minutes to remove any F-actin that might have formed. The assembly reaction was performed at room temperature, and the G-actin solution was kept at room temperature during the period of the experiment. 135µl of G-actin solution was used for each reaction and 15µl of 10xF-actin buffer (500mM KCl, 20mM $MgCl_2$, 10mM ATP, pH 7.5), 20µl of F-actin seeds, and 10µl of proteins in F-actin buffer were added separately. 10xF-actin buffer, F-actin seeds, and protein solutions were kept on ice and they were only warmed up to room temperature right before being added to the reaction. Pyrene fluorescence intensity was measured by a fluorometer (Photon Technology International, PTI) with a setting of 365nm for excitation and 407nm for emission. Because this fluorometer does not have an injection system, I opened the housing when adding to the reaction, which gave readings close to 0 during the open period.

Appendix 2. Lists of DNA constructs and yeast strains generated and used in this study

Table 1. List of DNA constructs generated and used in this study.

Location	Name	Bacteria strain	Plasmid Name	Source
4275	MP119	DH5α	pFA6a-yomNG-KanMX	This study
4276	MP120	DH5α	pFA6a-yomNG-NatMX	This study
4277	MP121	DH5α	pFA6a-yomNG-HIS3MX	This study
4278	MP122	DH5α	pFA6a-yomNG-LEU2	This study
4279	MP123	DH5α	pFA6a-yomNG-URA3	This study
4280	MP124	DH5α	pFA6a-yemCherry-KanMX	This study
4281	MP125	DH5α	pFA6a-yemCherry-NatMX	This study
4282	MP126	DH5α	pFA6a-yemCherry-HIS3MX	This study
4283	MP127	DH5α	pFA6a-yemCherry-LEU2	This study
4284	MP128	DH5α	pFA6a-yemCherry-URA3	This study
4306	MP150	DH5α	pFA6a-GFP(S65T)-LEU2	This study
4307	MP151	DH5α	pFA6a-GFP(S65T)-URA3	This study
4324	MP168	DH5α	pE-SUMO(pro)	LifeSensors Inc.
4325	MP169	DH5α	pE-SUMO(pro)-CAP1	This study
4326	MP170	DH5α	pE-SUMO(pro)-CAP2	This study
4327	MP171	DH5α	pE-SUMO(pro)-TDA2	This study
4328	MP172	DH5α	pE-SUMO(pro)-AIM21	This study
4329	MP173	Rosetta 2 (DE3) pLysS	pE-SUMO(pro)-CAP1	This study
4330	MP174	Rosetta 2 (DE3) pLysS	pE-SUMO(pro)-CAP2	This study
4331	MP175	Rosetta 2 (DE3) pLysS	pE-SUMO(pro)-TDA2	This study
4332	MP176	Rosetta 2 (DE3) pLysS	pE-SUMO(pro)-AIM21	This study
4333	MP177	DH5α	pE-SUMO(pro)-AIM21(PP1-4)	This study
4334	MP178	Rosetta 2 (DE3) pLysS	pE-SUMO(pro)-AIM21(PP1-4)	This study
4335	MP179	DH5α	pE-SUMO(pro)-AIM21(CT)	This study
4336	MP180	Rosetta 2 (DE3) pLysS	pE-SUMO(pro)-AIM21(CT)	This study
4341	MP185	DH5α	pFA6a-KanMX	Longtine et al. 1998
4342	MP186	DH5α	pFA6a-NatMX	This study
4344	MP188	DH5α	pFA6a-HIS3MX	Longtine et al. 1998
4345	MP189	DH5α	pFA6a-LEU2	This study
4346	MP190	DH5α	pFA6a-URA3	This study
4347	MP191	DH5α	pFA6a-mEGFP-KanMX	This study
4348	MP192	DH5α	pFA6a-mEGFP-NatMX	This study
4349	MP193	DH5α	pFA6a-mEGFP-HIS3MX	This study
4350	MP194	DH5α	pFA6a-mEGFP-LEU2	This study
4351	MP195	DH5α	pFA6a-mEGFP-URA3	This study
4352	MP196	DH5α	pFA6a-GFP(S65T)-KanMX	Longtine et al. 1998
4353	MP197	DH5α	pFA6a-GFP(S65T)-NatMX	This study

4354	MP198	DH5α	pFA6a-GFP(S65T)-HIS3MX	Longtine et al. 1998
4355	MP199	DH5α	pFA6a-GFP(S65T)-TRP1	Longtine et al. 1998
4359	MP203	DH5α	pFA6a-mCherry-KanMX	This study
4360	MP204	DH5α	pFA6a-mCherry-HIS3MX	This study

Table 2. List of yeast strains generated and used in this study.

Strain	Alias	Genotype	Source
ABY1656	BY4742	*MATα his3Δ1 leu2Δ0 lys2Δ0 ura3Δ0*	C. Boone
ABY6222		*MATα his3Δ1 leu2Δ0 lys2Δ0 ura3Δ0 aim21Δ::LEU2*	This study
ABY6165		*BY4741, Mat a: his3Δ1, leu2Δ0, met15Δ0, ura3Δ0 tpm1Δ::KanMX6*	Invitrogen
ABY6254		*MATα his3Δ1 leu2Δ0 lys2Δ0 ura3Δ0 tpm1Δ::LEU2*	This study
ABY6273		*MATα his3Δ1 leu2Δ0 lys2Δ0 ura3Δ0 aim21Δ::LEU2 tpm1Δ::URA3*	This study
ABY6384		*MATα his3Δ1 leu2Δ0 lys2Δ0 ura3Δ0 ABP1-mCherry::HIS3MX6 AIM21-mNeonGreen::URA3*	This study
ABY6422		*MATα his3Δ1 leu2Δ0 lys2Δ0 ura3Δ0 ABP1-mCherry::HIS3MX6 AIM21-mNeonGreen::URA3 sla2Δ::LEU2*	This study
ABY6322		*MATα his3Δ1 leu2Δ0 lys2Δ0 ura3Δ0 AIM21-mNeonGreen::HIS3MX6*	This study
ABY6336		*MATα his3Δ1 leu2Δ0 lys2Δ0 ura3Δ0 bbc1Δ::URA3 AIM21-mNeonGreen::HIS3MX6*	This study
ABY6287		*MATα his3Δ1 leu2Δ0 lys2Δ0 ura3Δ0 AIM21(PP1-2)-GFP::HIS3MX6*	This study
ABY6305		*MATα his3Δ1 leu2Δ0 lys2Δ0 ura3Δ0 AIM21(PP1-2)-GFP::HIS3MX6 bbc1Δ::LEU2*	This study
ABY6290		*MATα his3Δ1 leu2Δ0 lys2Δ0 ura3Δ0 AIM21(PP1-4)-GFP::HIS3MX6*	This study
ABY6334		*MATα his3Δ1 leu2Δ0 lys2Δ0 ura3Δ0 AIM21(PP1-4)-GFP::HIS3MX6 bbc1Δ::URA3*	This study
ABY6475		*MATα his3Δ1 leu2Δ0 lys2Δ0 ura3Δ0 AIM21(PP1-4)-GFP::URA3 abp1Δ::LEU2*	This study
ABY6365		*MATα his3Δ1 leu2Δ0 lys2Δ0 ura3Δ0 AIM21(PP1-4)-GFP::URA3 bbc1Δ::LEU2 abp1Δ::HIS3MX6*	This study
ABY6292		*MATα his3Δ1 leu2Δ0 lys2Δ0 ura3Δ0 AIM21-GFP::HIS3MX6*	This study
ABY6367		*MATα his3Δ1 leu2Δ0 lys2Δ0 ura3Δ0 AIM21-GFP::URA3 bbc1Δ::LEU2 abp1Δ::HIS3MX6*	This study
ABY6476		*MATα his3Δ1 leu2Δ0 lys2Δ0 ura3Δ0 AIM21-GFP::URA3 bbc1Δ::KanMX6 abp1Δ::HIS3MX6 tda2Δ::LEU2*	This study
ABY6423		*MATα his3Δ1 leu2Δ0 lys2Δ0 ura3Δ0 ABP1-mCherry::HIS3MX6 AIM21-mNeonGreen::URA3 bbc1Δ::KanMX6 sla2Δ::LEU2*	This study
ABY6426		*MATα his3Δ1 leu2Δ0 lys2Δ0 ura3Δ0 ABP1-mCherry::HIS3MX6 BBC1-GFP::URA3 sla2Δ::LEU2*	This study
ABY6491		*MATα his3Δ1 leu2Δ0 lys2Δ0 ura3Δ0 ABP1-mCherry::KanMX6 AIM21(PP3-4+CT)-mNeonGreen::LEU2 sla2Δ::URA3*	This study
ABY6478		*MATα his3Δ1 leu2Δ0 lys2Δ0 ura3Δ0 ABP1-mCherry::HIS3MX6 CAP1-GFP::LEU2 sla2Δ::URA3*	This study
ABY6369		*MATα his3Δ1 leu2Δ0 lys2Δ0 ura3Δ0 ABP1-mNeonGreen::HIS3MX6*	This study
ABY6370		*MATα his3Δ1 leu2Δ0 lys2Δ0 ura3Δ0 ABP1-mNeonGreen::HIS3MX6 aim21Δ::LEU2*	This study
ABY6456		*MATα his3Δ1 leu2Δ0 lys2Δ0 ura3Δ0 cap1Δ::LEU2*	This study

ABY6082		*Mat a: his3Δ1, leu2Δ0, met15Δ0, ura3Δ0 vrp1Δ::KanMX6*	Invitrogen
ABY6220		*Mat a: his3Δ1, leu2Δ0, met15Δ0, ura3Δ0 vrp1Δ::KanMX6, aim21Δ::URA3*	This study
ABY6187		*Mat a: his3Δ1, leu2Δ0, met15Δ0, ura3Δ0 sla1Δ::KanMX6*	Invitrogen
ABY6240		*Mat a: his3Δ1, leu2Δ0, met15Δ0, ura3Δ0 sla1Δ::KanMX6, pRS316-SLA1, aim21Δ::LEU2*	This study
ABY6296		*MATα his3Δ1 leu2Δ0 lys2Δ0 ura3Δ0 tpm1Δ::LEU2 AIM21-GFP::HIS3MX6*	This study
ABY6295		*MATα his3Δ1 leu2Δ0 lys2Δ0 ura3Δ0 tpm1Δ::LEU2 AIM21(PP1-4)-GFP::HIS3MX6*	This study
ABY6485		*MATα his3Δ1 leu2Δ0 lys2Δ0 ura3Δ0 TDA2-GFP::URA3 AIM21-yemCherry::HIS3MX6*	This study
ABY6483		*MATα his3Δ1 leu2Δ0 lys2Δ0 ura3Δ0 TDA2-GFP::URA3 AIM21(PP1-4)-yemCherry::HIS3MX6*	This study
ABY6466		*MATα his3Δ1 leu2Δ0 lys2Δ0 ura3Δ0 TDA2-GFP::URA3 aim21Δ::LEU2 BBC1-AIM21(CT)-yemCherry::HIS3MX6*	This study
ABY6447		*MATα his3Δ1 leu2Δ0 lys2Δ0 ura3Δ0 tda2Δ::LEU2*	This study
ABY6459		*MATα his3Δ1 leu2Δ0 lys2Δ0 ura3Δ0 tda2Δ::LEU2 tpm1Δ::URA3*	This study
ABY6501		*MATα his3Δ1 leu2Δ0 lys2Δ0 ura3Δ0 CAP1-GFP::URA3*	This study
ABY6502		*MATα his3Δ1 leu2Δ0 lys2Δ0 ura3Δ0 CAP1-GFP::URA3 aim21Δ::LEU2*	This study
ABY6503		*MATα his3Δ1 leu2Δ0 lys2Δ0 ura3Δ0 CAP1-GFP::URA3 tda2Δ::LEU2*	This study
ABY6457		*MATα his3Δ1 leu2Δ0 lys2Δ0 ura3Δ0 aim21Δ::LEU2 cap1Δ::URA3*	This study
ABY1655	BY4741	*MATa his3Δ1 leu2Δ0 met15Δ0 ura3Δ0*	C. Boone
ABY6068		*MATa his3Δ1 leu2Δ0 met15Δ0 ura3Δ0 cap1Δ::KanMX6*	Invitrogen
ABY6337		*MATa his3Δ1 leu2Δ0 met15Δ0 ura3Δ0 tpm1Δ::LEU2*	This study
ABY6394		*MATa his3Δ1 leu2Δ0 met15Δ0 ura3Δ0 cap1Δ::KanMX6 tpm1Δ::LEU2*	This study
ABY6307		*MATα his3Δ1 leu2Δ0 lys2Δ0 ura3Δ0 bni1Δ::URA3*	This study
ABY6338		*MATα his3Δ1 leu2Δ0 lys2Δ0 ura3Δ0 bni1Δ::URA3 tpm1Δ::LEU2*	This study
ABY6395		*MATα his3Δ1 leu2Δ0 lys2Δ0 ura3Δ0 BBC1-GFP::URA3*	This study
ABY6472		*MATα his3Δ1 leu2Δ0 lys2Δ0 ura3Δ0 AIM21(PP3-4+CT)-GFP::URA3*	This study
ABY6473		*MATα his3Δ1 leu2Δ0 lys2Δ0 ura3Δ0 AIM21(PP3-4+CT)-GFP::URA3 tpm1Δ::KanMX6*	This study

REFERENCES

Adams, A.E., D. Botstein, and D.G. Drubin. 1989. A yeast actin-binding protein is encoded by SAC6, a gene found by suppression of an actin mutation. *Science*. 243:231-233.

Adams, A.E., J.A. Cooper, and D.G. Drubin. 1993. Unexpected combinations of null mutations in genes encoding the actin cytoskeleton are lethal in yeast. *Mol Biol Cell*. 4:459-468.

Adams, A.E., and J.R. Pringle. 1984. Relationship of actin and tubulin distribution to bud growth in wild-type and morphogenetic-mutant Saccharomyces cerevisiae. *J Cell Biol*. 98:934-945.

Aggeli, D., E. Kish-Trier, M.C. Lin, B. Haarer, G. Cingolani, J.A. Cooper, S. Wilkens, and D.C. Amberg. 2014. Coordination of the filament stabilizing versus destabilizing activities of cofilin through its secondary binding site on actin. *Cytoskeleton (Hoboken)*. 71:361-379.

Aghamohammadzadeh, S., and K.R. Ayscough. 2009. Differential requirements for actin during yeast and mammalian endocytosis. *Nat Cell Biol*. 11:1039-1042.

Aghamohammadzadeh, S., R. Smaczynska-de, II, and K.R. Ayscough. 2014. An Abp1-dependent route of endocytosis functions when the classical endocytic pathway in yeast is inhibited. *PLoS One*. 9:e103311.

Alberts, A.S. 2001. Identification of a carboxyl-terminal diaphanous-related formin homology protein autoregulatory domain. *J Biol Chem*. 276:2824-2830.

Albuquerque, C.P., M.B. Smolka, S.H. Payne, V. Bafna, J. Eng, and H. Zhou. 2008. A multidimensional chromatography technology for in-depth phosphoproteome analysis. *Mol Cell Proteomics*. 7:1389-1396.

Amatruda, J.F., J.F. Cannon, K. Tatchell, C. Hug, and J.A. Cooper. 1990. Disruption of the actin cytoskeleton in yeast capping protein mutants. *Nature*. 344:352-354.

Amatruda, J.F., and J.A. Cooper. 1992. Purification, characterization, and immunofluorescence localization of Saccharomyces cerevisiae capping protein. *J Cell Biol*. 117:1067-1076.

Amatruda, J.F., D.J. Gattermeir, T.S. Karpova, and J.A. Cooper. 1992. Effects of null mutations and overexpression of capping protein on morphogenesis, actin distribution and polarized secretion in yeast. *J Cell Biol*. 119:1151-1162.

Asakura, T., T. Sasaki, F. Nagano, A. Satoh, H. Obaishi, H. Nishioka, H. Imamura, K. Hotta, K. Tanaka, H. Nakanishi, and Y. Takai. 1998. Isolation and characterization of a novel actin filament-binding protein from Saccharomyces cerevisiae. *Oncogene*. 16:121-130.

Atkinson, S.J., S.K. Doberstein, and T.D. Pollard. 1992. Moving off the beaten track. *Curr Biol*. 2:326-328.

Avinoam, O., M. Schorb, C.J. Beese, J.A. Briggs, and M. Kaksonen. 2015. ENDOCYTOSIS. Endocytic sites mature by continuous bending and remodeling of the clathrin coat. *Science*. 348:1369-1372.

Balcer, H.I., A.L. Goodman, A.A. Rodal, E. Smith, J. Kugler, J.E. Heuser, and B.L. Goode. 2003. Coordinated regulation of actin filament turnover by a high-molecular-weight Srv2/CAP complex, cofilin, profilin, and Aip1. *Curr Biol*. 13:2159-2169.

Bamburg, J.R., H.E. Harris, and A.G. Weeds. 1980. Partial purification and characterization of an actin depolymerizing factor from brain. *FEBS Lett*. 121:178-182.

Boettner, D.R., J.L. D'Agostino, O.T. Torres, K. Daugherty-Clarke, A. Uygur, A. Reider, B. Wendland, S.K. Lemmon, and B.L. Goode. 2009. The F-BAR protein Syp1 negatively

regulates WASp-Arp2/3 complex activity during endocytic patch formation. *Curr Biol*. 19:1979-1987.
Brach, T., C. Godlee, I. Moeller-Hansen, D. Boeke, and M. Kaksonen. 2014. The initiation of clathrin-mediated endocytosis is mechanistically highly flexible. *Curr Biol*. 24:548-554.
Brachmann, C.B., A. Davies, G.J. Cost, E. Caputo, J. Li, P. Hieter, and J.D. Boeke. 1998. Designer deletion strains derived from Saccharomyces cerevisiae S288C: a useful set of strains and plasmids for PCR-mediated gene disruption and other applications. *Yeast*. 14:115-132.
Brieher, W. 2013. Mechanisms of actin disassembly. *Mol Biol Cell*. 24:2299-2302.
Brieher, W.M., H.Y. Kueh, B.A. Ballif, and T.J. Mitchison. 2006. Rapid actin monomer-insensitive depolymerization of Listeria actin comet tails by cofilin, coronin, and Aip1. *J Cell Biol*. 175:315-324.
Burston, H.E., L. Maldonado-Baez, M. Davey, B. Montpetit, C. Schluter, B. Wendland, and E. Conibear. 2009. Regulators of yeast endocytosis identified by systematic quantitative analysis. *J Cell Biol*. 185:1097-1110.
Buttery, S.M., K. Kono, E. Stokasimov, and D. Pellman. 2012. Regulation of the formin Bnr1 by septins anda MARK/Par1-family septin-associated kinase. *Mol Biol Cell*. 23:4041-4053.
Buttery, S.M., S. Yoshida, and D. Pellman. 2007. Yeast formins Bni1 and Bnr1 utilize different modes of cortical interaction during the assembly of actin cables. *Mol Biol Cell*. 18:1826-1838.
Cai, L., A.M. Makhov, and J.E. Bear. 2007a. F-actin binding is essential for coronin 1B function in vivo. *J Cell Sci*. 120:1779-1790.
Cai, L., T.W. Marshall, A.C. Uetrecht, D.A. Schafer, and J.E. Bear. 2007b. Coronin 1B coordinates Arp2/3 complex and cofilin activities at the leading edge. *Cell*. 128:915-929.
Campellone, K.G., and M.D. Welch. 2010. A nucleator arms race: cellular control of actin assembly. *Nat Rev Mol Cell Biol*. 11:237-251.
Carlier, M.F., V. Laurent, J. Santolini, R. Melki, D. Didry, G.X. Xia, Y. Hong, N.H. Chua, and D. Pantaloni. 1997. Actin depolymerizing factor (ADF/cofilin) enhances the rate of filament turnover: implication in actin-based motility. *J Cell Biol*. 136:1307-1322.
Carlier, M.F., D. Pantaloni, and E.D. Korn. 1985. Polymerization of ADP-actin and ATP-actin under sonication and characteristics of the ATP-actin equilibrium polymer. *J Biol Chem*. 260:6565-6571.
Carlier, M.F., and S. Shekhar. 2017. Global treadmilling coordinates actin turnover and controls the size of actin networks. *Nat Rev Mol Cell Biol*. 18:389-401.
Carlsson, L., L.E. Nystrom, I. Sundkvist, F. Markey, and U. Lindberg. 1977. Actin polymerizability is influenced by profilin, a low molecular weight protein in non-muscle cells. *J Mol Biol*. 115:465-483.
Carroll, S.Y., H.E. Stimpson, J. Weinberg, C.P. Toret, Y. Sun, and D.G. Drubin. 2012. Analysis of yeast endocytic site formation and maturation through a regulatory transition point. *Mol Biol Cell*. 23:657-668.
Casella, J.F., D.J. Maack, and S. Lin. 1986. Purification and initial characterization of a protein from skeletal muscle that caps the barbed ends of actin filaments. *J Biol Chem*. 261:10915-10921.

Catlett, N.L., and L.S. Weisman. 1998. The terminal tail region of a yeast myosin-V mediates its attachment to vacuole membranes and sites of polarized growth. *Proc Natl Acad Sci U S A*. 95:14799-14804.

Chang, F., D. Drubin, and P. Nurse. 1997. cdc12p, a protein required for cytokinesis in fission yeast, is a component of the cell division ring and interacts with profilin. *J Cell Biol*. 137:169-182.

Chaudhry, F., D. Breitsprecher, K. Little, G. Sharov, O. Sokolova, and B.L. Goode. 2013. Srv2/cyclase-associated protein forms hexameric shurikens that directly catalyze actin filament severing by cofilin. *Mol Biol Cell*. 24:31-41.

Chen, H., B.W. Bernstein, and J.R. Bamburg. 2000. Regulating actin-filament dynamics in vivo. *Trends Biochem Sci*. 25:19-23.

Chernyakov, I., F. Santiago-Tirado, and A. Bretscher. 2013. Active segregation of yeast mitochondria by Myo2 is essential and mediated by Mmr1 and Ypt11. *Curr Biol*. 23:1818-1824.

Chesarone, M., C.J. Gould, J.B. Moseley, and B.L. Goode. 2009. Displacement of formins from growing barbed ends by bud14 is critical for actin cable architecture and function. *Dev Cell*. 16:292-302.

Cope, M.J., S. Yang, C. Shang, and D.G. Drubin. 1999. Novel protein kinases Ark1p and Prk1p associate with and regulate the cortical actin cytoskeleton in budding yeast. *J Cell Biol*. 144:1203-1218.

Costanzo, M., A. Baryshnikova, J. Bellay, Y. Kim, E.D. Spear, C.S. Sevier, H. Ding, J.L. Koh, K. Toufighi, S. Mostafavi, J. Prinz, R.P. St Onge, B. VanderSluis, T. Makhnevych, F.J. Vizeacoumar, S. Alizadeh, S. Bahr, R.L. Brost, Y. Chen, M. Cokol, R. Deshpande, Z. Li, Z.Y. Lin, W. Liang, M. Marback, J. Paw, B.J. San Luis, E. Shuteriqi, A.H. Tong, N. van Dyk, I.M. Wallace, J.A. Whitney, M.T. Weirauch, G. Zhong, H. Zhu, W.A. Houry, M. Brudno, S. Ragibizadeh, B. Papp, C. Pal, F.P. Roth, G. Giaever, C. Nislow, O.G. Troyanskaya, H. Bussey, G.D. Bader, A.C. Gingras, Q.D. Morris, P.M. Kim, C.A. Kaiser, C.L. Myers, B.J. Andrews, and C. Boone. 2010. The genetic landscape of a cell. *Science*. 327:425-431.

Costanzo, M., B. VanderSluis, E.N. Koch, A. Baryshnikova, C. Pons, G. Tan, W. Wang, M. Usaj, J. Hanchard, S.D. Lee, V. Pelechano, E.B. Styles, M. Billmann, J. van Leeuwen, N. van Dyk, Z.Y. Lin, E. Kuzmin, J. Nelson, J.S. Piotrowski, T. Srikumar, S. Bahr, Y. Chen, R. Deshpande, C.F. Kurat, S.C. Li, Z. Li, M.M. Usaj, H. Okada, N. Pascoe, B.J. San Luis, S. Sharifpoor, E. Shuteriqi, S.W. Simpkins, J. Snider, H.G. Suresh, Y. Tan, H. Zhu, N. Malod-Dognin, V. Janjic, N. Przulj, O.G. Troyanskaya, I. Stagljar, T. Xia, Y. Ohya, A.C. Gingras, B. Raught, M. Boutros, L.M. Steinmetz, C.L. Moore, A.P. Rosebrock, A.A. Caudy, C.L. Myers, B. Andrews, and C. Boone. 2016. A global genetic interaction network maps a wiring diagram of cellular function. *Science*. 353.

D'Silva, S., S.J. Haider, and E.M. Phizicky. 2011. A domain of the actin binding protein Abp140 is the yeast methyltransferase responsible for 3-methylcytidine modification in the tRNA anti-codon loop. *RNA*. 17:1100-1110.

Dayel, M.J., E.A. Holleran, and R.D. Mullins. 2001. Arp2/3 complex requires hydrolyzable ATP for nucleation of new actin filaments. *Proc Natl Acad Sci U S A*. 98:14871-14876.

Dayel, M.J., and R.D. Mullins. 2004. Activation of Arp2/3 complex: addition of the first subunit of the new filament by a WASP protein triggers rapid ATP hydrolysis on Arp2. *PLoS Biol*. 2:E91.

de Hostos, E.L., B. Bradtke, F. Lottspeich, R. Guggenheim, and G. Gerisch. 1991. Coronin, an actin binding protein of Dictyostelium discoideum localized to cell surface projections, has sequence similarities to G protein beta subunits. *EMBO J*. 10:4097-4104.

Diehl, B.E., and J.R. Pringle. 1991. Molecular analysis of Saccharomyces cerevisiae chromosome I: identification of additional transcribed regions and demonstration that some encode essential functions. *Genetics*. 127:287-298.

Doherty, G.J., and H.T. McMahon. 2009. Mechanisms of endocytosis. *Annu Rev Biochem*. 78:857-902.

Dong, Y., D. Pruyne, and A. Bretscher. 2003. Formin-dependent actin assembly is regulated by distinct modes of Rho signaling in yeast. *J Cell Biol*. 161:1081-1092.

Donnelly, S.F., M.J. Pocklington, D. Pallotta, and E. Orr. 1993. A proline-rich protein, verprolin, involved in cytoskeletal organization and cellular growth in the yeast Saccharomyces cerevisiae. *Mol Microbiol*. 10:585-596.

Drees, B., C. Brown, B.G. Barrell, and A. Bretscher. 1995. Tropomyosin is essential in yeast, yet the TPM1 and TPM2 products perform distinct functions. *J Cell Biol*. 128:383-392.

Drubin, D.G., K.G. Miller, and D. Botstein. 1988. Yeast actin-binding proteins: evidence for a role in morphogenesis. *J Cell Biol*. 107:2551-2561.

Drubin, D.G., J. Mulholland, Z.M. Zhu, and D. Botstein. 1990. Homology of a yeast actin-binding protein to signal transduction proteins and myosin-I. *Nature*. 343:288-290.

Edwards, M., P. McConnell, D.A. Schafer, and J.A. Cooper. 2015. CPI motif interaction is necessary for capping protein function in cells. *Nat Commun*. 6:8415.

Edwards, M., A. Zwolak, D.A. Schafer, D. Sept, R. Dominguez, and J.A. Cooper. 2014. Capping protein regulators fine-tune actin assembly dynamics. *Nat Rev Mol Cell Biol*. 15:677-689.

Ehrlich, M., W. Boll, A. Van Oijen, R. Hariharan, K. Chandran, M.L. Nibert, and T. Kirchhausen. 2004. Endocytosis by random initiation and stabilization of clathrin-coated pits. *Cell*. 118:591-605.

Evangelista, M., D. Pruyne, D.C. Amberg, C. Boone, and A. Bretscher. 2002. Formins direct Arp2/3-independent actin filament assembly to polarize cell growth in yeast. *Nat Cell Biol*. 4:32-41.

Fagarasanu, A., M. Fagarasanu, G.A. Eitzen, J.D. Aitchison, and R.A. Rachubinski. 2006. The peroxisomal membrane protein Inp2p is the peroxisome-specific receptor for the myosin V motor Myo2p of Saccharomyces cerevisiae. *Dev Cell*. 10:587-600.

Falck, S., V.O. Paavilainen, M.A. Wear, J.G. Grossmann, J.A. Cooper, and P. Lappalainen. 2004. Biological role and structural mechanism of twinfilin-capping protein interaction. *EMBO J*. 23:3010-3019.

Farrell, K.B., S. McDonald, A.K. Lamb, C. Worcester, O.B. Peersen, and S.M. Di Pietro. 2017. Novel function of a dynein light chain in actin assembly during clathrin-mediated endocytosis. *J Cell Biol*. 216:2565-2580.

Fazi, B., M.J. Cope, A. Douangamath, S. Ferracuti, K. Schirwitz, A. Zucconi, D.G. Drubin, M. Wilmanns, G. Cesareni, and L. Castagnoli. 2002. Unusual binding properties of the SH3 domain of the yeast actin-binding protein Abp1: structural and functional analysis. *J Biol Chem*. 277:5290-5298.

Feliciano, D., and S.M. Di Pietro. 2012. SLAC, a complex between Sla1 and Las17, regulates actin polymerization during clathrin-mediated endocytosis. *Mol Biol Cell*. 23:4256-4272.
Field, J., A. Vojtek, R. Ballester, G. Bolger, J. Colicelli, K. Ferguson, J. Gerst, T. Kataoka, T. Michaeli, S. Powers, and et al. 1990. Cloning and characterization of CAP, the S. cerevisiae gene encoding the 70 kd adenylyl cyclase-associated protein. *Cell*. 61:319-327.
Fowler, V.M. 1987. Identification and purification of a novel Mr 43,000 tropomyosin-binding protein from human erythrocyte membranes. *J Biol Chem*. 262:12792-12800.
Fowler, V.M. 1990. Tropomodulin: a cytoskeletal protein that binds to the end of erythrocyte tropomyosin and inhibits tropomyosin binding to actin. *J Cell Biol*. 111:471-481.
Fowler, V.M., M.A. Sussmann, P.G. Miller, B.E. Flucher, and M.P. Daniels. 1993. Tropomodulin is associated with the free (pointed) ends of the thin filaments in rat skeletal muscle. *J Cell Biol*. 120:411-420.
Frieden, C. 1985. Actin and tubulin polymerization: the use of kinetic methods to determine mechanism. *Annu Rev Biophys Biophys Chem*. 14:189-210.
Friesen, H., C. Humphries, Y. Ho, O. Schub, K. Colwill, and B. Andrews. 2006. Characterization of the yeast amphiphysins Rvs161p and Rvs167p reveals roles for the Rvs heterodimer in vivo. *Mol Biol Cell*. 17:1306-1321.
Fujiwara, T., K. Tanaka, A. Mino, M. Kikyo, K. Takahashi, K. Shimizu, and Y. Takai. 1998. Rho1p-Bni1p-Spa2p interactions: implication in localization of Bni1p at the bud site and regulation of the actin cytoskeleton in Saccharomyces cerevisiae. *Mol Biol Cell*. 9:1221-1233.
Gallwitz, D., and R. Seidel. 1980. Molecular cloning of the actin gene from yeast Saccharomyces cerevisiae. *Nucleic Acids Res*. 8:1043-1059.
Gandhi, M., V. Achard, L. Blanchoin, and B.L. Goode. 2009. Coronin switches roles in actin disassembly depending on the nucleotide state of actin. *Mol Cell*. 34:364-374.
Gandhi, M., B.A. Smith, M. Bovellan, V. Paavilainen, K. Daugherty-Clarke, J. Gelles, P. Lappalainen, and B.L. Goode. 2010. GMF is a cofilin homolog that binds Arp2/3 complex to stimulate filament debranching and inhibit actin nucleation. *Curr Biol*. 20:861-867.
Gao, L., and A. Bretscher. 2008. Analysis of unregulated formin activity reveals how yeast can balance F-actin assembly between different microfilament-based organizations. *Mol Biol Cell*. 19:1474-1484.
Gao, L., W. Liu, and A. Bretscher. 2010. The yeast formin Bnr1p has two localization regions that show spatially and temporally distinct association with septin structures. *Mol Biol Cell*. 21:1253-1262.
Gao, X.D., S. Albert, S.E. Tcheperegine, C.G. Burd, D. Gallwitz, and E. Bi. 2003. The GAP activity of Msb3p and Msb4p for the Rab GTPase Sec4p is required for efficient exocytosis and actin organization. *J Cell Biol*. 162:635-646.
Gavin, A.C., P. Aloy, P. Grandi, R. Krause, M. Boesche, M. Marzioch, C. Rau, L.J. Jensen, S. Bastuck, B. Dumpelfeld, A. Edelmann, M.A. Heurtier, V. Hoffman, C. Hoefert, K. Klein, M. Hudak, A.M. Michon, M. Schelder, M. Schirle, M. Remor, T. Rudi, S. Hooper, A. Bauer, T. Bouwmeester, G. Casari, G. Drewes, G. Neubauer, J.M. Rick, B. Kuster, P. Bork, R.B. Russell, and G. Superti-Furga. 2006. Proteome survey reveals modularity of the yeast cell machinery. *Nature*. 440:631-636.

Ge, P., Z.A. Durer, D. Kudryashov, Z.H. Zhou, and E. Reisler. 2014. Cryo-EM reveals different coronin binding modes for ADP- and ADP-BeFx actin filaments. *Nat Struct Mol Biol*. 21:1075-1081.

Geli, M.I., R. Lombardi, B. Schmelzl, and H. Riezman. 2000. An intact SH3 domain is required for myosin I-induced actin polymerization. *EMBO J*. 19:4281-4291.

Gerst, J.E., K. Ferguson, A. Vojtek, M. Wigler, and J. Field. 1991. CAP is a bifunctional component of the Saccharomyces cerevisiae adenylyl cyclase complex. *Mol Cell Biol*. 11:1248-1257.

Gietz, R.D., and R.H. Schiestl. 2007. High-efficiency yeast transformation using the LiAc/SS carrier DNA/PEG method. *Nat Protoc*. 2:31-34.

Goley, E.D., S.E. Rodenbusch, A.C. Martin, and M.D. Welch. 2004. Critical conformational changes in the Arp2/3 complex are induced by nucleotide and nucleation promoting factor. *Mol Cell*. 16:269-279.

Goley, E.D., and M.D. Welch. 2006. The ARP2/3 complex: an actin nucleator comes of age. *Nat Rev Mol Cell Biol*. 7:713-726.

Goode, B.L., D.G. Drubin, and P. Lappalainen. 1998. Regulation of the cortical actin cytoskeleton in budding yeast by twinfilin, a ubiquitous actin monomer-sequestering protein. *J Cell Biol*. 142:723-733.

Goode, B.L., and M.J. Eck. 2007. Mechanism and function of formins in the control of actin assembly. *Annu Rev Biochem*. 76:593-627.

Goode, B.L., J.A. Eskin, and B. Wendland. 2015. Actin and endocytosis in budding yeast. *Genetics*. 199:315-358.

Goode, B.L., A.A. Rodal, G. Barnes, and D.G. Drubin. 2001. Activation of the Arp2/3 complex by the actin filament binding protein Abp1p. *J Cell Biol*. 153:627-634.

Gould, C.J., M. Chesarone-Cataldo, S.L. Alioto, B. Salin, I. Sagot, and B.L. Goode. 2014. Saccharomyces cerevisiae Kelch proteins and Bud14 protein form a stable 520-kDa formin regulatory complex that controls actin cable assembly and cell morphogenesis. *J Biol Chem*. 289:18290-18301.

Graziano, B.R., A.G. DuPage, A. Michelot, D. Breitsprecher, J.B. Moseley, I. Sagot, L. Blanchoin, and B.L. Goode. 2011. Mechanism and cellular function of Bud6 as an actin nucleation-promoting factor. *Mol Biol Cell*. 22:4016-4028.

Graziano, B.R., E.M. Jonasson, J.G. Pullen, C.J. Gould, and B.L. Goode. 2013. Ligand-induced activation of a formin-NPF pair leads to collaborative actin nucleation. *J Cell Biol*. 201:595-611.

Graziano, B.R., H.Y. Yu, S.L. Alioto, J.A. Eskin, C.A. Ydenberg, D.P. Waterman, M. Garabedian, and B.L. Goode. 2014. The F-BAR protein Hof1 tunes formin activity to sculpt actin cables during polarized growth. *Mol Biol Cell*. 25:1730-1743.

Gunning, P.W., U. Ghoshdastider, S. Whitaker, D. Popp, and R.C. Robinson. 2015. The evolution of compositionally and functionally distinct actin filaments. *J Cell Sci*. 128:2009-2019.

Haarer, B.K., A. Corbett, Y. Kweon, A.S. Petzold, P. Silver, and S.S. Brown. 1996. SEC3 mutations are synthetically lethal with profilin mutations and cause defects in diploid-specific bud-site selection. *Genetics*. 144:495-510.

Haarer, B.K., A. Petzold, S.H. Lillie, and S.S. Brown. 1994. Identification of MYO4, a second class V myosin gene in yeast. *J Cell Sci*. 107 (Pt 4):1055-1064.

Harris, H.E., J.R. Bamburg, and A.G. Weeds. 1980. Actin filament disassembly in blood plasma. *FEBS Lett*. 121:175-177.
Hayakawa, K., S. Sakakibara, M. Sokabe, and H. Tatsumi. 2014. Single-molecule imaging and kinetic analysis of cooperative cofilin-actin filament interactions. *Proc Natl Acad Sci U S A*. 111:9810-9815.
Heiss, S.G., and J.A. Cooper. 1991. Regulation of CapZ, an actin capping protein of chicken muscle, by anionic phospholipids. *Biochemistry*. 30:8753-8758.
Helfer, E., E.M. Nevalainen, P. Naumanen, S. Romero, D. Didry, D. Pantaloni, P. Lappalainen, and M.F. Carlier. 2006. Mammalian twinfilin sequesters ADP-G-actin and caps filament barbed ends: implications in motility. *EMBO J*. 25:1184-1195.
Hess, D.C., C.L. Myers, C. Huttenhower, M.A. Hibbs, A.P. Hayes, J. Paw, J.J. Clore, R.M. Mendoza, B.S. Luis, C. Nislow, G. Giaever, M. Costanzo, O.G. Troyanskaya, and A.A. Caudy. 2009. Computationally driven, quantitative experiments discover genes required for mitochondrial biogenesis. *PLoS Genet*. 5:e1000407.
Higgs, H.N., L. Blanchoin, and T.D. Pollard. 1999. Influence of the C terminus of Wiskott-Aldrich syndrome protein (WASp) and the Arp2/3 complex on actin polymerization. *Biochemistry*. 38:15212-15222.
Higgs, H.N., and K.J. Peterson. 2005. Phylogenetic analysis of the formin homology 2 domain. *Mol Biol Cell*. 16:1-13.
Hill, K.L., N.L. Catlett, and L.S. Weisman. 1996. Actin and myosin function in directed vacuole movement during cell division in Saccharomyces cerevisiae. *J Cell Biol*. 135:1535-1549.
Hinnebusch, A.G. 1988. Mechanisms of gene regulation in the general control of amino acid biosynthesis in Saccharomyces cerevisiae. *Microbiol Rev*. 52:248-273.
Hoepfner, D., S.B. Helliwell, H. Sadlish, S. Schuierer, I. Filipuzzi, S. Brachat, B. Bhullar, U. Plikat, Y. Abraham, M. Altorfer, T. Aust, L. Baeriswyl, R. Cerino, L. Chang, D. Estoppey, J. Eichenberger, M. Frederiksen, N. Hartmann, A. Hohendahl, B. Knapp, P. Krastel, N. Melin, F. Nigsch, E.J. Oakeley, V. Petitjean, F. Petersen, R. Riedl, E.K. Schmitt, F. Staedtler, C. Studer, J.A. Tallarico, S. Wetzel, M.C. Fishman, J.A. Porter, and N.R. Movva. 2014. High-resolution chemical dissection of a model eukaryote reveals targets, pathways and gene functions. *Microbiol Res*. 169:107-120.
Hoepfner, D., M. van den Berg, P. Philippsen, H.F. Tabak, and E.H. Hettema. 2001. A role for Vps1p, actin, and the Myo2p motor in peroxisome abundance and inheritance in Saccharomyces cerevisiae. *J Cell Biol*. 155:979-990.
Hubberstey, A.V., and E.P. Mottillo. 2002. Cyclase-associated proteins: CAPacity for linking signal transduction and actin polymerization. *FASEB J*. 16:487-499.
Humphries, C.L., H.I. Balcer, J.L. D'Agostino, B. Winsor, D.G. Drubin, G. Barnes, B.J. Andrews, and B.L. Goode. 2002. Direct regulation of Arp2/3 complex activity and function by the actin binding protein coronin. *J Cell Biol*. 159:993-1004.
Huxley, H.E. 1963. Electron Microscope Studies on the Structure of Natural and Synthetic Protein Filaments from Striated Muscle. *J Mol Biol*. 7:281-308.
Idrissi, F.Z., H. Grotsch, I.M. Fernandez-Golbano, C. Presciatto-Baschong, H. Riezman, and M.I. Geli. 2008. Distinct acto/myosin-I structures associate with endocytic profiles at the plasma membrane. *J Cell Biol*. 180:1219-1232.
Imamura, H., K. Tanaka, T. Hihara, M. Umikawa, T. Kamei, K. Takahashi, T. Sasaki, and Y. Takai. 1997. Bni1p and Bnr1p: downstream targets of the Rho family small G-proteins

which interact with profilin and regulate actin cytoskeleton in Saccharomyces cerevisiae. *EMBO J*. 16:2745-2755.
Ingerman, E., J.Y. Hsiao, and R.D. Mullins. 2013. Arp2/3 complex ATP hydrolysis promotes lamellipodial actin network disassembly but is dispensable for assembly. *J Cell Biol*. 200:619-633.
Itoh, T., E.A. Toh, and Y. Matsui. 2004. Mmr1p is a mitochondrial factor for Myo2p-dependent inheritance of mitochondria in the budding yeast. *EMBO J*. 23:2520-2530.
Itoh, T., A. Watabe, E.A. Toh, and Y. Matsui. 2002. Complex formation with Ypt11p, a rab-type small GTPase, is essential to facilitate the function of Myo2p, a class V myosin, in mitochondrial distribution in Saccharomyces cerevisiae. *Mol Cell Biol*. 22:7744-7757.
Janji, B., A. Giganti, V. De Corte, M. Catillon, E. Bruyneel, D. Lentz, J. Plastino, J. Gettemans, and E. Friederich. 2006. Phosphorylation on Ser5 increases the F-actin-binding activity of L-plastin and promotes its targeting to sites of actin assembly in cells. *J Cell Sci*. 119:1947-1960.
Johnston, A.B., A. Collins, and B.L. Goode. 2015. High-speed depolymerization at actin filament ends jointly catalysed by Twinfilin and Srv2/CAP. *Nat Cell Biol*. 17:1504-1511.
Johnston, G.C., J.A. Prendergast, and R.A. Singer. 1991. The Saccharomyces cerevisiae MYO2 gene encodes an essential myosin for vectorial transport of vesicles. *J Cell Biol*. 113:539-551.
Jung, G., K. Remmert, X. Wu, J.M. Volosky, and J.A. Hammer, 3rd. 2001. The Dictyostelium CARMIL protein links capping protein and the Arp2/3 complex to type I myosins through their SH3 domains. *J Cell Biol*. 153:1479-1497.
Kaksonen, M., Y. Sun, and D.G. Drubin. 2003. A pathway for association of receptors, adaptors, and actin during endocytic internalization. *Cell*. 115:475-487.
Kaksonen, M., C.P. Toret, and D.G. Drubin. 2005. A modular design for the clathrin- and actin-mediated endocytosis machinery. *Cell*. 123:305-320.
Kamei, T., K. Tanaka, T. Hihara, M. Umikawa, H. Imamura, M. Kikyo, K. Ozaki, and Y. Takai. 1998. Interaction of Bnr1p with a novel Src homology 3 domain-containing Hof1p. Implication in cytokinesis in Saccharomyces cerevisiae. *J Biol Chem*. 273:28341-28345.
Kelleher, J.F., S.J. Atkinson, and T.D. Pollard. 1995. Sequences, structural models, and cellular localization of the actin-related proteins Arp2 and Arp3 from Acanthamoeba. *J Cell Biol*. 131:385-397.
Kikyo, M., K. Tanaka, T. Kamei, K. Ozaki, T. Fujiwara, E. Inoue, Y. Takita, Y. Ohya, and Y. Takai. 1999. An FH domain-containing Bnr1p is a multifunctional protein interacting with a variety of cytoskeletal proteins in Saccharomyces cerevisiae. *Oncogene*. 18:7046-7054.
Kilchert, C., and A. Spang. 2011. Cotranslational transport of ABP140 mRNA to the distal pole of S. cerevisiae. *EMBO J*. 30:3567-3580.
Kilmartin, J.V., and A.E. Adams. 1984. Structural rearrangements of tubulin and actin during the cell cycle of the yeast Saccharomyces. *J Cell Biol*. 98:922-933.
Kim, K., A. Yamashita, M.A. Wear, Y. Maeda, and J.A. Cooper. 2004. Capping protein binding to actin in yeast: biochemical mechanism and physiological relevance. *J Cell Biol*. 164:567-580.
Kirchhausen, T., D. Owen, and S.C. Harrison. 2014. Molecular structure, function, and dynamics of clathrin-mediated membrane traffic. *Cold Spring Harb Perspect Biol*. 6:a016725.

Kishimoto, T., Y. Sun, C. Buser, J. Liu, A. Michelot, and D.G. Drubin. 2011. Determinants of endocytic membrane geometry, stability, and scission. *Proc Natl Acad Sci U S A*. 108:E979-988.

Kohno, H., K. Tanaka, A. Mino, M. Umikawa, H. Imamura, T. Fujiwara, Y. Fujita, K. Hotta, H. Qadota, T. Watanabe, Y. Ohya, and Y. Takai. 1996. Bni1p implicated in cytoskeletal control is a putative target of Rho1p small GTP binding protein in Saccharomyces cerevisiae. *EMBO J*. 15:6060-6068.

Kono, K., Y. Saeki, S. Yoshida, K. Tanaka, and D. Pellman. 2012. Proteasomal degradation resolves competition between cell polarization and cellular wound healing. *Cell*. 150:151-164.

Korn, E.D. 1982. Actin polymerization and its regulation by proteins from nonmuscle cells. *Physiol Rev*. 62:672-737.

Korn, E.D., M.F. Carlier, and D. Pantaloni. 1987. Actin polymerization and ATP hydrolysis. *Science*. 238:638-644.

Kovar, D.R., E.S. Harris, R. Mahaffy, H.N. Higgs, and T.D. Pollard. 2006. Control of the assembly of ATP- and ADP-actin by formins and profilin. *Cell*. 124:423-435.

Kubler, E., and H. Riezman. 1993. Actin and fimbrin are required for the internalization step of endocytosis in yeast. *EMBO J*. 12:2855-2862.

Kueh, H.Y., G.T. Charras, T.J. Mitchison, and W.M. Brieher. 2008. Actin disassembly by cofilin, coronin, and Aip1 occurs in bursts and is inhibited by barbed-end cappers. *J Cell Biol*. 182:341-353.

Kulak, N.A., G. Pichler, I. Paron, N. Nagaraj, and M. Mann. 2014. Minimal, encapsulated proteomic-sample processing applied to copy-number estimation in eukaryotic cells. *Nat Methods*. 11:319-324.

Lawrimore, J., K.S. Bloom, and E.D. Salmon. 2011. Point centromeres contain more than a single centromere-specific Cse4 (CENP-A) nucleosome. *J Cell Biol*. 195:573-582.

Layton, A.T., N.S. Savage, A.S. Howell, S.Y. Carroll, D.G. Drubin, and D.J. Lew. 2011. Modeling vesicle traffic reveals unexpected consequences for Cdc42p-mediated polarity establishment. *Curr Biol*. 21:184-194.

Le Clainche, C., D. Didry, M.F. Carlier, and D. Pantaloni. 2001. Activation of Arp2/3 complex by Wiskott-Aldrich Syndrome protein is linked to enhanced binding of ATP to Arp2. *J Biol Chem*. 276:46689-46692.

Le Clainche, C., D. Pantaloni, and M.F. Carlier. 2003. ATP hydrolysis on actin-related protein 2/3 complex causes debranching of dendritic actin arrays. *Proc Natl Acad Sci U S A*. 100:6337-6342.

Lechler, T., G.A. Jonsdottir, S.K. Klee, D. Pellman, and R. Li. 2001. A two-tiered mechanism by which Cdc42 controls the localization and activation of an Arp2/3-activating motor complex in yeast. *J Cell Biol*. 155:261-270.

Levy, S.F., N. Ziv, and M.L. Siegal. 2012. Bet hedging in yeast by heterogeneous, age-correlated expression of a stress protectant. *PLoS Biol*. 10:e1001325.

Li, F., and H.N. Higgs. 2003. The mouse Formin mDia1 is a potent actin nucleation factor regulated by autoinhibition. *Curr Biol*. 13:1335-1340.

Li, F., and H.N. Higgs. 2005. Dissecting requirements for auto-inhibition of actin nucleation by the formin, mDia1. *J Biol Chem*. 280:6986-6992.

Li, R. 1997. Bee1, a yeast protein with homology to Wiscott-Aldrich syndrome protein, is critical for the assembly of cortical actin cytoskeleton. *J Cell Biol*. 136:649-658.
Lipatova, Z., A.A. Tokarev, Y. Jin, J. Mulholland, L.S. Weisman, and N. Segev. 2008. Direct interaction between a myosin V motor and the Rab GTPases Ypt31/32 is required for polarized secretion. *Mol Biol Cell*. 19:4177-4187.
Liu, H., and A. Bretscher. 1992. Characterization of TPM1 disrupted yeast cells indicates an involvement of tropomyosin in directed vesicular transport. *J Cell Biol*. 118:285-299.
Liu, H.P., and A. Bretscher. 1989a. Disruption of the single tropomyosin gene in yeast results in the disappearance of actin cables from the cytoskeleton. *Cell*. 57:233-242.
Liu, H.P., and A. Bretscher. 1989b. Purification of tropomyosin from Saccharomyces cerevisiae and identification of related proteins in Schizosaccharomyces and Physarum. *Proc Natl Acad Sci U S A*. 86:90-93.
Longtine, M.S., A. McKenzie, 3rd, D.J. Demarini, N.G. Shah, A. Wach, A. Brachat, P. Philippsen, and J.R. Pringle. 1998. Additional modules for versatile and economical PCR-based gene deletion and modification in Saccharomyces cerevisiae. *Yeast*. 14:953-961.
Lu, R., D.G. Drubin, and Y. Sun. 2016. Clathrin-mediated endocytosis in budding yeast at a glance. *J Cell Sci*. 129:1531-1536.
Luan, Q., and B.J. Nolen. 2013. Structural basis for regulation of Arp2/3 complex by GMF. *Nat Struct Mol Biol*. 20:1062-1068.
Machesky, L.M., R.D. Mullins, H.N. Higgs, D.A. Kaiser, L. Blanchoin, R.C. May, M.E. Hall, and T.D. Pollard. 1999. Scar, a WASp-related protein, activates nucleation of actin filaments by the Arp2/3 complex. *Proc Natl Acad Sci U S A*. 96:3739-3744.
MacLean-Fletcher, S., and T.D. Pollard. 1980. Identification of a factor in conventional muscle actin preparations which inhibits actin filament self-association. *Biochem Biophys Res Commun*. 96:18-27.
Madania, A., P. Dumoulin, S. Grava, H. Kitamoto, C. Scharer-Brodbeck, A. Soulard, V. Moreau, and B. Winsor. 1999. The Saccharomyces cerevisiae homologue of human Wiskott-Aldrich syndrome protein Las17p interacts with the Arp2/3 complex. *Mol Biol Cell*. 10:3521-3538.
Martin, A.C., M.D. Welch, and D.G. Drubin. 2006. Arp2/3 ATP hydrolysis-catalysed branch dissociation is critical for endocytic force generation. *Nat Cell Biol*. 8:826-833.
Martin, A.C., X.P. Xu, I. Rouiller, M. Kaksonen, Y. Sun, L. Belmont, N. Volkmann, D. Hanein, M. Welch, and D.G. Drubin. 2005. Effects of Arp2 and Arp3 nucleotide-binding pocket mutations on Arp2/3 complex function. *J Cell Biol*. 168:315-328.
Maruyama, K. 1965a. A New Protein-Factor Hindering Network Formation of F-Actin in Solution. *Biochim Biophys Acta*. 94:208-225.
Maruyama, K. 1965b. Some physico-chemical properties of beta-actinin, "actin-factor", isolated from striated muscle. *Biochim Biophys Acta*. 102:542-548.
Maruyama, K., S. Kimura, T. Ishi, M. Kuroda, and K. Ohashi. 1977. beta-actinin, a regulatory protein of muscle. Purification, characterization and function. *J Biochem*. 81:215-232.
Maruyama, K., H. Kurokawa, M. Oosawa, S. Shimaoka, H. Yamamoto, M. Ito, and K. Maruyama. 1990. Beta-actinin is equivalent to Cap Z protein. *J Biol Chem*. 265:8712-8715.

Mattila, P.K., O. Quintero-Monzon, J. Kugler, J.B. Moseley, S.C. Almo, P. Lappalainen, and B.L. Goode. 2004. A high-affinity interaction with ADP-actin monomers underlies the mechanism and in vivo function of Srv2/cyclase-associated protein. *Mol Biol Cell*. 15:5158-5171.

Mayor, S., R.G. Parton, and J.G. Donaldson. 2014. Clathrin-independent pathways of endocytosis. *Cold Spring Harb Perspect Biol*. 6.

Maytum, R., M.A. Geeves, and M. Konrad. 2000. Actomyosin regulatory properties of yeast tropomyosin are dependent upon N-terminal modification. *Biochemistry*. 39:11913-11920.

McGough, A., B. Pope, W. Chiu, and A. Weeds. 1997. Cofilin changes the twist of F-actin: implications for actin filament dynamics and cellular function. *J Cell Biol*. 138:771-781.

Merrifield, C.J., and M. Kaksonen. 2014. Endocytic accessory factors and regulation of clathrin-mediated endocytosis. *Cold Spring Harb Perspect Biol*. 6:a016733.

Miao, Y., X. Han, L. Zheng, Y. Xie, Y. Mu, J.R. Yates, 3rd, and D.G. Drubin. 2016. Fimbrin phosphorylation by metaphase Cdk1 regulates actin cable dynamics in budding yeast. *Nat Commun*. 7:11265.

Michelot, A., A. Grassart, V. Okreglak, M. Costanzo, C. Boone, and D.G. Drubin. 2013. Actin filament elongation in Arp2/3-derived networks is controlled by three distinct mechanisms. *Dev Cell*. 24:182-195.

Mikati, M.A., D. Breitsprecher, S. Jansen, E. Reisler, and B.L. Goode. 2015. Coronin Enhances Actin Filament Severing by Recruiting Cofilin to Filament Sides and Altering F-Actin Conformation. *J Mol Biol*. 427:3137-3147.

Mockrin, S.C., and E.D. Korn. 1980. Acanthamoeba profilin interacts with G-actin to increase the rate of exchange of actin-bound adenosine 5'-triphosphate. *Biochemistry*. 19:5359-5362.

Moon, A.L., P.A. Janmey, K.A. Louie, and D.G. Drubin. 1993. Cofilin is an essential component of the yeast cortical cytoskeleton. *J Cell Biol*. 120:421-435.

Mooren, O.L., B.J. Galletta, and J.A. Cooper. 2012. Roles for actin assembly in endocytosis. *Annu Rev Biochem*. 81:661-686.

Moseley, J.B., and B.L. Goode. 2005. Differential activities and regulation of Saccharomyces cerevisiae formin proteins Bni1 and Bnr1 by Bud6. *J Biol Chem*. 280:28023-28033.

Moseley, J.B., and B.L. Goode. 2006. The yeast actin cytoskeleton: from cellular function to biochemical mechanism. *Microbiol Mol Biol Rev*. 70:605-645.

Mullins, R.D., J.A. Heuser, and T.D. Pollard. 1998. The interaction of Arp2/3 complex with actin: nucleation, high affinity pointed end capping, and formation of branching networks of filaments. *Proc Natl Acad Sci U S A*. 95:6181-6186.

Nadkarni, A.V., and W.M. Brieher. 2014. Aip1 destabilizes cofilin-saturated actin filaments by severing and accelerating monomer dissociation from ends. *Curr Biol*. 24:2749-2757.

Namba, Y., M. Ito, Y. Zu, K. Shigesada, and K. Maruyama. 1992. Human T cell L-plastin bundles actin filaments in a calcium-dependent manner. *J Biochem*. 112:503-507.

Nefsky, B., and A. Bretscher. 1992. Yeast actin is relatively well behaved. *Eur J Biochem*. 206:949-955.

Ng, R., and J. Abelson. 1980. Isolation and sequence of the gene for actin in Saccharomyces cerevisiae. *Proc Natl Acad Sci U S A*. 77:3912-3916.

Nishida, E., S. Maekawa, and H. Sakai. 1984. Cofilin, a protein in porcine brain that binds to actin filaments and inhibits their interactions with myosin and tropomyosin. *Biochemistry*. 23:5307-5313.

Normoyle, K.P., and W.M. Brieher. 2012. Cyclase-associated protein (CAP) acts directly on F-actin to accelerate cofilin-mediated actin severing across the range of physiological pH. *J Biol Chem*. 287:35722-35732.

Ojala, P.J., V.O. Paavilainen, M.K. Vartiainen, R. Tuma, A.G. Weeds, and P. Lappalainen. 2002. The two ADF-H domains of twinfilin play functionally distinct roles in interactions with actin monomers. *Mol Biol Cell*. 13:3811-3821.

Okada, K., L. Blanchoin, H. Abe, H. Chen, T.D. Pollard, and J.R. Bamburg. 2002. Xenopus actin-interacting protein 1 (XAip1) enhances cofilin fragmentation of filaments by capping filament ends. *J Biol Chem*. 277:43011-43016.

Okada, K., H. Ravi, E.M. Smith, and B.L. Goode. 2006. Aip1 and cofilin promote rapid turnover of yeast actin patches and cables: a coordinated mechanism for severing and capping filaments. *Mol Biol Cell*. 17:2855-2868.

Okreglak, V., and D.G. Drubin. 2007. Cofilin recruitment and function during actin-mediated endocytosis dictated by actin nucleotide state. *J Cell Biol*. 178:1251-1264.

Okreglak, V., and D.G. Drubin. 2010. Loss of Aip1 reveals a role in maintaining the actin monomer pool and an in vivo oligomer assembly pathway. *J Cell Biol*. 188:769-777.

Ono, S., K. Mohri, and K. Ono. 2004. Microscopic evidence that actin-interacting protein 1 actively disassembles actin-depolymerizing factor/Cofilin-bound actin filaments. *J Biol Chem*. 279:14207-14212.

Ozaki-Kuroda, K., Y. Yamamoto, H. Nohara, M. Kinoshita, T. Fujiwara, K. Irie, and Y. Takai. 2001. Dynamic localization and function of Bni1p at the sites of directed growth in Saccharomyces cerevisiae. *Mol Cell Biol*. 21:827-839.

Paavilainen, V.O., M. Hellman, E. Helfer, M. Bovellan, A. Annila, M.F. Carlier, P. Permi, and P. Lappalainen. 2007. Structural basis and evolutionary origin of actin filament capping by twinfilin. *Proc Natl Acad Sci U S A*. 104:3113-3118.

Paavilainen, V.O., E. Oksanen, A. Goldman, and P. Lappalainen. 2008. Structure of the actin-depolymerizing factor homology domain in complex with actin. *J Cell Biol*. 182:51-59.

Palmgren, S., P.J. Ojala, M.A. Wear, J.A. Cooper, and P. Lappalainen. 2001. Interactions with PIP2, ADP-actin monomers, and capping protein regulate the activity and localization of yeast twinfilin. *J Cell Biol*. 155:251-260.

Park, E., B.R. Graziano, W. Zheng, M. Garabedian, B.L. Goode, and M.J. Eck. 2015. Structure of a Bud6/Actin Complex Reveals a Novel WH2-like Actin Monomer Recruitment Motif. *Structure*. 23:1492-1499.

Peng, Y., A. Grassart, R. Lu, C.C. Wong, J. Yates, 3rd, G. Barnes, and D.G. Drubin. 2015. Casein kinase 1 promotes initiation of clathrin-mediated endocytosis. *Dev Cell*. 32:231-240.

Picco, A., M. Mund, J. Ries, F. Nedelec, and M. Kaksonen. 2015. Visualizing the functional architecture of the endocytic machinery. *Elife*. 4.

Polevoda, B., T.S. Cardillo, T.C. Doyle, G.S. Bedi, and F. Sherman. 2003. Nat3p and Mdm20p are required for function of yeast NatB Nalpha-terminal acetyltransferase and of actin and tropomyosin. *J Biol Chem*. 278:30686-30697.

Pollard, T.D. 1986. Rate constants for the reactions of ATP- and ADP-actin with the ends of actin filaments. *J Cell Biol*. 103:2747-2754.
Pollard, T.D. 1990. Actin. *Curr Opin Cell Biol*. 2:33-40.
Pollard, T.D. 2016. Actin and Actin-Binding Proteins. *Cold Spring Harb Perspect Biol*. 8.
Pollard, T.D., and J.A. Cooper. 1984. Quantitative analysis of the effect of Acanthamoeba profilin on actin filament nucleation and elongation. *Biochemistry*. 23:6631-6641.
Pollard, T.D., and J.A. Cooper. 1986. Actin and actin-binding proteins. A critical evaluation of mechanisms and functions. *Annu Rev Biochem*. 55:987-1035.
Prendergast, J.A., L.E. Murray, A. Rowley, D.R. Carruthers, R.A. Singer, and G.C. Johnston. 1990. Size selection identifies new genes that regulate Saccharomyces cerevisiae cell proliferation. *Genetics*. 124:81-90.
Pringle, J.R., R.A. Preston, A.E. Adams, T. Stearns, D.G. Drubin, B.K. Haarer, and E.W. Jones. 1989. Fluorescence microscopy methods for yeast. *Methods Cell Biol*. 31:357-435.
Prosser, D.C., T.G. Drivas, L. Maldonado-Baez, and B. Wendland. 2011. Existence of a novel clathrin-independent endocytic pathway in yeast that depends on Rho1 and formin. *J Cell Biol*. 195:657-671.
Prosser, D.C., and B. Wendland. 2012. Conserved roles for yeast Rho1 and mammalian RhoA GTPases in clathrin-independent endocytosis. *Small GTPases*. 3:229-235.
Protopopov, V., B. Govindan, P. Novick, and J.E. Gerst. 1993. Homologs of the synaptobrevin/VAMP family of synaptic vesicle proteins function on the late secretory pathway in S. cerevisiae. *Cell*. 74:855-861.
Pruyne, D., M. Evangelista, C. Yang, E. Bi, S. Zigmond, A. Bretscher, and C. Boone. 2002. Role of formins in actin assembly: nucleation and barbed-end association. *Science*. 297:612-615.
Pruyne, D., A. Legesse-Miller, L. Gao, Y. Dong, and A. Bretscher. 2004. Mechanisms of polarized growth and organelle segregation in yeast. *Annu Rev Cell Dev Biol*. 20:559-591.
Pruyne, D.W., D.H. Schott, and A. Bretscher. 1998. Tropomyosin-containing actin cables direct the Myo2p-dependent polarized delivery of secretory vesicles in budding yeast. *J Cell Biol*. 143:1931-1945.
Rodal, A.A., A.L. Manning, B.L. Goode, and D.G. Drubin. 2003. Negative regulation of yeast WASp by two SH3 domain-containing proteins. *Curr Biol*. 13:1000-1008.
Rodal, A.A., O. Sokolova, D.B. Robins, K.M. Daugherty, S. Hippenmeyer, H. Riezman, N. Grigorieff, and B.L. Goode. 2005. Conformational changes in the Arp2/3 complex leading to actin nucleation. *Nat Struct Mol Biol*. 12:26-31.
Rodal, A.A., J.W. Tetreault, P. Lappalainen, D.G. Drubin, and D.C. Amberg. 1999. Aip1p interacts with cofilin to disassemble actin filaments. *J Cell Biol*. 145:1251-1264.
Romero, S., C. Le Clainche, D. Didry, C. Egile, D. Pantaloni, and M.F. Carlier. 2004. Formin is a processive motor that requires profilin to accelerate actin assembly and associated ATP hydrolysis. *Cell*. 119:419-429.
Safer, D., M. Elzinga, and V.T. Nachmias. 1991. Thymosin beta 4 and Fx, an actin-sequestering peptide, are indistinguishable. *J Biol Chem*. 266:4029-4032.
Safer, D., R. Golla, and V.T. Nachmias. 1990. Isolation of a 5-kilodalton actin-sequestering peptide from human blood platelets. *Proc Natl Acad Sci U S A*. 87:2536-2540.

Sagot, I., S.K. Klee, and D. Pellman. 2002a. Yeast formins regulate cell polarity by controlling the assembly of actin cables. *Nat Cell Biol*. 4:42-50.
Sagot, I., A.A. Rodal, J. Moseley, B.L. Goode, and D. Pellman. 2002b. An actin nucleation mechanism mediated by Bni1 and profilin. *Nat Cell Biol*. 4:626-631.
Schott, D., J. Ho, D. Pruyne, and A. Bretscher. 1999. The COOH-terminal domain of Myo2p, a yeast myosin V, has a direct role in secretory vesicle targeting. *J Cell Biol*. 147:791-808.
Schutt, C.E., J.C. Myslik, M.D. Rozycki, N.C. Goonesekere, and U. Lindberg. 1993. The structure of crystalline profilin-beta-actin. *Nature*. 365:810-816.
Schwob, E., and R.P. Martin. 1992. New yeast actin-like gene required late in the cell cycle. *Nature*. 355:179-182.
Sheu, Y.J., B. Santos, N. Fortin, C. Costigan, and M. Snyder. 1998. Spa2p interacts with cell polarity proteins and signaling components involved in yeast cell morphogenesis. *Mol Cell Biol*. 18:4053-4069.
Shortle, D., J.E. Haber, and D. Botstein. 1982. Lethal disruption of the yeast actin gene by integrative DNA transformation. *Science*. 217:371-373.
Singer, J.M., and J.M. Shaw. 2003. Mdm20 protein functions with Nat3 protein to acetylate Tpm1 protein and regulate tropomyosin-actin interactions in budding yeast. *Proc Natl Acad Sci U S A*. 100:7644-7649.
Skruzny, M., T. Brach, R. Ciuffa, S. Rybina, M. Wachsmuth, and M. Kaksonen. 2012. Molecular basis for coupling the plasma membrane to the actin cytoskeleton during clathrin-mediated endocytosis. *Proc Natl Acad Sci U S A*. 109:E2533-2542.
Skruzny, M., A. Desfosses, S. Prinz, S.O. Dodonova, A. Gieras, C. Uetrecht, A.J. Jakobi, M. Abella, W.J. Hagen, J. Schulz, R. Meijers, V. Rybin, J.A. Briggs, C. Sachse, and M. Kaksonen. 2015. An organized co-assembly of clathrin adaptors is essential for endocytosis. *Dev Cell*. 33:150-162.
Stark, B.C., M.H. Lanier, and J.A. Cooper. 2017. CARMIL family proteins as multidomain regulators of actin-based motility. *Mol Biol Cell*. 28:1713-1723.
Suarez, C., J. Roland, R. Boujemaa-Paterski, H. Kang, B.R. McCullough, A.C. Reymann, C. Guerin, J.L. Martiel, E.M. De la Cruz, and L. Blanchoin. 2011. Cofilin tunes the nucleotide state of actin filaments and severs at bare and decorated segment boundaries. *Curr Biol*. 21:862-868.
Sun, Y., S. Carroll, M. Kaksonen, J.Y. Toshima, and D.G. Drubin. 2007. PtdIns(4,5)P2 turnover is required for multiple stages during clathrin- and actin-dependent endocytic internalization. *J Cell Biol*. 177:355-367.
Sun, Y., A.C. Martin, and D.G. Drubin. 2006. Endocytic internalization in budding yeast requires coordinated actin nucleation and myosin motor activity. *Dev Cell*. 11:33-46.
Tilney, L.G., E.M. Bonder, L.M. Coluccio, and M.S. Mooseker. 1983. Actin from Thyone sperm assembles on only one end of an actin filament: a behavior regulated by profilin. *J Cell Biol*. 97:112-124.
Tonikian, R., X. Xin, C.P. Toret, D. Gfeller, C. Landgraf, S. Panni, S. Paoluzi, L. Castagnoli, B. Currell, S. Seshagiri, H. Yu, B. Winsor, M. Vidal, M.B. Gerstein, G.D. Bader, R. Volkmer, G. Cesareni, D.G. Drubin, P.M. Kim, S.S. Sidhu, and C. Boone. 2009. Bayesian modeling of the yeast SH3 domain interactome predicts spatiotemporal dynamics of endocytosis proteins. *PLoS Biol*. 7:e1000218.

Toret, C.P., L. Lee, M. Sekiya-Kawasaki, and D.G. Drubin. 2008. Multiple pathways regulate endocytic coat disassembly in Saccharomyces cerevisiae for optimal downstream trafficking. *Traffic*. 9:848-859.

Uruno, T., K. Remmert, and J.A. Hammer, 3rd. 2006. CARMIL is a potent capping protein antagonist: identification of a conserved CARMIL domain that inhibits the activity of capping protein and uncaps capped actin filaments. *J Biol Chem*. 281:10635-10650.

Usaj, M., Y. Tan, W. Wang, B. VanderSluis, A. Zou, C.L. Myers, M. Costanzo, B. Andrews, and C. Boone. 2017. TheCellMap.org: A Web-Accessible Database for Visualizing and Mining the Global Yeast Genetic Interaction Network. *G3 (Bethesda)*. 7:1539-1549.

Vallen, E.A., J. Caviston, and E. Bi. 2000. Roles of Hof1p, Bni1p, Bnr1p, and myo1p in cytokinesis in Saccharomyces cerevisiae. *Mol Biol Cell*. 11:593-611.

van Leeuwen, J., C. Pons, J.C. Mellor, T.N. Yamaguchi, H. Friesen, J. Koschwanez, M.M. Usaj, M. Pechlaner, M. Takar, M. Usaj, B. VanderSluis, K. Andrusiak, P. Bansal, A. Baryshnikova, C.E. Boone, J. Cao, A. Cote, M. Gebbia, G. Horecka, I. Horecka, E. Kuzmin, N. Legro, W. Liang, N. van Lieshout, M. McNee, B.J. San Luis, F. Shaeri, E. Shuteriqi, S. Sun, L. Yang, J.Y. Youn, M. Yuen, M. Costanzo, A.C. Gingras, P. Aloy, C. Oostenbrink, A. Murray, T.R. Graham, C.L. Myers, B.J. Andrews, F.P. Roth, and C. Boone. 2016. Exploring genetic suppression interactions on a global scale. *Science*. 354.

Vinson, V.K., E.M. De La Cruz, H.N. Higgs, and T.D. Pollard. 1998. Interactions of Acanthamoeba profilin with actin and nucleotides bound to actin. *Biochemistry*. 37:10871-10880.

Wang, J., S.P. Neo, and M. Cai. 2009. Regulation of the yeast formin Bni1p by the actin-regulating kinase Prk1p. *Traffic*. 10:528-535.

Watanabe, N., T. Kato, A. Fujita, T. Ishizaki, and S. Narumiya. 1999. Cooperation between mDia1 and ROCK in Rho-induced actin reorganization. *Nat Cell Biol*. 1:136-143.

Weber, A., C.R. Pennise, G.G. Babcock, and V.M. Fowler. 1994. Tropomodulin caps the pointed ends of actin filaments. *J Cell Biol*. 127:1627-1635.

Welch, M.D., A. Iwamatsu, and T.J. Mitchison. 1997. Actin polymerization is induced by Arp2/3 protein complex at the surface of Listeria monocytogenes. *Nature*. 385:265-269.

Wen, K.K., and P.A. Rubenstein. 2005. Acceleration of yeast actin polymerization by yeast Arp2/3 complex does not require an Arp2/3-activating protein. *J Biol Chem*. 280:24168-24174.

Winder, S.J., T. Jess, and K.R. Ayscough. 2003. SCP1 encodes an actin-bundling protein in yeast. *Biochem J*. 375:287-295.

Winter, D., T. Lechler, and R. Li. 1999a. Activation of the yeast Arp2/3 complex by Bee1p, a WASP-family protein. *Curr Biol*. 9:501-504.

Winter, D., A.V. Podtelejnikov, M. Mann, and R. Li. 1997. The complex containing actin-related proteins Arp2 and Arp3 is required for the motility and integrity of yeast actin patches. *Curr Biol*. 7:519-529.

Winter, D.C., E.Y. Choe, and R. Li. 1999b. Genetic dissection of the budding yeast Arp2/3 complex: a comparison of the in vivo and structural roles of individual subunits. *Proc Natl Acad Sci U S A*. 96:7288-7293.

Wioland, H., B. Guichard, Y. Senju, S. Myram, P. Lappalainen, A. Jegou, and G. Romet-Lemonne. 2017. ADF/Cofilin Accelerates Actin Dynamics by Severing Filaments and Promoting Their Depolymerization at Both Ends. *Curr Biol*. 27:1956-1967 e1957.

Yang, C., M. Pring, M.A. Wear, M. Huang, J.A. Cooper, T.M. Svitkina, and S.H. Zigmond. 2005. Mammalian CARMIL inhibits actin filament capping by capping protein. *Dev Cell*. 9:209-221.

Yang, H.C., and L.A. Pon. 2002. Actin cable dynamics in budding yeast. *Proc Natl Acad Sci U S A*. 99:751-756.

Ydenberg, C.A., S.B. Padrick, M.O. Sweeney, M. Gandhi, O. Sokolova, and B.L. Goode. 2013. GMF severs actin-Arp2/3 complex branch junctions by a cofilin-like mechanism. *Curr Biol*. 23:1037-1045.

Yin, H., D. Pruyne, T.C. Huffaker, and A. Bretscher. 2000. Myosin V orientates the mitotic spindle in yeast. *Nature*. 406:1013-1015.

Yu, H., P. Braun, M.A. Yildirim, I. Lemmens, K. Venkatesan, J. Sahalie, T. Hirozane-Kishikawa, F. Gebreab, N. Li, N. Simonis, T. Hao, J.F. Rual, A. Dricot, A. Vazquez, R.R. Murray, C. Simon, L. Tardivo, S. Tam, N. Svrzikapa, C. Fan, A.S. de Smet, A. Motyl, M.E. Hudson, J. Park, X. Xin, M.E. Cusick, T. Moore, C. Boone, M. Snyder, F.P. Roth, A.L. Barabasi, J. Tavernier, D.E. Hill, and M. Vidal. 2008. High-quality binary protein interaction map of the yeast interactome network. *Science*. 322:104-110.

Zigmond, S.H. 1993. Recent quantitative studies of actin filament turnover during cell locomotion. *Cell Motil Cytoskeleton*. 25:309-316.